PERFORMANCE OF HOLLOWCORE FLOOR SEATING CONNECTION DETAILS

A thesis
submitted in partial fulfilment
of the requirements for the Degree
of
Master of Engineering
at the
University of Canterbury
by
Horng Yih, LIEW

University of Canterbury
Christchurch, New Zealand

2004

Abstract:

Hollowcore floor slabs are the dominant flooring systems used in New Zealand since the 1980's. This study examines the performance of three different types of beam to hollowcore floor slab seating connection detail under seismic loading conditions. Two of these connection details tested are used in present New Zealand practise and the other is a potential retrofit detail to construction practice of the 1980's and 1990's. In this sub-assemblage research, relative rotation between the supporting beam and hollowcore floor is used as the dominant source of damage instead of the traditional pull and push approach. The sub-assemblages were tested up to inter-storey drifts of ±4.0% and visual and instrumental observations from the experiments are outlined. An analytical study is conducted to better understand the observed failure modes and strength capacity for each seating connection details is also predicted. Finally, fragility analysis is used to determine the seismic vulnerability for all three types of connection detail. Results show that hollowcore units should have some reinforcing in their cells. However, the cells should not be over reinforced as this becomes detrimental to performances.

Acknowledgements:

The research presented in this thesis was conducted at the Department of Civil Engineering at the University of Canterbury under the supervision of Professor John Mander and Professor Des Bull. I would like to thank both John and Des for their support and guidance throughout my thesis.

This project would not be possible without the support from University of Canterbury, Firth Industries Ltd, and Stresscrete for their funding and sponsorship in materials. I also like to thanks the technician staff in the department of Civil Engineering, especially Russell McConchie, for their friendship and guidance.

A huge thank you must go to Jeff Matthews for his friendship and guidance. He has helped me a lot with my thesis. Special thanks also to other postgraduate students like Renee Lindsay, Victor Wong, Vincent Wong, Iwan Surdano and Dave Arnold for their support. I also want to thank Alan Nicholson, Louise Barton and Melody Callahan too for their help during my time studying a master degree.

Finally, a special thanks to my family and friend for their love, support and guidance throughout my time in university.

Table of Contents:

3. Implications of Experimental Observation

4.Summary, Conclusions and Recommendations

Appendix A

Appendix B: Experimental Photos

Appendix C: Full Detail Calculations

List of Figures:

List of Tables:

Section 1

Introduction

1.1 BACKGROUND

Prestressed hollowcore floor units are extensively used in precast construction and it has been a dominant form of construction in New Zealand practise since the 1980s. The main structural functions of hollowcore floor are span, load bearing, transverse distribution of vertical loads, diaphragm distribution of horizontal actions as well as resistance against fire and accidental actions affecting the floor elements or the supporting structure.

In precast floors, individual slab units are mounted together and connected to form a complete floor. Generally, the prestressed hollowcore floor units have no reinforcement other than the longitudinal prestressing tendons anchored by bond. Due to the absence of complementary reinforcement at the support and in the transverse direction, the tensile strength of the concrete has to be taken into account for the determination of the shear capacity, load distribution and etc.

In order to fulfill all the required functions of hollowcore floor slab, the design of hollowcore floors should meet a certain specific criteria. One of the most important criteria is the tensile stresses in un-reinforced zones should be avoided whenever possible. Normally, a hollowcore floor should be designed to adequately resist negative bending moments caused by rotation at the supports. Precautions should also be taken to cope with unintended transverse restraint in the connections at edge supports.

New Zealand standards now recognize the widespread use of precast concrete construction, and include specific reference to precast concrete support details. Research in this area is expanding however; new issues and newly recommended support details continue to simplify the design and construction of precast concrete floor systems. Detailed design requirements on precast hollowcore floor system can be found in FIP (1998), PCI (1985) and FIP (1994).

After the collapse of several precast concrete structures in the 1994 Northridge California earthquake (Norton et al, 1994), concern was raised as to the dependability of performance of precast buildings with hollowcore flooring systems in New Zealand. One of the major concern with hollowcore flooring unit was the connection of these precast hollowcore units to the surrounding lateral load resisting system. When these hollowcore units loose their seating due to a connection failure with the surrounding perimeter beam, entire sections of the floor could possibly collapse leading to a partial (or full) collapse of the building. Figure 1-1 shows examples of hollowcore flooring system failure observed in Northridge earthquake.

In the past, research has focussed on the performance of the lateral loading resisting systems and floor diaphragms have been overlooked. This is because floor diaphragms have been assumed to act rigidly and hence ease the computational effort required when designing a building. Research work conducted by Matthews (2004) and Lindsay (2004) has aimed at determining whether New Zealand designed and built precast concrete structures, which incorporate precast hollowcore floor units structure, possess adequate or inadequate seating details.

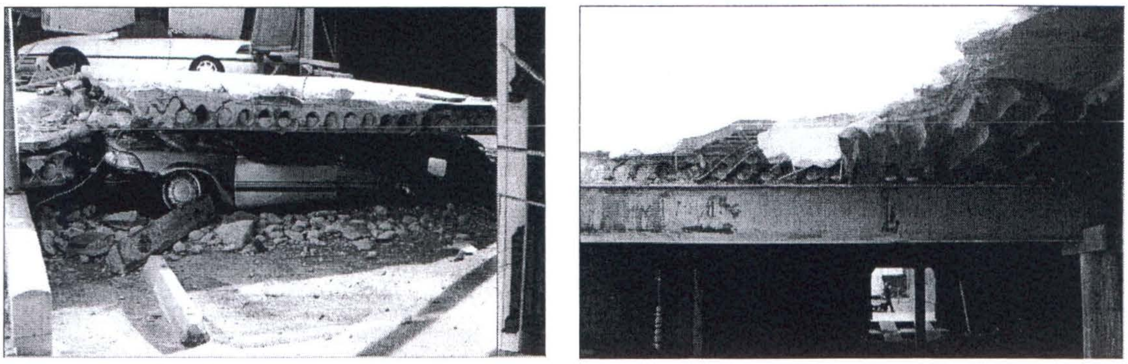

(a) complete collapse of a hollowcore unit **(b) Partial collapse of a hollowcore unit**

Figure 1-1 Hollowcore floor failure observed in 1994 Northridge

This thesis follows on from recent research work completed by Bull and Matthews (2003). This chapter firstly discusses the investigation undertaken by previous researchers on the performance of the connection detail used for seating hollowcore floor slabs. Next, an introduction on New Zealand recommended seating connection detail is made. Finally, a brief discussion on the seating connection detail that will be examined in this research is presented.

1.2 SUB-ASSEMBLAGE RESEARCH

Previous hollowcore research undertaken by Mejia-McMaster and Park (1994), Oliver (1998) and Herlihy and Park (2000) have focused on the connection between a precast hollowcore floor unit and its supporting beam. These tests were undertaken to investigate the seating requirements of a hollowcore unit during an earthquake when supporting beam undergoes beam elongation. These tests were conducted by pulling and pushing the units longitudinally on their seats to investigate whether the cast-in-place topping concrete and the starter bars had sufficient strength to prevent the floor from collapsing. Various connection details were examined and were pulled off the supporting beam by a cyclic horizontal load.

Mejia-McMaster and Park (1994) investigated hollowcore connection detail recommended by FIP (1988) and New Zealand Guidelines (CAE, 1999) as shown in Figure 1-2. Mejia-McMaster and Park (1994) shows that the FIP (1998) recommended tie connection detail was able to behave in a ductile manner. Next, Oliver (1998) investigated the use of "paperclip" tie-bars connection detail and the advantage of incorporating steel fibre reinforced concrete (SFRC) at the support detail. Oliver (1998) found that the fibre reinforced concrete has vastly improved the tensile capacity of connection detail. Herlihy and Park (2000) has further describe a set of tests that compromised a monotonic vertical push down of the hollowcore unit relative to the supporting beam to induce tension in the starter bars and determine the amount of additional bending moment resistance added to the seating connection by the continuity steel. Test layouts for both the pull-off and rotation tests are shown in Figure 1-3.

Failure observed in previous research was due purely to tension. Figure 1-4 shows the failure of Herlihy and Park (2000) test when compared with the actual damage from an earthquake. None of the previous test looked at the relative rotation between the hollowcore and supporting beam as a dominant source of damage to the hollowcore units. Therefore, the failure mechanisms observed in these tests was not consistent with the failure mechanisms observed in Northridge earthquake.

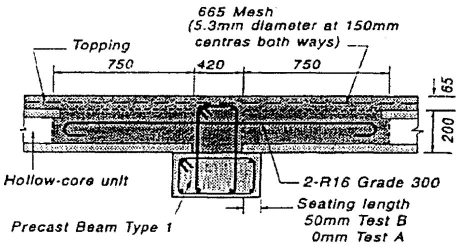

(a) Type 1 connection detail

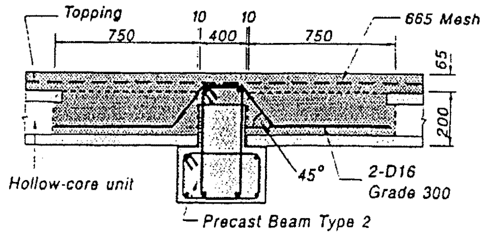

(b) Type 2 connection detail

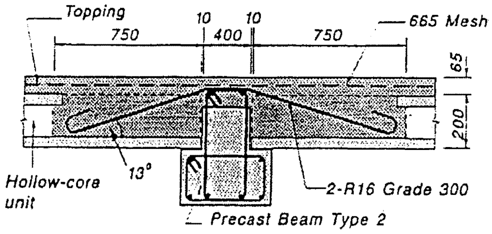

(c) Type 3 connection detail

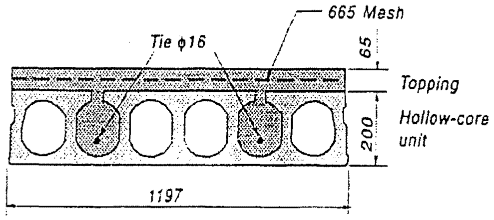

(d) Typical cross section

Figure 1-2 Connection detail tested by Mejia-McMaster and Park (1994)

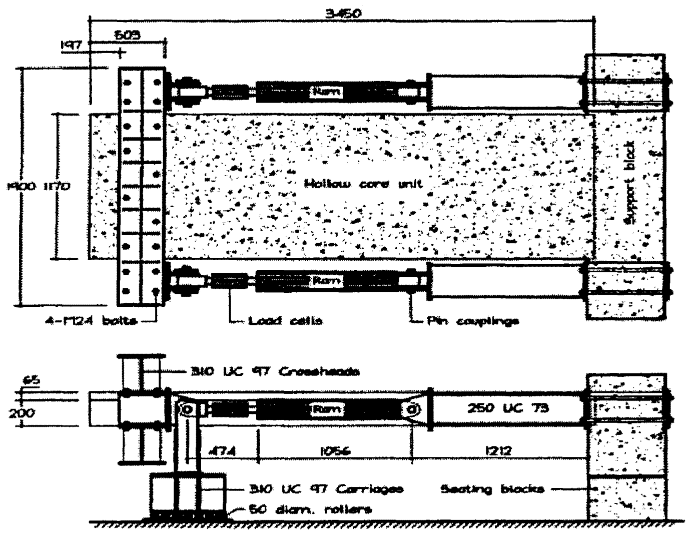

(a) Pull-off test set-up

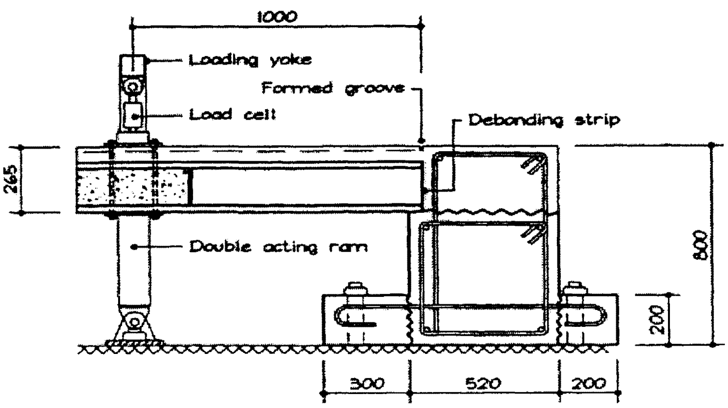

(b) Cantilever test set-up

Figure 1-3 Previous hollowcore pull off and rotation tests (Herlihy and Park, 2000)

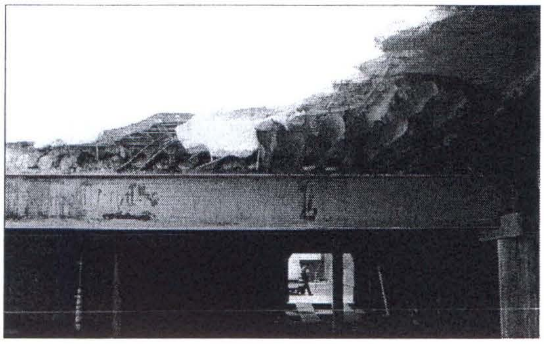

(a) Meadows Apartment Building, Northridge 1994 (Norton et al, 1994)

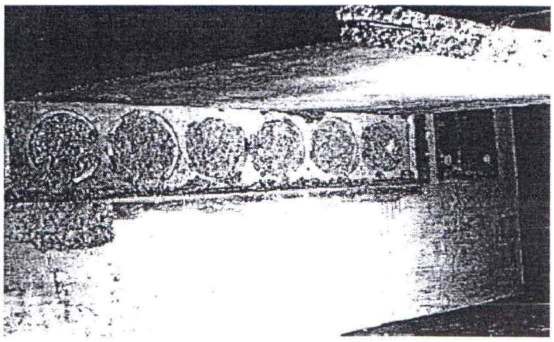

(b) Herlihy and Park (2000)

Figure 1-4 Failure of hollowcore in 1994 Northridge earthquake (Norton et al, 1994) and Herlihy and Park (2000)

Bull and Matthews (2003) has specifically addressed the relative rotation between the hollowcore unit and supporting beam as the damage initiating factor. Figure 1-5 shows four connection details tested by Bull and Matthews (2003). Firstly, a 300 series hollowcore unit seated on a mortar bed was tested as a control specimen to determine whether the failure mechanism similar to Matthews (2004) experiment. A 200 series hollowcore unit was tested to investigate whether there is any size dependent effect. Finally, two new recommended connection details; a pinned type connection joint consisted of a low-friction bearing strip and 10mm compressible material at the units ends and; a more rigid connection with 2-R12 paperclip in two cells of the hollowcore unit filled with concrete.

Bull and Matthews (2003) concluded that the performance of the connection detail of the control specimen agreed well with the observed behaviour in Matthews (2004) super assemblage experiment. Bull and Matthews (2003) also concluded that both new recommended seating connection details has performed well and out performed the control specimen, as expected. The compressible backing board solution has shown to perform better than the "paperclip" detail. Bull and Matthews (2003) experimental setup did not, however, include three dimensional effects such as no net tension applied, no plasticity forming in the supporting beam and secondary effects were not monitored.

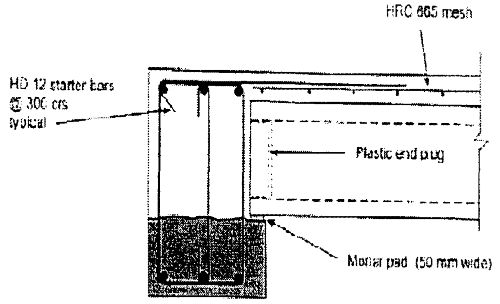

(a) Control Specimen (200 and 300 series)

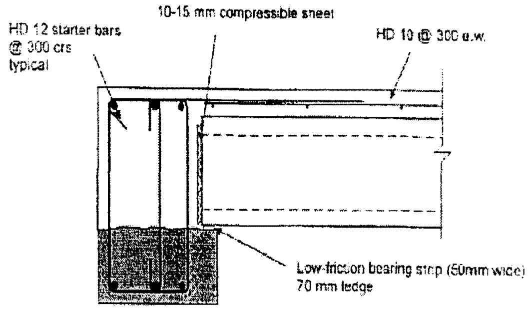

(b) Flexible seating detail

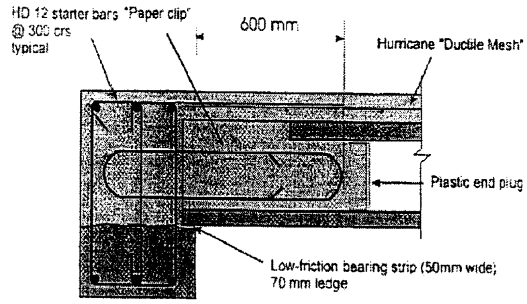

(c) Paperclip seating detail recommended by TAG

Figure 1-5 Seating detail tested by Matthews and Bull (2003)

1.3 SUPER-ASSEMBLAGE RESEARCH

Matthews (2004) investigated the performance of a beam-floor connection joint detail in a three dimensional manner by constructing a one storey slice from a precast concrete building as shown in Figure 1-6. The super assemblage was loaded cyclically in both longitudinal (parallel to hollowcore units) and transverse directions describe in Figure 1-7. Matthews focused on the beam elongation effect and seating length requirement for hollowcore floor units.

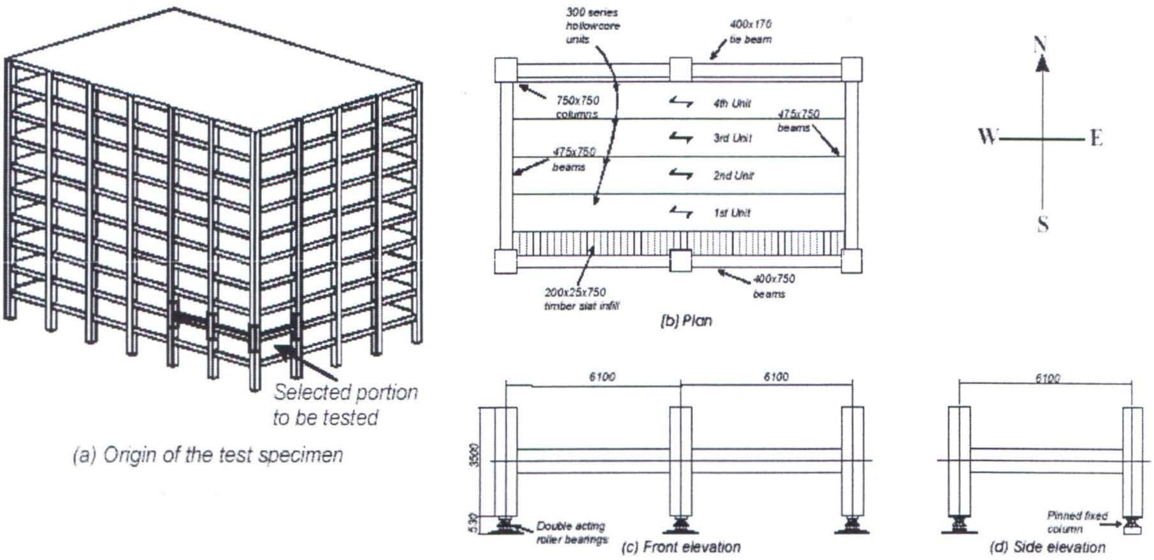

Figure 1-6 Layout and dimensions of the super-assembly

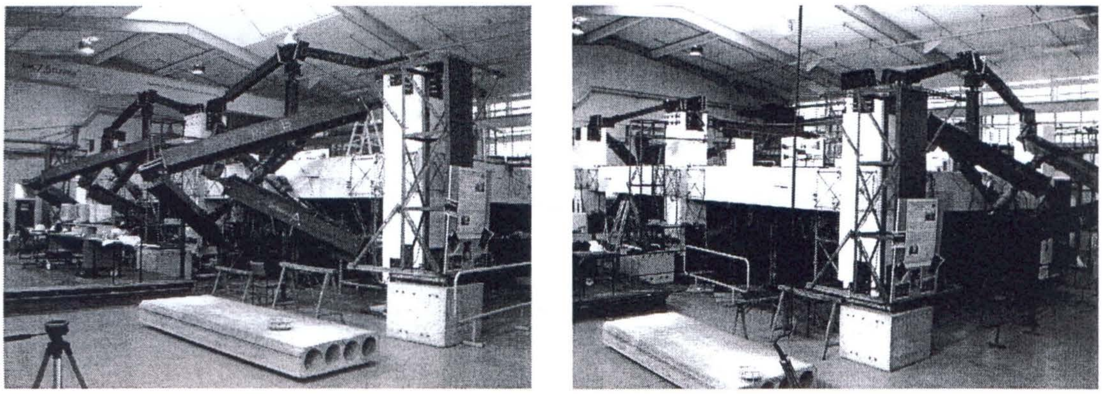

(a) Longitudinal loading **(b) Transverse loading**

Figure 1-7 Specimen setup of Matthews (2004) and Lindsay (2004) super-assemblage

Matthews (2004) concluded that failure mode of the hollowcore floor unit was different to those assumed by design. Relative rotation between the supporting beam and the hollowcore unit was identified as the dominant source of damage to the hollowcore unit. There was sufficient bond/friction to cause the hollowcore unit to rotate rather than sliding. Figure 1-8 shows that Matthews (2004) super-assemblage gives the same failure mechanism as those observed in the 1994 Northridge earthquake. Matthews (2004) also pointed out that the performance of the beam-floor connection detail is inferior to the structural frame. Although the floor has failed, the perimeter frames (beams, columns, beam and column joints) remained relatively undamaged.

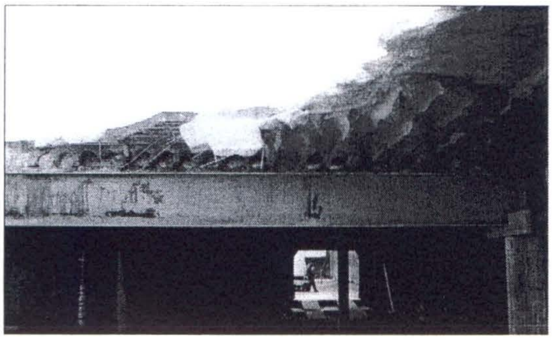

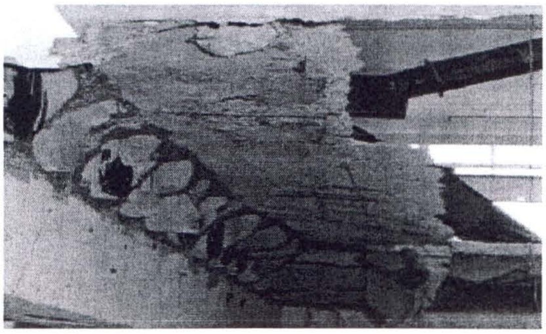

(a) Meadows Apartment Building, Northridge 1994 (Norton et al, 1994) **(b) Matthews (2004) failure mode**

Figure 1-8 Failure modes between 1994 Northridge earthquake and Matthews (2004)

A theory was developed by Matthews (2004) on beam elongation. A "rainflow counting" method has been employed to predict the beam elongation using rigid body kinematics. The principal advantage for using rigid body kinematics is that it allows for a simplified set of equations to be used. The seat width requirement, U_T, determined in term of inter-storey drift is given by:

$$U_T = \frac{\omega}{2} n e_{cr} \left(|\theta_p^+| + |\theta_p^-| + |\theta_y| \right) \frac{L}{L_b} + 15mm + cover \quad \textbf{(1-1)}$$

in which ω = a dynamic magnification factor (a value of 1.5 is suggested); n = number of hinges within the span of the floor section under consideration; e_{cr} = depth between the beam centreline and the instantaneous centre of rotation; θ_p^+ = maximum positive plastic rotation; θ_p^- = maximum negative plastic rotation; θ_y = yield drift of structure; L = distance between column centrelines and L_b = distance between the assumed centre of rotation of the plastic hinges.

Lindsay (2004) has followed on Matthews (2004) experimental work. She reconstructed and retested Matthews's super-assemblage specimen. Lindsay has addressed some of the issues encountered by Matthews (2004) and modifications were made to improve the performance of the overall hollowcore flooring system. Lindsay (2004) employed a beam to floor connection detail using a low-friction bearing strip with a compressible backing replacing the plastic bungs in the end of the units. The low-friction bearing strips were observed to slide and the compressive backing board used in the experiment did not compress enough. Lindsay (2004) concluded that hollowcore units not be seated in the potential plastic hinge zones of the supporting beams. This is because the plastic hinge zones lead to areas of high stresses and strains as this is evident in the corner cracking of the hollowcore unit and it was contributing factors in Matthews (2004) floor failure. Lindsay (2004) has answered several questions left by Matthews (2004), particularly the lateral support of the first hollowcore unit to the perimeter beam, tying of the central column to the floor slab and torsion effect in structures. Lindsay (2004) experiment also verified the beam elongation theory developed by Matthews (2004)

1.4 NEW ZEALAND RECOMMENDED DETAILS FOR HOLLOWCORE UNITS CONNECTIONS

1.4.1 Seating detail

Adequate support of precast concrete floor units is one of the most basic requirements for a safe structure. Particular issues such as tolerances, construction methodology, transverse load distribution, volume changes, thermal effects, seismic effects and appropriate seating needed to be consider carefully both during the designing and constructing stage. All these factors must be considered when determining required seating length.

The New Zealand Concrete Structures Standard (NZS 3101:1995) requires a minimum bearing lengths, as shown in Figure 1-9 (Fig C4.3 NZS3101:1995 Part 2), to maintain the structural integrity of precast flooring systems. The code specifies that a beam support length of L/180 must be satisfied. The minimum allowable seating length is 50 mm for a slab unit and 75 mm for a beams or ribbed floor. Cl 4.3.6.4 of the NZS3101:1995 gives guidance on the recommended seat length and placing requirements. None of the connection details specify that a bearing strip should be used. Centre for Advanced Engineering (CAE, 1999) did recommend the use of bearing pads or mortar seating pads at the seating connection. The evenness of the contact zone along the support will affect the bearing capacity. The bearing strips or packing may be sand cement mortar, neoprene rubber pads, proprietary plastic shims or strips or epoxy mortar.

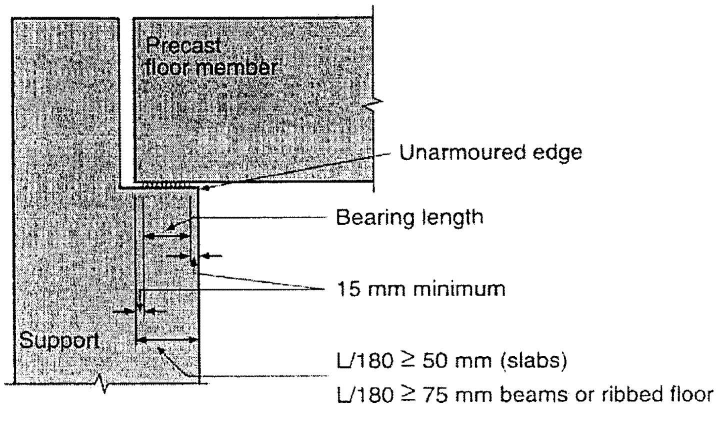

Figure 1-9 Required bearing length at support of a member

1.4.2 New Zealand Guideline recommended connection detail

Centre for Advanced Engineering (CAE, 1999) identifies three basic types of support for precast floor units as shown in Figure 1-10. The differences between these three groups of connections support are the depth of the supporting beam prior to the cast in place concrete being poured. The chosen connection depends on the depth of supporting beam prior to the cast in-situ concrete topping slab being poured. CAE also gives additional guidance to the hollowcore units placed in a ductile moment resisting frame or when the unit arrives on site and is too short to be seated on the beam (or its seat length is less than the standard specifies minimum).

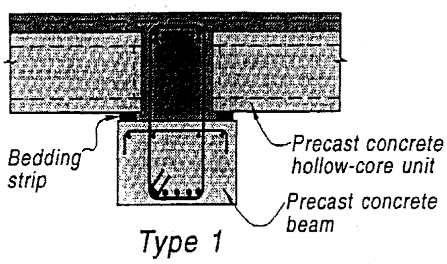

(a) Type 1 beam support system

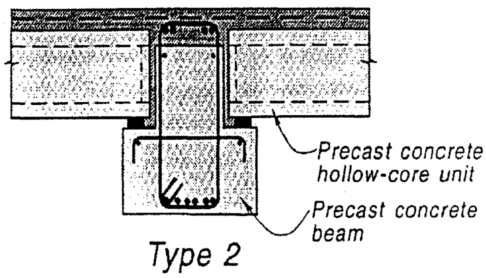

(b) Type 2 beam support system

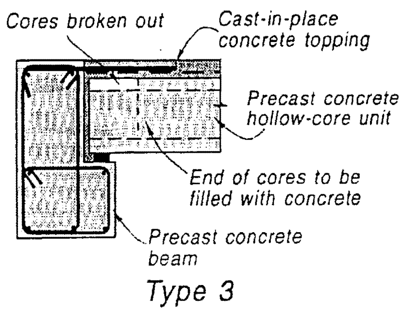

(a) Type 3 beam support system

Figure 1-10 NZ recommended details for the support of hollowcore floor units (CAE, 1999)

Type 1 support usually has the advantage of overcome the problems of construction tolerances easily on site. Type 2 support has a greater beam depth when the floor units are erected. This generally requires less propping and the amount of work involved is less. Finally, type 3 support is usually used for perimeter beams or lift and stairwells. There is no edge formwork needed for the slab topping concrete since the entire supporting beam is pre-cast.

1.4.3 Design Consideration for Connection at Support

In a multi-storey building, the primary role of diaphragms is to ensure efficient interaction of all lateral force resisting elements. Generally, two types of diaphragm actions are encountered in buildings (Paulay and Priestley, 1992). The first type of action occurs at every floor where the floor system, acting as a horizontal deep beam, transmits forces generated by wind or an earthquake to various lateral force resisting components. The second type of action is where large in-plane shear forces need to be transferred from one vertical lateral force component to others. In such transfer diaphragms, shear effects may be critical and connection joint will be critical too. Therefore, connection joint will be crucial on the ability of diaphragm to transfer the in-plane force and vertical shear force.

The structural connections, especially the connections at the supports, should be designed and detailed aiming to provide structural integrity and ductility in a building during collapse. Not only a connection joint need to provide a load path to transfer tensile force, it also should withstand large imposed deformations results from effects of creep, shrinkage, temperature changes and differential settlements. The connection joint should also be designed to prevent horizontal relative displacements of the hollowcore floor units both in the longitudinal and the transverse directions and prevent possible joint cracks from opening uncontrollably.

It is very important that brittle failures do not occur at connection joints. As buildings are generally designed not to collapse and for life-safety purposes, incident of loss of anchorage and splitting at the connection should be prevented. In order to avoid brittle failure, it is essential that sufficient shear capacity (shear friction effect) is developed at longitudinal and transverse joint interfaces and the splitting effect from tie bars anchored in the joint is also taken care of.

1.5 DETAILS OF TEST SPECIMEN TO BE INVESTIGATED

1.5.1 Test Specimen Dimensions

Three different types of end connection details were investigated. Details of the connection are summarised in Figure 1-11. Firstly, two of the seating connection details use paperclip. Specimen 1 and 2 comprised of a 4 R-16 (Grade 500) paperclip, one paperclip in each of the four cells of the unit. The specimen consisted of a 300 mm deep hollowcore unit, HD12 (Grade 500) deformed starter bars and a ductile mesh centrally positioned in a 75 mm cast-in-placed topping. Specimen 2 differs from Specimen 1 in that it had additional seating of 70 mm as depicted in Figure 1-11(a) and (b). Finally, Specimen 3 represents a potential retrofit detail utilising a 150 x 150 x 12mm angle seat as a catcher as shown in Figure 1-11(c). This specimen consisted of a 20mm mortar pack seating, 300mm deep hollowcore unit, HD12 (Grade 500) deformed starter bars; a high strength mesh and a low friction bearing strip positioned on the angle seat. A cross section of the 300 series hollowcore unit used in each three of the connection details are shown Figure 1-11(d).

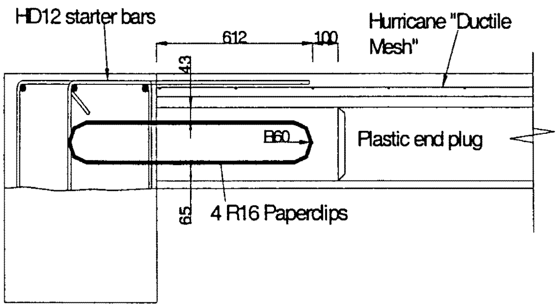

(a) Specimen 1 dimensions

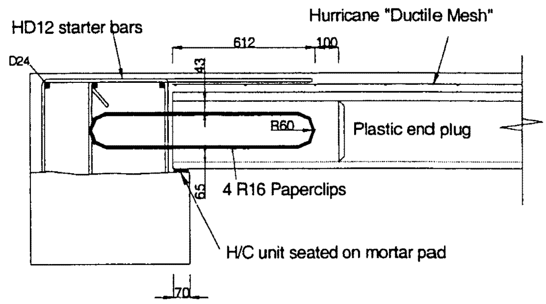

(b) Specimen 2 dimensions

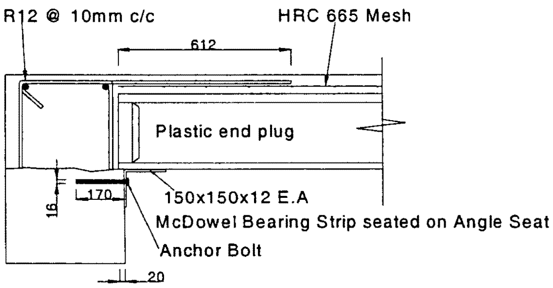

(c) Specimen 3 dimensions

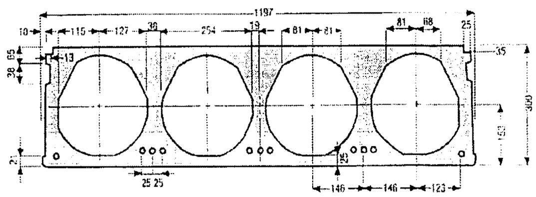

(d) Cross section of hollowcore unit

Figure 1-11 Dimensions of Test Specimens

1.5.2 Experiment Set-up

Figure 1-12 shows the layout of the experimental setup used to investigate the seismic performance of these hollowcore units end support connection detail. The setup of the experiment focused on the relative rotation between hollowcore end unit and the supporting beam as the damage initiating factor. The experimental setup consisted of a 6m length hollowcore unit; a supporting beam clamped down onto the ground and a computer controlled hydraulic actuator. To ensure shear force stimulate between specimen and prototype, a constant vertical load of 35 kN was applied at the mid-span of the hollowcore unit.

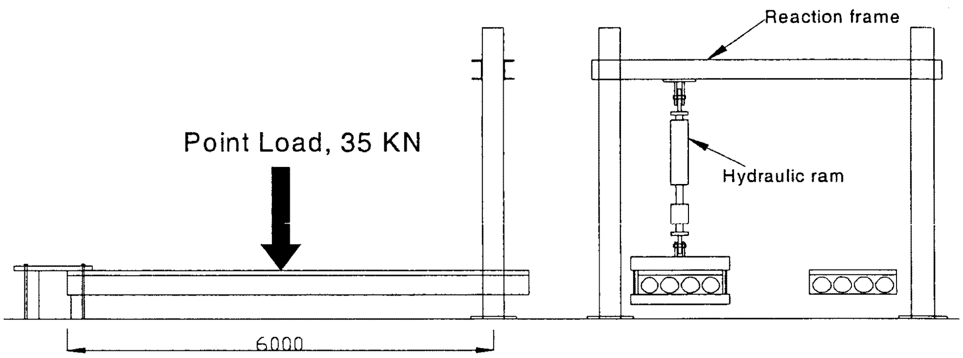

Figure 1-12 Layout of experimental setup

1.6 CONNECTION CAPACITY

Tie-bar connections for precast concrete floor units with their supporting elements should be designed and constructed to provide adequate strength, stiffness, and ductility to resist not only the gravity loads but also imposed movements, such as volume changes of structural members and elongation associated with plastic hinging of adjacent beams in a ductile frame.

To achieve a higher resistance to accidental loading and a higher endurance of damage, the structure should display a ductile behaviour. However, the behaviour of a precast concrete structure is to a great extent dependent on the properties of the structural connections. If the connections have high ductility and high energy absorption, large relative displacements can be reached without loss of structural integrity, whereby redistributions of forces are facilitated and it may be possible to achieve new alternative bearing paths if vital structural units are completely destroyed or out of function. It is of importance that the supporting function remains even if large relative displacements occur. Falling structural members inside the building may otherwise initiate a progressive collapse in the event of accidental or seismic loading.

One possibility often discussed is to utilise catenary action within the floor slab.

1.6.1 Kinking Mechanism of Paperclip

Special reinforcement for tie connections can be designed to prevent collapse as a result of loss of support of the precast floor units. The shear force carried by the kinking of reinforcement (Figure 1-13) can often be utilized by the designer. However the imposed movements cannot be catered for by the kinking of conventional top reinforcement in cast-in-place concrete topping slabs since normally the connection between the topping slab and the precast unit is inadequate to prevent concrete splitting.

Referring to Figure 1-13, the shear strength, V_n, of kinking mechanism can be expressed as,

$$V_n = A_s f_s \sin\alpha \tag{1-2}$$

Where A_s = area of reinforcement; f_s = stress in the reinforcement crossing the crack and α = Angle of the kinking crossing the crack. Centre for Advanced Engineering (CAE, 1999) recommended that the kinking angle, α, should not exceed 30° and that the stress in the bar crossing the crack can be taken as the yield strength of the reinforcement.

1.6.2 Predicted Elongation Capacity

At the ultimate limit state, the yield stress of the bar is exceeded and causing the bar to yield and consequently elongate. For a deformed bar, most of the elongation within the paperclips will be concentrated at the crack. However for plain round bars the friction between the bar and the surrounding concrete is significantly lower than that for that deformed bars. The elongation capacity of the paperclips tie reinforcement can be based on the length between the end anchors. FIP guidelines (1985) suggested that the ultimate elongation, δ_u, can be estimated by:

$$\delta_u = 0.8 L_a \varepsilon_u \qquad \textbf{(1-3)}$$

where L_a = the embedded length of the paperclips ties and ε_u = the steel strain at ultimate strength.

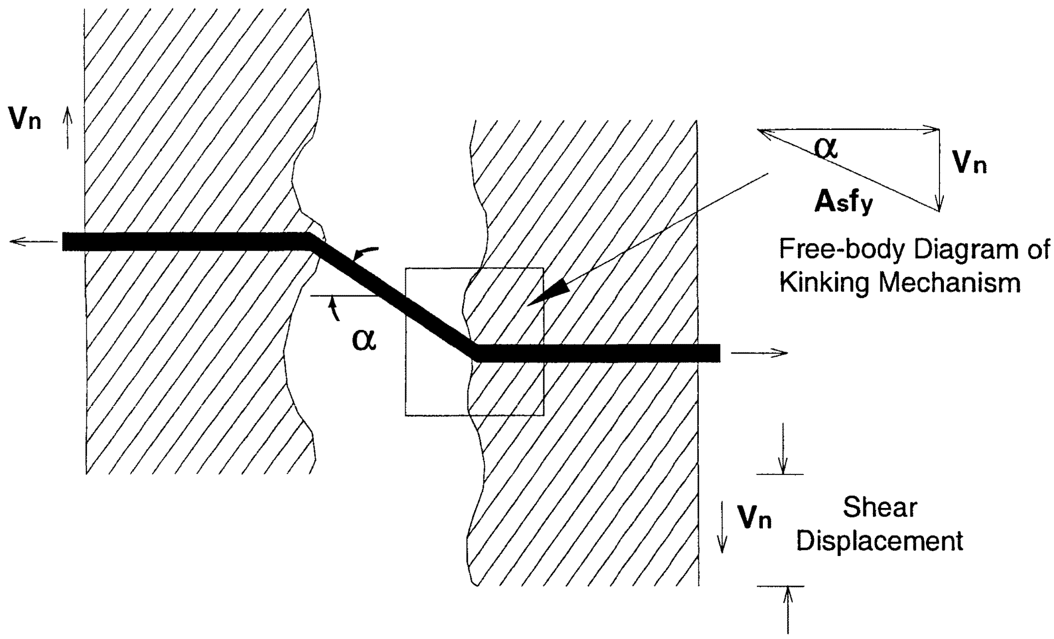

Figure 1-13 Shear Transfer across a Crack by Kinking of Reinforcement

1.7 WHAT IS PARTICULARLY NEW IN THIS THESIS?

The experiments described herein followed on work recently completed by Bull and Matthews (2003), Matthews (2004) and Lindsay (2004). It provides a valuable data and insight into the behaviour of the precast hollowcore floor units end support connection with various details. The connection details that are tested incorporate details that are used in existing structures and a potential retrofit solution.

Performing several of these component tests in the two dimensional format will allow a better understanding of the performance of many different seating connection details. Two-dimensional testing can be done in a relatively short space of time and Bull and Matthews (2003) has showed that the failure mechanism observed in these tests was seen similar to Matthews (2004). Full scale testing of large super-assemblages may give more insight into the overall performance of the seating connection details. However, such testing is time consuming and costly. On the other hand, component testing allows a database of results to be built, which in turn can be adopted for predicting the performance of other connection details.

1.8 REFERENCES

CAE, 1999, *Guidelines for the Use of Structural Precast Concrete in Buildings*, Centre for Advanced Engineering, Report of a Study Group of the New Zealand Concrete Society and the New Zealand Society for Earthquake Engineering.

FIP Recommendations, 1988, *Precast prestressed hollow core floors*, Thomas Telford London.

FIP Prefabrication Commission, 1994, *Planning and Design Handbook on Precast Building Structures*, SETO, London.

Herlihy M.D and Park, 2000, *Precast Concrete Floor Support and Diaphragm Action*, Research Report 2000-13, Department of Civil Engineering, University of Canterbury, Christchurch, New Zealand

Linsay R, 2004, *Experiments On The Seismic Performance of Hollow-core Floor Systems in Precast Concrete Buildings*, Master of Engineering Thesis, Department of Civil Engineering, University of Canterbury, Christchurch.

Matthews J.G, Bull D.K and Mander J.B, 2003, *Preliminary Results from the Testing of a Precast Hollowcore Floor Slab Building*, 2003 Pacific Conferences on Earthquake Engineering, February, Christchurch.

Matthews J.G, Bull D.K, Mander J.B, 2003, *Background to the Testing of a Precast Concrete Hollowcore Floor Slab Building*, 2003 Pacific Conferences on Earthquake Engineering, February, Christchurch.

Matthews J.G, 2004, *Hollow-core Floor Slab Performance Following a Severe Earthquake*, PhD Thesis, Department of Civil Engineering, University of Canterbury, Christchurch, New Zealand.

Matthews J.G, Bull D.K, 2003, *Proof of Concept Tests for Hollowcore Floor Unit Connections*, Precast NZ report, Feb.

Mejia-McMaster J.C and Park R., 1994, *Tests on Special Reinforcement for the End Support of Hollow-Core Slabs*, PCI Journal, Vol 39, No. 5, pp. 90-105, September-October.

Norton, J.A, King, A.B, Bull, D.K, Chapman, H.E, McVerry, G.H, Larkin, T.J, Spring, KC, 1994, *Northridge Earthquake Reconnaissance Report*, Bulletin of the New Zealand National Society for Earthquake Engineering Vol. 27, No.4, December.

NZS3101, 2003, *Draft Amendment No.3 to 1995 Standard (NZS 3101)*, Standards New Zealand, Wellington, New Zealand

NZS3101, 1995, *Concrete Structures Standard, NZS 3101, Part 1 & 2*, Standards New Zealand, Wellington, New Zealand

Oliver S. J and Restrepo J, 1998, *The Performance of Concrete Topped Precast Hollowcore Flooring Systems Reinforced With and Without Dramix Steel Fibres Under Simulated Seismic Loading*, Master of Engineering Thesis, Department of Civil Engineering, University of Canterbury, Christchurch, New Zealand.

Paulay T, Priestley, M.J.N, 1992, *Seismic Design of Reinforced Concrete and Masonry Buildings,* John Wiley and Sons, pp.767.

PCI, 1985, *Manual for the Design of Hollow-Core Slabs*, Prestressed Concrete Institute, Chicago.

PCI, 1985, *Design Handbook – Precast and Prestressed Concrete*, Prestressed Concrete Institute, Chicago, 3rd Edition

PCI, 1985, *Manual for Quality Control for Plants and Production of Precast and Prestressed Concrete*, Prestressed Concrete Institute, Chicago.

Section 2

Experimental Study of Hollowcore Support Details

SECTION SUMMARY

An experimental investigation on the cyclic load performance of three precast/prestressed hollowcore floor units is described. Specimen 1 had reinforced end cells with zero seating. Specimen 2 had a 70mm seat width along with heavily reinforced cells. The cells in Specimen 1 and 2 were reinforced with reinforcing bars bent to form a "paperclip" shape. Specimen 3 was constructed with seating details representative of 1980's and 90's detailing practise in which no reinforcement was used in the cells adjacent to the seats. However it was retrofitted with a supplementary seat in the form of an "angle catcher". Incipient failure occurred at 1.6% for Specimen 1 due to inadequate seating. Although loss of negative moment capacity occurred at a drift of -0.8% for Specimen 2 it was able to function without collapse at drifts of ±4%. Specimen 3 "broke its back" under negative moments at a drift of -1.5%, however the "catcher" was effective in sustaining positive moments up to +3% drift.

2.1 INTRODUCTION

Precast concrete buildings that use prestressed hollowcore floor units have been a dominant form of construction used in New Zealand over the past two decades. The popularity of precast concrete is essentially due to the benefits of reduced construction time frames, the high quality of factory made components, and overall cost reduction.

Due to collapses in the 1994 Northridge earthquake, some deficiencies in hollowcore flooring systems were exposed (Norton, 1994). Since precast construction in New Zealand has similar construction characteristics to the United States, it has considerably raised awareness regarding the potential lack of safety and reliability of hollowcore flooring units used in New Zealand's multi-storey moment resisting frame buildings. Following the hollowcore floor failures observed in the 1994 Northridge earthquake, several research efforts including experimental work has been conducted targeting detailing deficiencies. The purpose of this research is to provide a further understanding of the behaviour of hollowcore floor systems during a severe earthquake.

In particular, the research presented herein investigates life-safety and post-earthquake behaviour implications of hollowcore construction joint details utilised in present New Zealand practice. A potential retrofit detail is also examined to provide a possible solution to mitigate vulnerability of existing structures. This study first examines hollowcore performance in light of recent research findings, and then goes on to conduct an experimental investigation examining several hollowcore to seat details under reversed cyclic loadings.

2.2 Summary of Findings from Previous Research

Mejia-McMaster and Park (1994) examined a number of hollowcore support details involving longitudinal tie bar reinforcement. The tie-bar connections tested were designed to carry the precast floor unit in the event of failure of the support, or lateral movement of precast units off a supporting beam. Mejia-McMaster (1994) showed that all tested connection details were able to perform well under service load. Mejia-McMaster's test also illustrated that the FIP (1998) recommended tie-bar connection detail was able to behave in a ductile manner. This is largely due to the use of plain round reinforcement for the tie bars which enabled bond failure to propagate making large plastic elongations possible. Mejia-McMaster also noted that the Centre for Advanced Engineering (CAE, 1999) guidelines recommended that the tie-bar connection detail should not be used in structures subjected to large horizontal movement.

Herlihy et al (1995) investigated the performance of traditional hollowcore seat connection details used in New Zealand and particularly the "hair pin" end support detail. A "hair pin" is a U-shape bar (one-half of a "paperclip" where a paperclip is defined below) aligned longitudinally down the axis of a hollowcore. Herlihy et al (1995) concluded that the traditional starter bar detail does not provide sufficient composite bond strength to maintain a ductile tie connection between flooring units and support members when beam elongation occurs. Herlihy suggested that the "hair pin" connection detail generally performed adequately. However, there was still a general concern regarding the elongation capacity of this reinforcement subjected to large horizontal movements. Herlihy et al (1995) also suggested an alternate "paperclip" detail incorporating plain round bar which can be used to resist large horizontal movement during a earthquake.

Oliver (1998) examined more closely the use of the "paperclip" tie connection detail proposed by Herlihy et al (1995). The advantages of incorporating steel fibre reinforced concrete (SFRC) at the support detail was also investigated. Oliver (1998) concluded that deformed bars traditionally placed in topping slabs to transmit horizontal forces are not sufficient to resist the effect of beam-elongation that occurs in a ductile frame structure. Oliver (1998) also suggested that SFRC incorporated at the connection increased the tensile capacity of the concrete topping and hence was able to sustain a larger horizontal displacement at failure. However, Oliver (1998) concluded that "paperclip" tie-bar reinforcement is not suited for applications at the corner region of ductile reinforced concrete frames where the effects of beam elongation are most critical.

Matthews et al (2003) and Matthews (2004) investigated the performance of a beam-floor connection joint detail in a three dimensional manner. Matthews (2004) constructed a full scale (1:1) super-assemblage experiment on a one-storey slice from a precast concrete building as shown in Figure 2-1. The super-assemblage was loaded cyclically in both longitudinal (parallel to hollowcore units) and transverse directions. Testing of the full-scale super-assemblage created a boundary condition that would exist in real structures under seismic loading. This research also examined the beam elongation effect and its seating length requirements for hollowcore floor units. Matthews (2004) found that the expected seating performance of a floor unit moving relative to the beam it was seated on was different from the observed performance as summarised in Figure 2-2. In design, it is customary to assume that hollowcore units would slide relative to the beam; this was not observed in the super assemblage experiment. There was sufficient bond/friction to cause the end of the unit to fracture rather than slide. Moreover, Matthews (2004) also showed that the failure mode of the hollowcore floor units was similar to that observed in a building that collapsed in the 1994 Northridge earthquake.

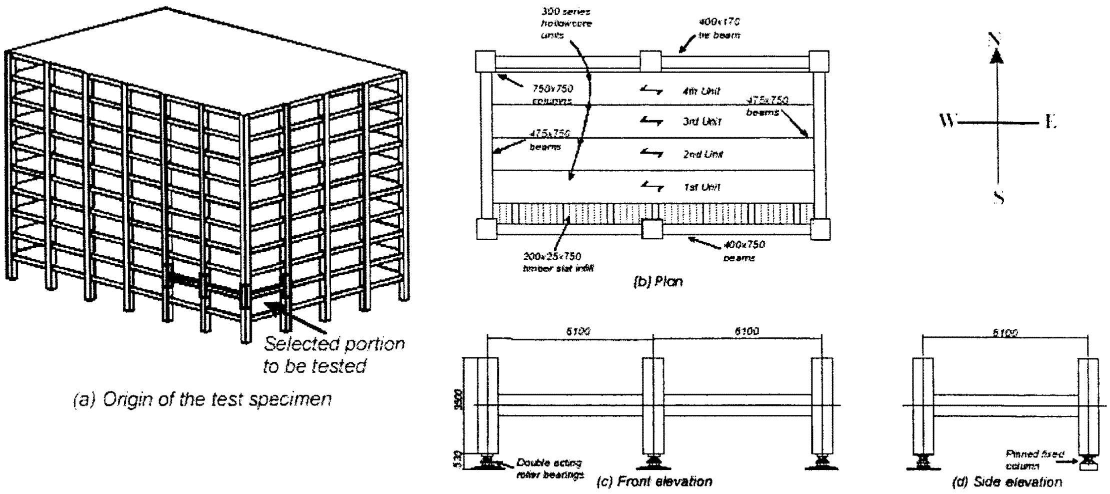

Figure 2-1 Layout and dimensions of the super-assembly (Matthews, 2004)

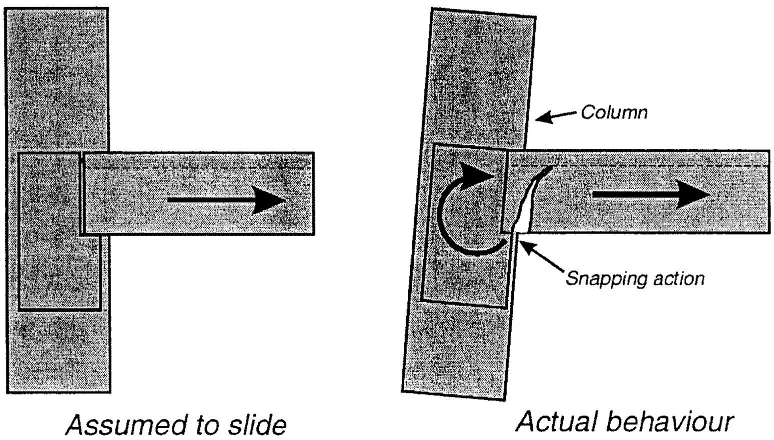

Figure 2-2 Assumed versus observed hollowcore to support beam performance (Matthews, 2004)

Bull and Matthews (2003) conducted a series of hollowcore-to-beam seat connection experiments to investigate the seismic performance and crack pattern formation. Figure 2-3 summarises connection details tested by Bull and Matthews (2003). In the past studies (Mejia-McMaster and Park 1994; Herlihy et al 1995; and Oliver 1998), connection testing had been conducted by a longitudinal pull and push of the units sliding back and forth on their seats. However, Bull and Matthews (2003) have shown that the assumed failure mechanism that was tested in the earlier work was incorrect by virtue of the effects of rotation of the supporting beam. They show that the bond between hollowcore unit and the beam seat is sufficient to cause fracture at the end support rather than sliding. Therefore, a cyclic rotation effect was induced in this study at the support. This rotation mimics the rotation that developed in moment resisting sway frames. Matthews (2004) showed that inter-storey drifts up to 3.5% can be expected in an earthquake.

Bull and Matthews (2003) demonstrated that the traditional connection detail gave a similar floor crack pattern as that found in Matthews (2004) super-assemblage experiment. Matthews (2004) also suggested that both the compressible backboard solution and the "paperclip" detail provide satisfactory performance. These details performed better than the traditional connection detail examined in Matthews (2004) super-assemblage experiment. Furthermore, Bull and Matthews (2003) also showed that the compressible backing board solution performed better than the "paperclip" detail. Following Matthews initial findings, in 2002 a "Technical Advisory Group" (TAG) was formed. New research was conducted by Bull and Matthews (2003) sponsored by Precast NZ. The TAG endorsed their findings. Subsequently recommendations were added to the Concrete Design Standard (NZS3101, 1995) by way of an official amendment in the form of two prescriptive "acceptable solutions" to thc Standard (see NZS3101, 2004).

Lindsay (2004) and Lindsay et al (2004) followed on from experimental work conducted by Matthews (2004). In contrast to Matthews (2004) who investigated past construction techniques (1985-2000) and the resulting problems with seismic performance, Lindsay (2004) looked toward developing details for improved performance for future precast concrete construction practice. Lindsay (2004) repaired and reconstructed Matthews (2004) full-scale super-assemblage specimen and then retested it. Modifications were made to improve the performance of the hollowcore floor system in both the lateral and end seating details as well as more adequately tying the central column into the floor system. As shown in Figure 2-3(b), Lindsay (2004) employed the beam to floor connection detail using a low-friction bearing strip with a compressible backing replacing the plastic bungs in the end of the units. There were some performance problems with the low-friction bearing strips used. They were observed to slide in Lindsay's experiment. Thus Lindsay (2004) concluded that a second generation bearing strip with bigger teeth or bonding the underside of the bearing be specified in future construction. The backing board did not compress significantly during the experiment, hence only a bond breaker may be necessary at the end of the units as compression at the bottom of the floor seating is not observed after the first cycle of displacement.

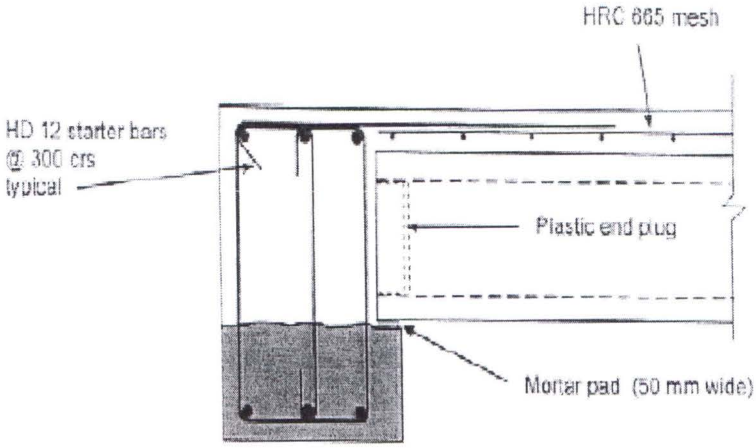

(a) Control Specimen (200 and 300 series)

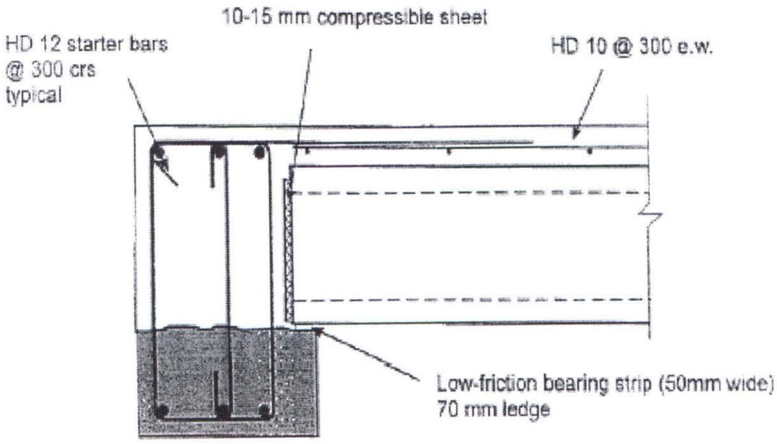

(b) Flexible seating detail

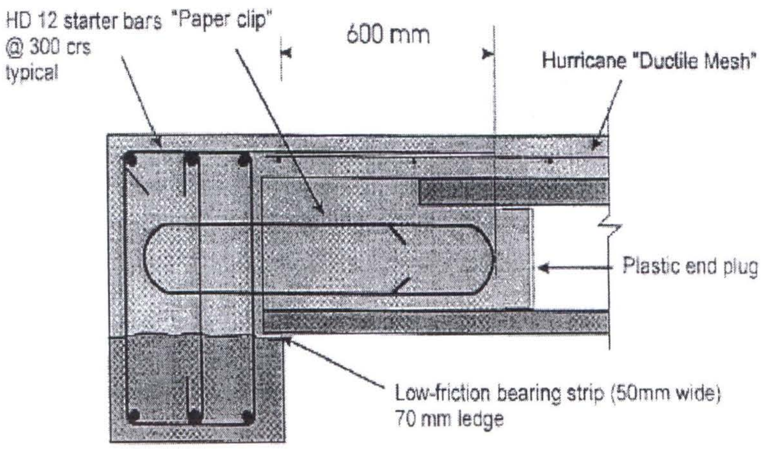

(c) Paperclip seating detail recommended by TAG

Figure 2-3 Seating detail tested by Bull and Matthews (2003)

Much progress has been made since commencement of Bull and Matthews (2003), Matthews (2004), Lindsay (2004) research. However, the work on precast floor systems in reinforced moment resisting frames is still in its infancy. Several key questions remain, including: (i) What is the affect of negative seating (precast unit being cut short and placed with a bridging connection)? (ii) What reliable retrofit solution can be applied to existing buildings with the inferior connection details demonstrated in Matthews (2004) research? (iii) How well will the paperclip seating detail (recommended by TAG) perform? (iv) What is the affect of over-reinforcing a connection? (v) What is the vulnerability of other major precast floor types (e.g. double Tees etc) to earthquake damage?

The research described in what follows attempts to address question (i) to (iv) above.

2.3 THE TEST SPECIMENS

Specimen construction details, summarised in Figure 2-4, are described in the following subsection. Some additional details of the specimens are also given in Appendix A.

2.3.1 Specimen 1: Paperclip Detail with Zero Seating

It is not uncommon for hollowcore units to arrive at the job site cut to a shorter length than specified. Rather than rejecting the units as unsatisfactory, they are often still used, one end is seated while the other end is propped and reinforced cells used to strengthen the connection. A popular connection used in such circumstances is the "paperclip" detail. This connection detail tested herein consisted of 4-R16 (Grade 500) paperclips; one paperclip in each of the four cells of the unit as shown in Figure 2-4(a). The specimen was a 6m long half-unit consisting of a 300 mm deep hollowcore unit. Starter bars from the support beam consisted of HD12 (Grade 500) rebars. A ductile mesh was centrally positioned in the 75 mm cast-in-placed topping.

2.3.2 Specimen 2: Paperclip Detail with 70 mm Seating

Specimen 2 is representative of a hollowcore unit with normal end seats. It had a similar connection detail to Specimen 1 but with an additional seating of 70 mm as shown in Figure 2-4(b). As before, HD12 (Grade 500) starter bars were used along with in the topping slab. With the unit seated on a mortar bed, a small amount of friction or bond was induced at the bottom of the unit within the seating. The purpose of this connection was to consider what difference is made when a positive seat is provided.

2.3.3 Specimen 3: Retrofit Detail

Matthews (2004) super-assemblage experiment and subsequent analysis openly questioned the overall safety of existing buildings with hollowcore floor systems. Some skeptics may contend that his experiment, which used 300 series hollowcore, was not representative of the overall building stock in New Zealand. However, when Precast NZ sponsored component tests were conducted by Bull and Matthews (2003), similar findings were revealed between the 200 and 300 series units – both performed poorly. The purpose of Specimen 3 was to investigate potential retrofit solutions by improving the seat details of existing hollowcore units. Figure 2-4(c) presents the retrofit detail. A normal hollowcore seat was constructed on a mortar bed and retrofitted. A 150 x 150 x 12 mm angle seat was positioned at the soffit of the hollowcore unit, as shown in Figure 2-5, and bolted to the side of the support beam. Views from beneath the specimen and side are shown in Figure 2-5(c) and (d), respectively.

The purpose of the angle seat is to act as a "catcher" in the event of expected end shear failure as shown in Figure 2-5(a). Thus Specimen 3 used a traditional connection detail which consisted of 50 mm seating, HD-12 (Grade 500) starter bars and high strength mesh. Figure 2-5(b) shows a bearing strip beneath the hollowcore unit attached to the angle seat. This detail has two functions. First, it is used to reduce the friction between the hollowcore floor and the angle seat. Secondly the bearing strip exerts a compression force into the bottom strand away from the end of the unit, thereby enhancing the anchorage/bond of the strand, consequently leading to improved shear capacity of the unit.

2.3.4 Material Properties

The reinforcing steel used had measured yield strengths of 302 MPa for the beam longitudinal bar and 563 MPa for the starter bars, respectively. Ready mixed concrete had a specified strength of 30 MPa with 19mm aggregate and slump of 100 mm. At the time of testing, cylinder strengths of 33 MPa and 40 MPa were measured for the beam and floor topping, respectively. The stress-strain plots for the reinforcing bars, paperclip and the compressive strength test results for the concrete are given in Appendix A.

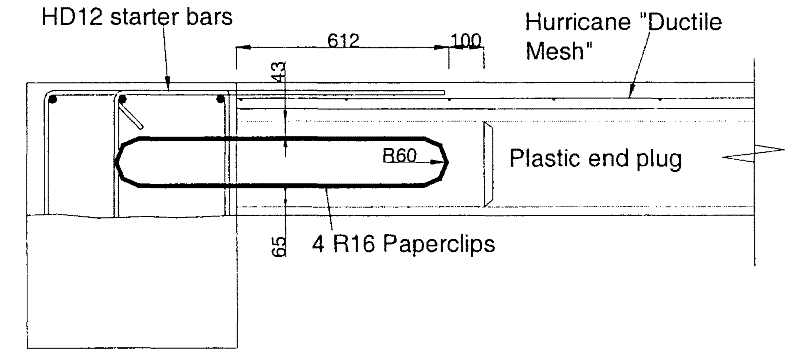

(a) Specimen 1: Paperclip detail with zero Seating

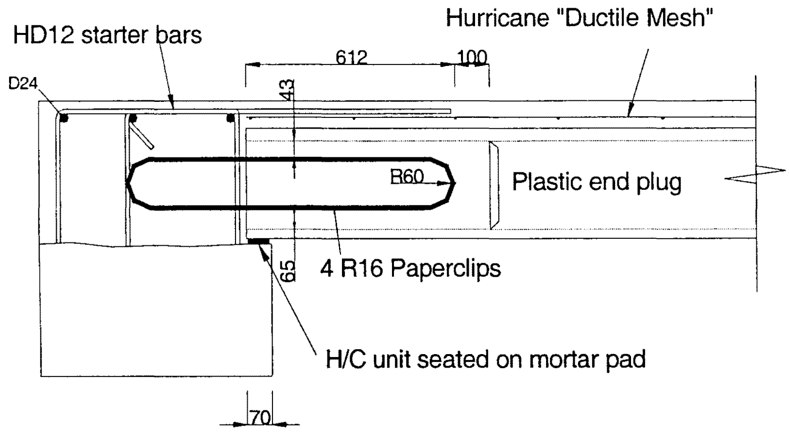

(b) Specimen 2: Paperclip detail with 70mm seating

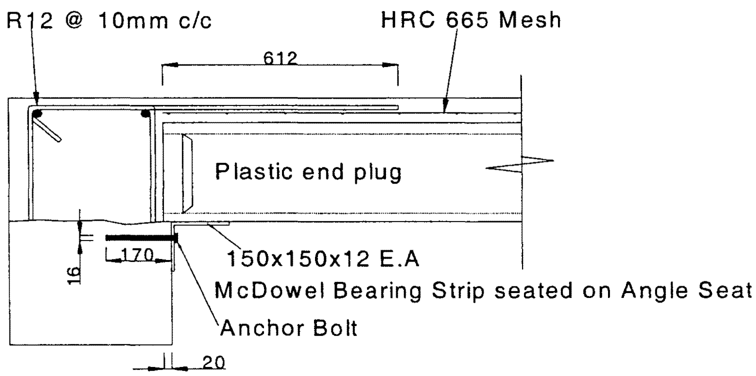

(c) Specimen 3: Retrofit of a grouted seat

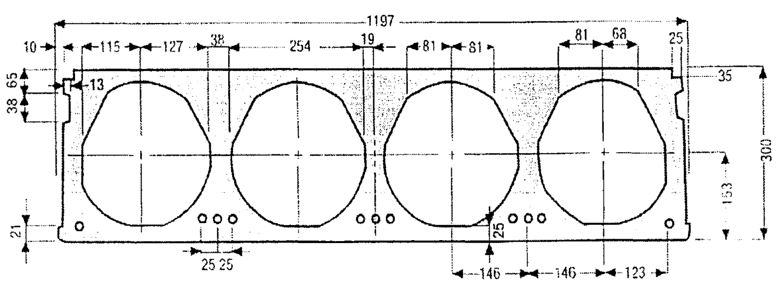

(d) Cross section of hollowcore unit

Figure 2-4 Test specimens and their dimensions

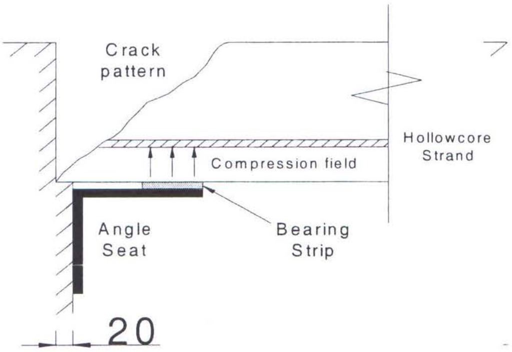

(a) Benefit of using a longer angle seat

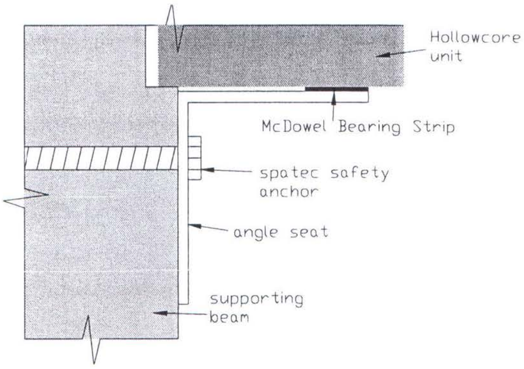

(b) Bearing strip position on angle seat

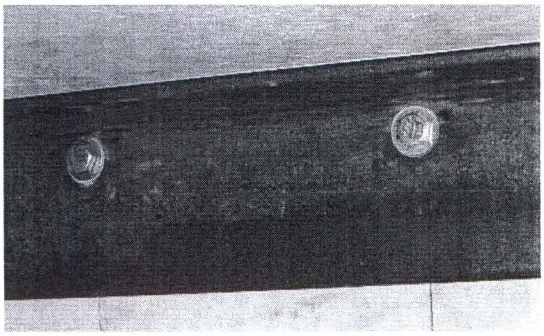

(c) Plain view of the angle seat

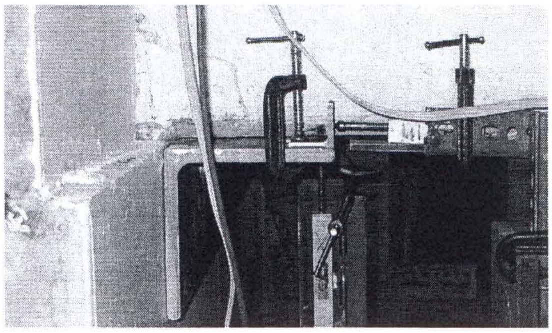

(d) Elevation view of the angle seat

Figure 2-5 Retrofit details applied to Specimen 3

2.3.5 Construction of the Test Specimens

The construction process for each of the three test specimen was carried out in two phases aimed at emulating site conditions. The initial phase consisted of casting the supporting beam while the second phase dealt with positioning the hollowcore unit on the beam, placing the reinforcing steel and finally pouring the 75mm topping concrete. For the support beam, half-depth formwork was made, the reinforcing cage placed and 30 MPa concrete poured and cured for 28 days. With the exception of Specimen 1, the units were then positioned on the beam seat on a dry pack mortar bed to ensure the floor units sit on an even surface to avoid high stress concentrations.

The top flanges of the hollowcore voids, 75mm wide and 700mm long, were then cut to make way for the "paperclip" reinforcement that was inserted into each cell of

Specimen 1 and 2. Finally, mesh and starter bars were placed and the 75 mm topping slab was poured. The angle seat retrofit was bolted onto Specimen 3 after all concrete had cured.

2.3.6 Instrumentation

Figure 2-6 presents the instrumentation used in the connection region for each of the hollowcore units. This consisted of a series of linear potentiometers used to measure the starter bar strains and the strain transfer to the concrete topping. Relative movement and rotation of the beam to the ground and floor was also measured. Strains within two of the four paperclips were monitored via six strain gauges that affixed to each of the paperclip bars. The strain gauges were spaced 200 mm apart.

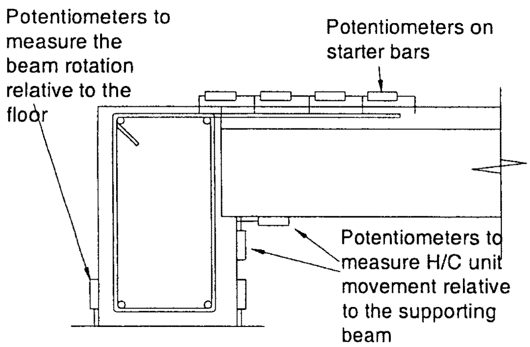

(a) Location of potentiometers attached on the test specimens

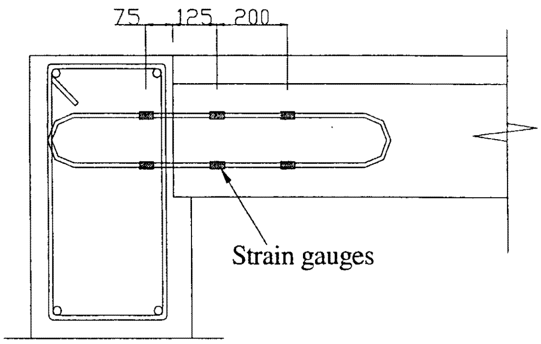

(b) Location of all the strain gauges on the "paperclips"

Figure 2-6 Specimen Instrumentation in the connection region

2.4 TEST APPARATUS AND LOADING

The testing of these connection details was designed and carried out in a two dimensional sub-assembly component format. Full scale three-dimensional effects such as the net tension in slab beam connection, plastic hinge formation in the beam which the hollowcore unit is seated, etc was ignored. The experimental set up used for testing the connection detail was required to satisfy several criteria so that the applied loading matched the in-situ performance as close as possible. The most essential criterion was to induce a rotation effect between the hollowcore floor unit and the supporting beam.

The experimental setup of this research was based on the procedures developed by Bull and Matthews (2003) and shown schematically in Figure 2-7(a). The specimens were loaded cantilevers, 6m in length from their seat to the load point. Vertical loading was applied onto the floor unit to match the shear force at the connection for prototype 12m long span floor units. Further design details are shown in the Appendix A.

The experimental setup used to test each specimen is presented in Figure 2-7(b). The adapted setup was similar to that adopted by Bull and Matthews (2003). Over the free end of the cantilever a steel reaction frame was used to hang a computer controlled hydraulic actuator. The reaction frame, both column and beam, was made up of two 300 mm channels and bolted to the laboratory strong floor. Instead of rotating the beam to create the rotation effect, the supporting beams were securely clamped down to the strong floor and at the free-end of the hollowcore cyclic vertical load were applied in displacement control to mimic beam to floor rotations or inter-storey drifts. To ensure shear force similitude between specimen and prototype, a 100 kN capacity hydraulic jack with an in-line pressure relief valve was used to apply a constant 35 kN vertical load.

The displacement history used was in keeping with the traditional ductility based loading protocol described by Park (1989). Each of the three test specimens was loaded cyclically in the same manner. The displacement controlled history consisted of two completely reversed load cycles equivalent to inter-storey drift amplitudes of ±0.1%, ±0.5%, ±1%, ±2%, ±3% and ±4%. Note that in this research equivalent inter-storey drifts equate to the relative rotation between the hollowcore unit and the supporting beam. A positive drift results in tension on the bottom of the hollowcore unit, while a negative drift results in tension on the top of the hollowcore unit. Similarly, positive and negative drifts respectively induce positive and negative moments in the support beam connection.

It should be noted that upon the completion of the data analysis the target drifts from ±0.5% to ±4.0% were not always achieved during the testing programme. This was due to flexibility in the support beam. A correction has been applied to remove this effect. The true inter-storey drift is obtained by subtracting the measured supporting beam rotation from the target drift. Table A-4 in Appendix gives a summary of the target drifts versus the actual drifts for all the tests undertaken. Herein, the North side will be referred to as the left hand side of the test specimen and the South side as the right hand side.

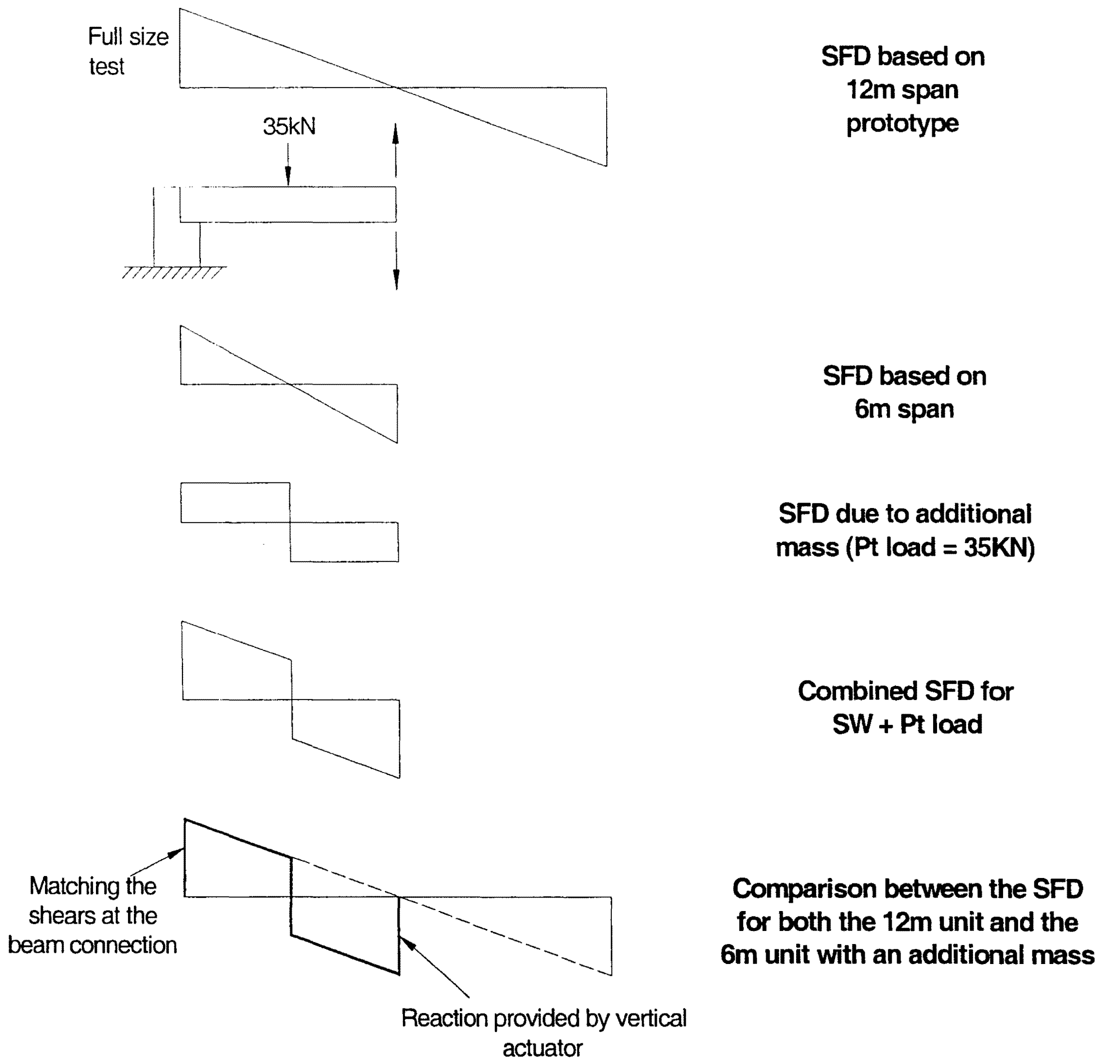

(a) Schematic showing the determination of experimental setup

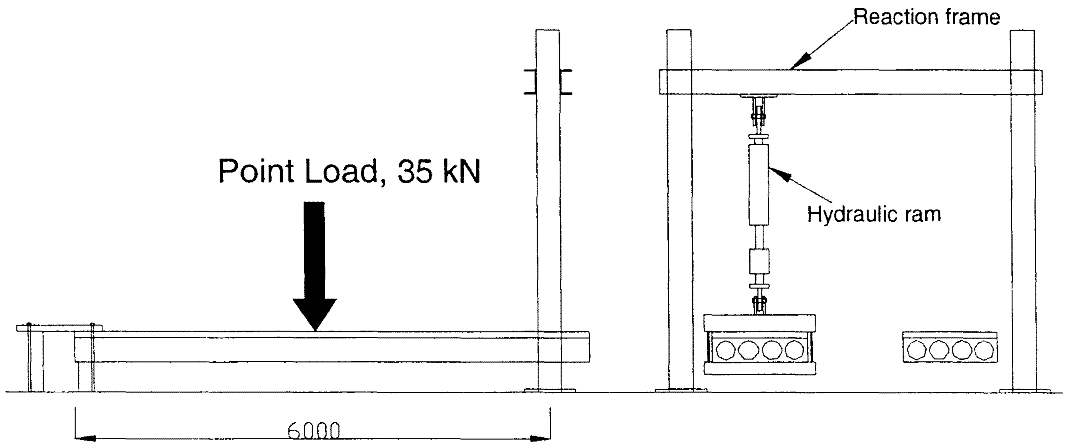

(b) Elevation view of experimental setup

Figure 2-7 Layout of experimental setup

2.5 EXPERIMENTAL RESULTS: VISUAL OBSERVATIONS

Figure 2-8 presents some key photographs of the behaviour observed during the cyclic loading experiments. Details on each unit are described in what follows.

2.5.1 Specimen 1

Hairline cracks of 0.5mm first appeared at the connection interface and concrete topping ±0.5% drift. Figure 2-8a(i) shows a 2 mm shear crack developed at 800mm away from the beam face, at -1.0% drift. This shear crack located just outside the end zone of the starter bars and the 4-R16 paperclip. Significant stiffening of the joint resulted to the high amount of steel (paperclip) reinforcement at the beam precast floor to seat. This caused a shear crack to form where major strength discontinuity occurred, rather than near the beam face. At 1.75% drift, the hollowcore unit dropped 20mm as shown in Figure 2-8a(ii). A wide horizontal split can be observed at the web of the hollowcore unit and this diagonal crack has extended from the outside region of the starter bars down toward the bottom of the unit end support. The connection integrity deteriorated and the floor dropped further as testing continued. Shortly after the horizontal split occurred, at 2.0% drift the unit failed completely and separated from the topping. Ductile mesh within the topping did not fail throughout the experiment. Figure 2-8a(iii) shows the hollowcore unit has broken off from the supporting beam at the end of the experiment of 2.0% drift.

2.5.2 Specimen 2

Small cracks first appeared in the early stage of the experiment at ±0.5% drift. At 1.0% drift, some spalling of beam concrete cover was found. Similar to Specimen 1, a major shear crack developed at the end zone of the starter bar region at a drift of -1.0%. Figure 2-8b(i) clearly shows that the shear crack (1.9 mm at this stage at topping surface – opening up to 8 mm and 6 mm at -2.0% and -3.0%, respectively) extended from the concrete topping and split into two near the bottom of the unit. The vertical drop of the floor for Specimen 2 was measured as 0.7mm, 2.5 mm and 20 mm at drift of 2.0%, -2.0% and -3.0%, respectively. At a drift of -3.0%, the ductile mesh of the specimen fractured. Finally at ±4.0%, the hollowcore unit separated from supporting beam and collapsed. Figure 2-8b(ii) shows the bottom strand of the hollowcore unit can be spotted through the cracks at 4.0% drift. Figure 2-8b(iii) presents the status of the hollowcore unit at the end of the experiment of Specimen 2. The bottom of the hollowcore unit ruptured and remained hanging by the hollowcore strand.

2.5.3 Specimen 3

At ±0.5% and ±1.0% drift, hairline cracks formed and propagated near the interface between the supporting beam and the hollowcore unit. At -2.0% drift, shear cracks developed at the end zone of the starter bar (700mm from the beam face). This crack was due to the angle seat, situated tightly against the hollowcore unit, restraining the rotation of the hollowcore unit at the end support. The effect of the angle seat was to move the hinge away from the end of the precast unit. However, as a result of greater negative moments the high strength mesh fractured. The hollowcore unit also measured a drop of 4mm and 17mm at the second cycles at drift amplitude of -2.0% and -3.0% drift, respectively. Figure 2-8c(i) shows the bearing strip which slipped outward during the experiment. Figure 2-8c(ii) shows the behaviour of the hollowcore unit at the end of the experiment at ±3.0% drift. This specimen, which used a traditional connection detail, formed a different crack pattern compared to the control detail (300 series) tested by Bull and Matthews (2003). The 150 x 150 x 12mm angle seat successfully served its purpose as a "catcher". However, the angle seat did not prevent the hollowcore unit failure due to an excessive negative moment demand in the vicinity of the end of the top starter bars, as shown in Figure 2-8c(iii).

2.6 INSTRUMENTAL OBSERVATIONS FROM EXPERIMENTS

2.6.1 Specimen 1

Figure 2-9 presents all the basic experimental results for Specimen 1 that was derived from the instrumentation. From the overall cyclic loading hysteretic performance for presented in Figure 2-9(a) it may be observed that a maximum positive shear capacity of 30.2 kN and a maximum negative shear capacity of -12.12 kN were recorded. The plot also clearly shows the instants where failure of the connection was induced as indicated by sudden drops in load during the experiment. These events occurred at the formation of the shear crack and the dropping of hollowcore unit respective drifts of -1.0% and +1.75%.

Figure 2-9 (b) presents the northern starter bar strain distribution plotted at both positive and negative drift amplitude peaks. Evidently the starter bar remained in the elastic range most of the time and it only yielded at the negative drift at the connection interface where most of the continuity cracks concentrated.

Figure 2-9 (c) presents the northern paperclip strain distribution in both drift direction. The paperclip did not yield during the experiment; in fact it appears to have done little work. This is because once the shear crack formed, most of the deformation concentrated on the diagonal crack plane. It should be noted that both top and bottom paperclip strain registered tensile strains throughout the experiment under both positive and negative (moments) drift.

2.6.2 Specimen 2

Figure 2-10 presents all the basic experimental results for Specimen 2 that was derived from the instrumentation. Figure 2-10 (a) presents the performance of Specimen 2 under cyclic loading. Specimen 2 reached a maximum positive shear capacity of 38.5 kN at 2.0% drift and a maximum negative shear capacity of -11.21 kN at -1.0% drift where a shear crack formed. The stiffness of the connection deteriorated with increasing drift amplitude and cycling.

Figure 2-10 (b) shows the northern starter bar strain profile in the positive and negative drift direction showing that the majority of the strains were concentrated at the beam to floor interface and at the end of the starter bars concrete topping. The starter bars remained in the elastic range throughout the experiment. After shear crack formed, the starter bars evidently carried little loads.

Figure 2-10 (c) shows the northern paperclip strain distribution of Specimen 2. The paperclip did not appear to yield at any stage during the experiment and remained in tension throughout testing. Similar to Specimen 1, after a diagonal plane shear crack formed in the hollowcore, the paperclip did not take any additional load.

2.6.3 Specimen 3

Figure 2-11 presents all the basic experimental results for Specimen 3 that was derived from the instrumentation. The shape of this hysteresis plot, Figure 2-11 (a), was different from the two above mentioned experiments. Initially, up to the completion of the ±0.5% drift the behaviour appeared looked to be essentially elastic. Specimen 3 reached a shear force of 11.5 kN at the second cycle of 1.0% drift and the cracks at the beam-floor connection joint interface were seen to extend to 3mm. On the way to the first cycle of drift amplitude of -2.0%, the high strength mesh was observed to fracture and a shear crack formed at the end zone of the starter bars. At the instance the first mesh fracture, the strength capacity of Specimen 3 dropped suddenly from -13.4 kN to -11.7 kN. All the mesh within the concrete topping then fractured during the second cycle to -2.0% and the strength dropped to -2.15 kN. Note that when the diagonal shear crack formed and the mesh first fractured, the stiffness of Specimen 3 deteriorated rapidly.

Figure 2-11 (b) presents the northern and southern starter bar strain distribution of Specimen 3 at the peaks of the positive and negative drift amplitudes. Instrument failure and the preservation of instrumentation prevented a complete set of results to be shown. The results shows that a majority of the strain induced in this region occurred in two places. Firstly, due to lack of continuity, cracks occurred in the topping concrete above the end of the hollowcore unit. The second region was in the topping concrete at the end of the starter bars. Cracking at both locations results from stress concentrations at locations of strength discontinuity.

(i) Shear crack at -1.0% **(ii) Unit dropped at 1.75%** **(iii) Connection at failure**

(a) Observed damage to Specimen 1

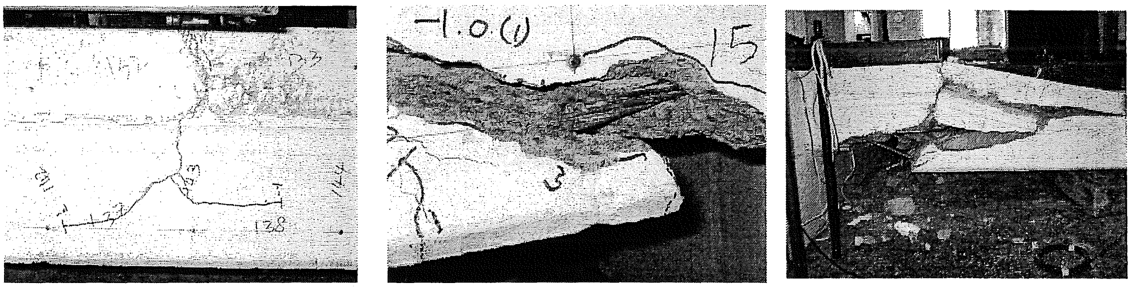

(i) Shear crack at -1.0% **(ii) Strand seen at 4.0%** **(iii) Connection at failure**

(b) Observed damage to Specimen 2

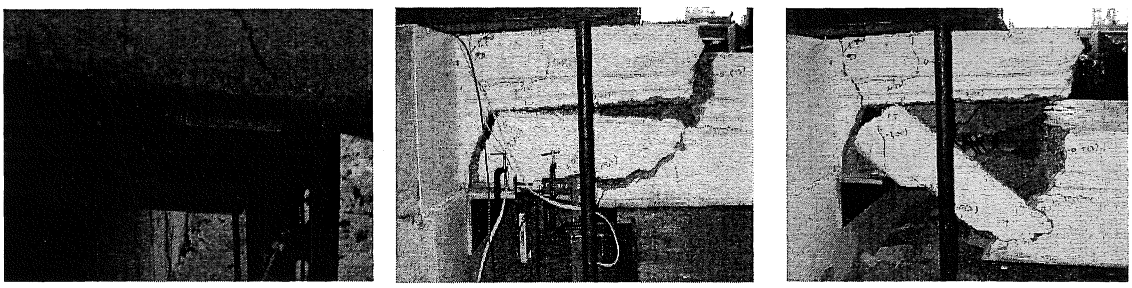

(i) Bearing strip slipped **(ii) Floor unit at -3.0%** **(iii) Floor unit at failure**

(c) Observed damage to Specimen 3

Figure 2-8 Photographs of damage observed during the experiments

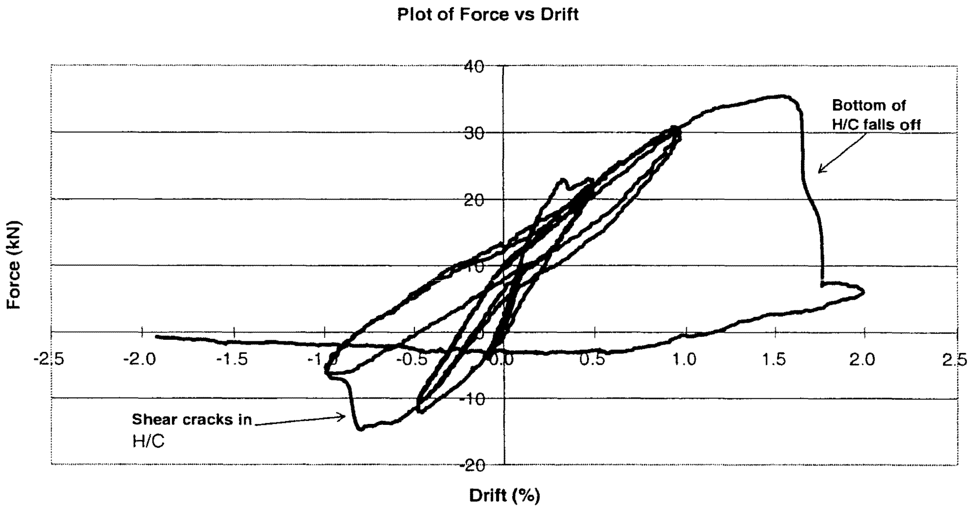

(a) Hysteresis performance of Specimen 1

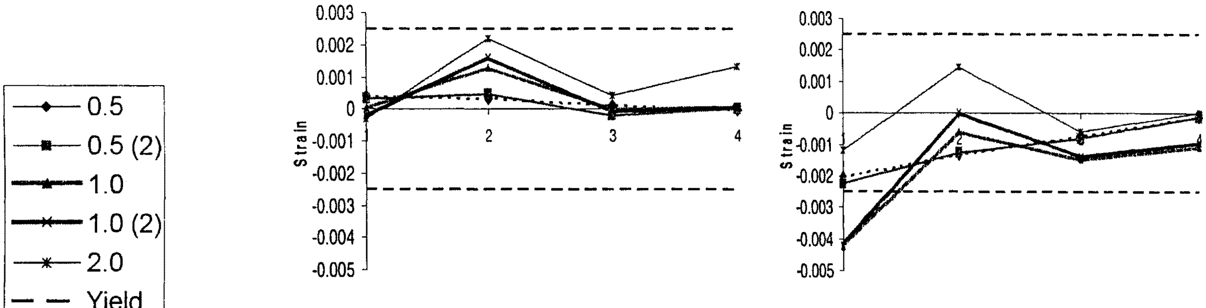

(i) Positive drift **(ii) Negative drift**

(b) Northern starter bar strains

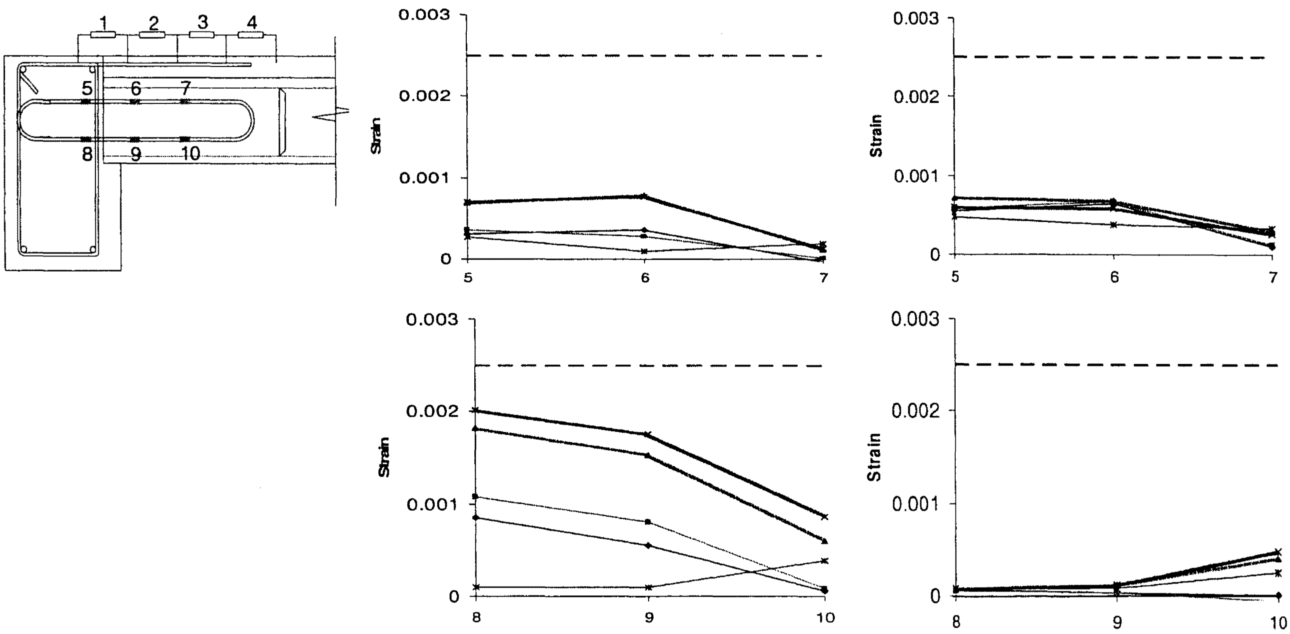

(i) Positive drift direction **(ii) Negative drift direction**

Instrumental Layout **(c) Northern paperclip strains**

Figure 2-9 Experimental Results for Specimen 1: Zero seating

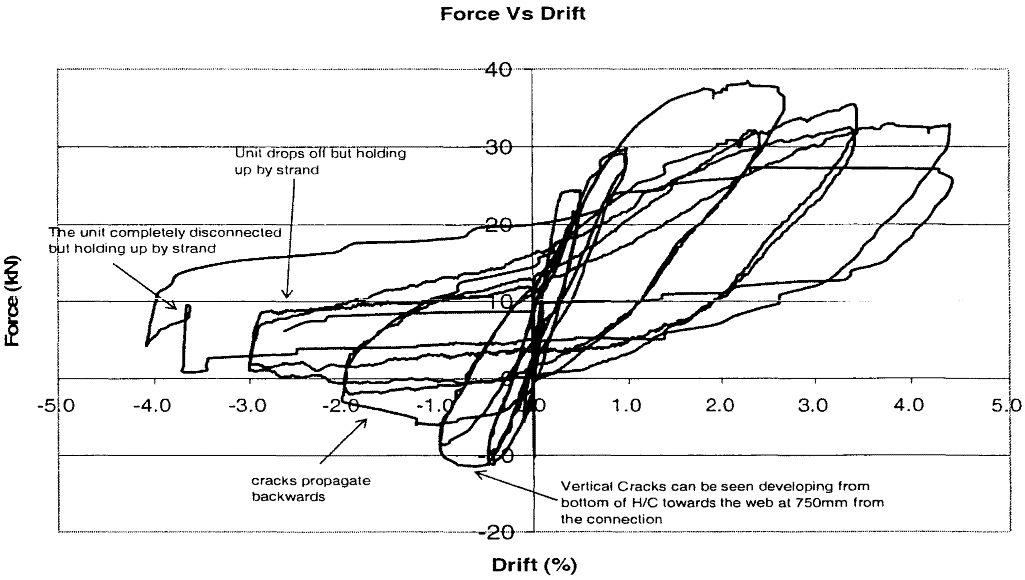

(a) Hysteresis performance of Specimen 2

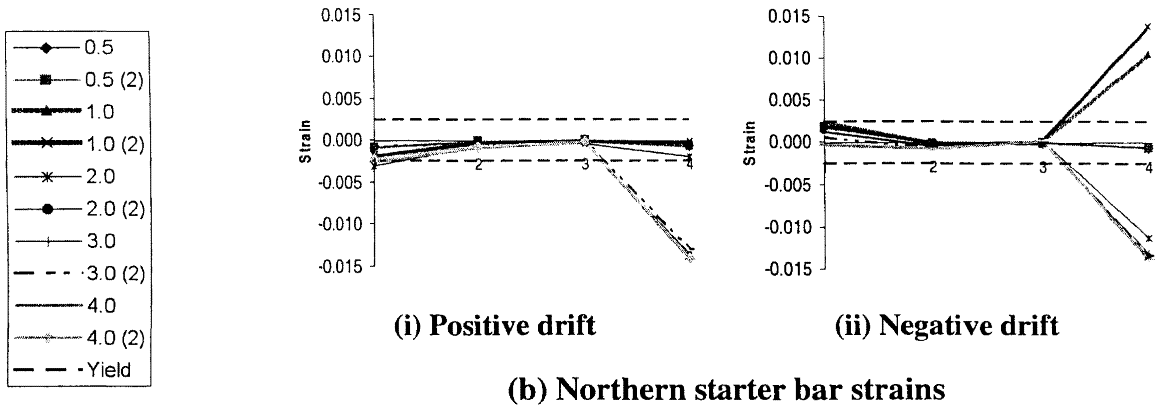

(i) Positive drift

(ii) Negative drift

(b) Northern starter bar strains

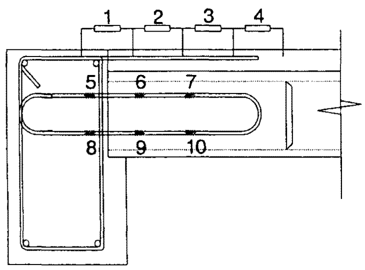

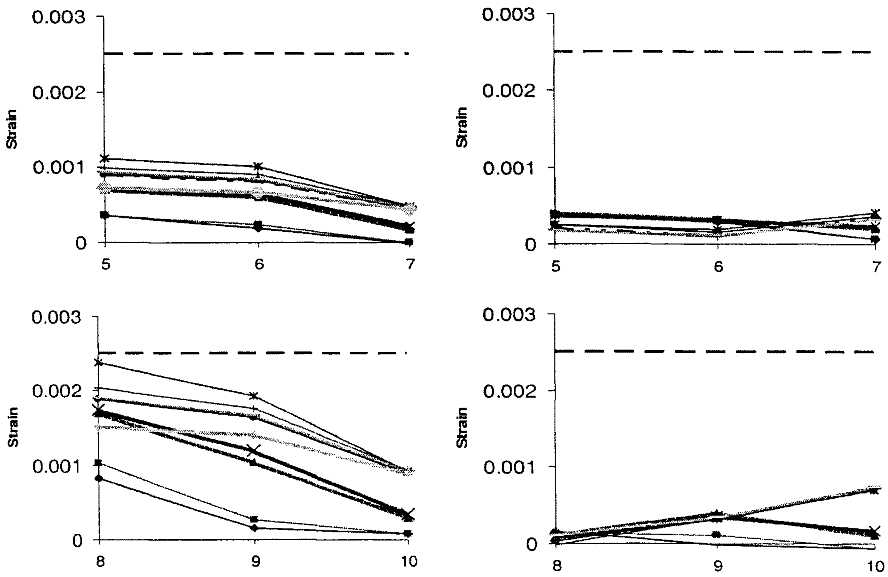

(i) Positive drift direction

(ii) Negative drift direction

Instrumental Layout

(c) Northern paperclip strains

Figure 2-10 Experimental Results for Specimen 2 (70mm seating)

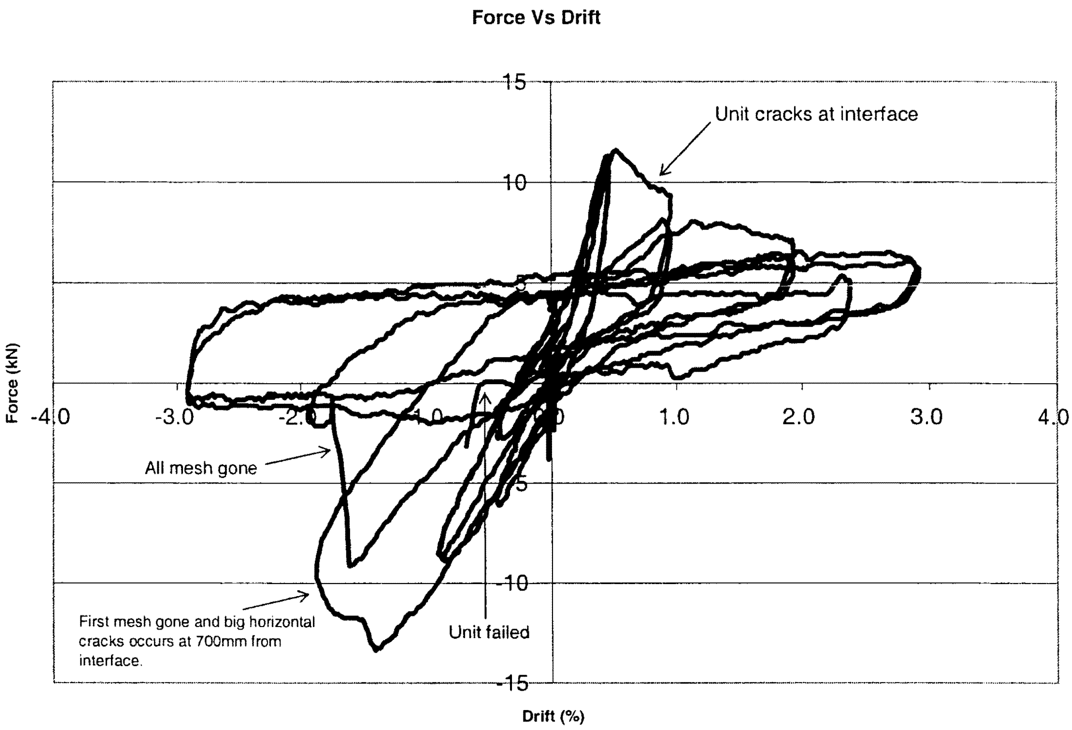

(b) Hysteresis performance of Specimen 3

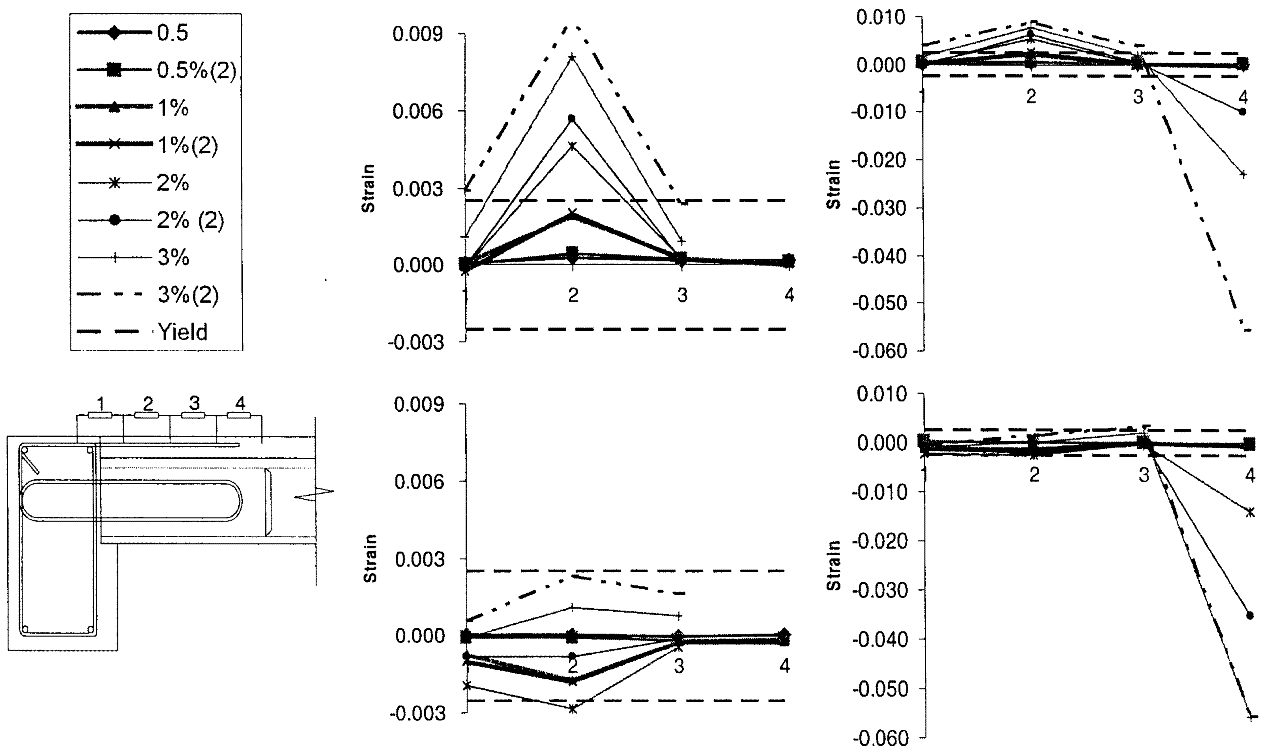

Instrumental Layout **(i) Northern Starter Bar** **(ii) Southern Starter Bar**

(b) Starter Bar strains profile

Figure 2-11 Experimental result of Specimen 3: Retrofit seating detail

2.7 COMPARISON OF RESULTS

Figure 2-12 compares the end moment-rotation hysteretic performance of Specimen 1 and 2. It is evident that the hysteresis plots are somewhat similar up to drifts of about 1%; both tests indicate about the same peak magnitude in the positive and negative directions of loading. While Specimen 2 survived the entire cyclic loading regime up to and including 4% drift, Specimen 1 failed at 2% drift. The reason Specimen 2 performed better is because the 70mm seat provided supported the hollowcore unit better accommodated the damage inflicted by the end rotations. Nevertheless, shear cracks developed in both specimens. Such cracking is not a particularly positive outcome and future research needs to address the detrimental effect.

Figure 2-13 presents the overall end moment-rotation curve for Specimen 3 and Bull and Matthews (2003) control specimen. Figure 2-13 shows that the "catcher" in Specimen 3 has significantly improved the connection joint performances under positive moments when compare with Bull and Matthews (2003). The paperclip specimen gives a stiffer connection detail than the retrofit detail which utilised a traditional connection detail used in New Zealand practise. Comparing Figure 2-12 and 2-13(b), it can be concluded that the paperclip has significantly improved the seating connection performance under positive drift amplitude. Specimen 3 has out-performed Specimen 1, where incipient failure occurred at 1.6% drift amplitude. This has further emphasised the necessity of a seating availability in a connection detail. All three test specimens show the formation of shear cracks at the end of the starter bars—it is clearly evident that this can be mitigated by preferably removing the lap splice and placing continuous decking reinforcement in the reinforced concrete topping, or at least continuing the lap well beyond any negative moment region.

Figure 2-14 shows the effect of steel quantity used to reinforce the cells on the moment-rotation performance. Figure 2-14(a) and (b) compares the moment-rotation performance of 4-R16 and 2-R12 paperclip specimen. 4-R16 paperclip connection detail has a higher strength capacity than 2-R12 paperclip connection detail. Both Specimens have observed to sustain the entire cyclic loading regime of ±4.0% drift amplitude. Figure 2-14 shows that the 4-R16 paperclip specimen reached a higher force magnitude and gave a bigger hysteric loop (more work done). According to experimental observation, 2-R12 paperclip specimen by Bull and Matthews (2003) has performed better than 4-R16 paperclip specimen. At the end of the testing, 4-R16 paperclip specimen was badly damage and the 2-R12 paperclip specimen has only sustained a modest level of damage that is repairable after earthquake. Therefore, it is evident that there is a limit on how much reinforcement should be placed on beam to floor connection joint. Over reinforcement of a connection joint should be avoided.

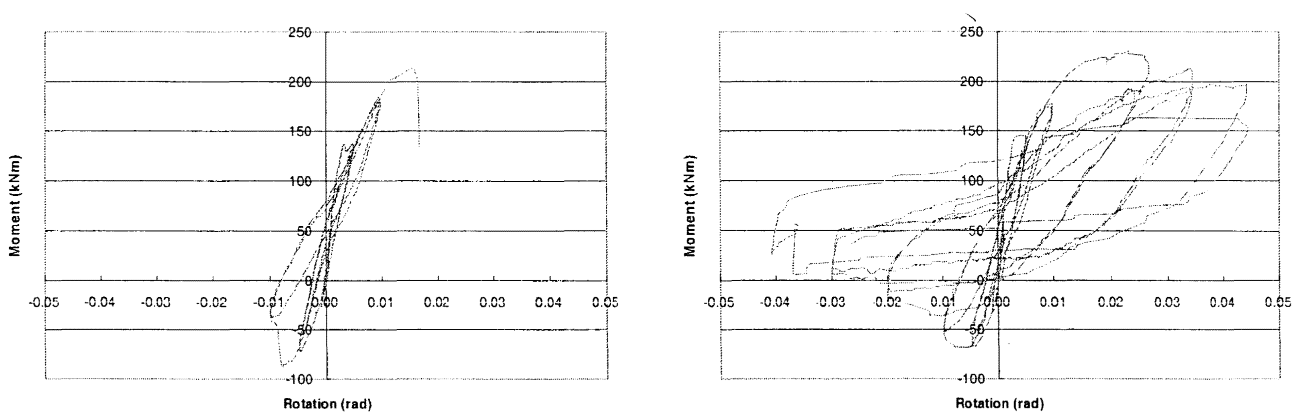

(a) Specimen 1: no seat

(b) Specimen 2: 70mm seat

Figure 2-12 Moment-rotation comparison showing the effect of a seat

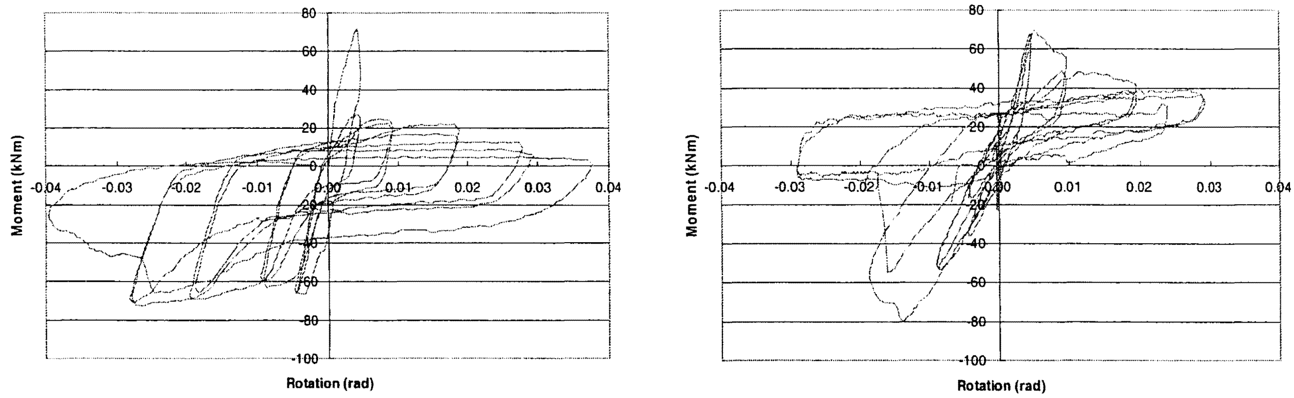

(a) Pre-retrofit, Bull and Matthews (2003)

(b) Specimen 3— Angle Retrofit

Figure 2-13 Effectiveness of a "catcher" retrofit on the moment-rotation performance of existing hollowcore construction where the cells are un-reinforced

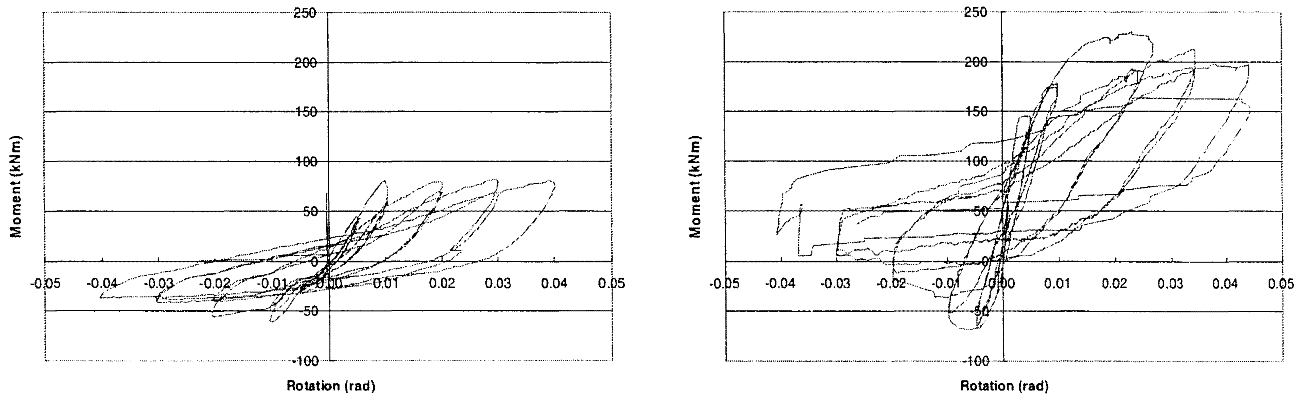

(a) 2-R12 Paperclips, Bull and Matthews (2003)

(b) 4-R16 Paperclips (Specimen 2)

Figure 2-14 Effect of quantity of Steel used to reinforce the cells on the moment-rotation performance

2.8 CONCLUSIONS

Based on the experimental study presented herein, the following conclusions are drawn.

2. Specimen 1 which had the zero seating demonstrated that although the moment capacity was adequate, the shear resistance under negative moments was totally inadequate. Incipient failure occurred at drift of 1.6%, well below the expected demand of 2% drift and a desirable rotational capacity in excess of 3%.
3. The failure of Specimen 2, which had the positive seating, was not dissimilar to Specimen 1. Incipient failure occurred due to negative moments in the connection at a drift of -1.0%. However, due to the presence of the seat the shear resistance was superior. Specimen 2 was still able to function without collapse up to 4% drift, although it was in a badly damaged state.
4. The experiments on Specimen 1 and 2 demonstrated that over-reinforcement of the cores can lead to inferior performance. In contrast to Specimen 2 (which was reinforced with 4 R-16 paperclips), the Bull and Matthews (2003) paperclip detail (2-R12 paperclips, see Figure 2-3 (c)) showed more stable performance up to inter-storey drifts of ±4%. Clearly, over-reinforcement of the connection should be avoided.
5. Three dimensional effects including the effect of beam elongation were ignored in these experiments. It would be interesting to repeat the experiments with these effects included, as it is unclear whether such effects are beneficial or detrimental in terms of overall performance.

6. All three test specimens "broke their back" under negative moment. This accured due to the formation of a shear crack plane at the end of the starter bars. Clearly, some negative moment enhancement is needed. One method of providing this is to ensure the negative moment capacity beyond the starter bars is maintained. To achieve this, reinforcing steel should be continuous in the topping slab from the end supports to at least the quarter points of the span.
7. Over reinforcement at a seating connection detail must be avoided. However, the boundary on how much steel placed in a connection joint is defined as over reinforcement is still unclear. Therefore, further research is required to come up with a quantifiable approach for defining over-reinforcement.

2.9 REFERENCES

CAE, 1999, *Guidelines for the Use of Structural Precast Concrete in Buildings*, Centre for Advanced Engineering, Report of a Study Group of the New Zealand Concrete Society and the New Zealand Society for Earthquake Engineering, 1999.

FIP Recommendations, 1988, *Precast prestressed hollow core floors*, Thomas Telford London.

Herlihy M.D, Park R. and Bull D.K, 1995, *Precast Concrete Floor Unit Support and Continuity*, Research Report 93/103, Department of Civil Engineering, University of Canterbury, Christchurch, New Zealand

Lindsay R, Mander J.G and Bull D.K, 2004, *Experiments On the Seismic Performance of Hollow-core Floor Systems in Precast Concrete Buildings*, Master of Engineering Thesis, Department of Civil Engineering, University of Canterbury, Christchurch.

Matthews J.G, Bull D.K and Mander J.B, 2003, *Preliminary Results from the Testing of a Precast Hollowcore Floor Slab Building*, 2003 Pacific Conference on Earthquake Engineering, February, Christchurch.

Matthews J.G, Bull D.K, Mander J.B, 2003, *Background to the Testing of a Precast Concrete Hollowcore Floor Slab Building*, 2003 Pacific Conference on Earthquake Engineering, February, Christchurch.

Matthews J.G, 2004, *Hollow-core Floor Slab Performance Following a Severe Earthquake*, PhD Thesis, Department of Civil Engineering, University of Canterbury, Christchurch, New Zealand.

Bull D.K, Matthews J.G, 2003, *Proof of Concept Tests for Hollowcore Floor Unit Connections*, Precast NZ report, Feb 2003.

Mejia-McMaster J.C and Park R., 1994, *Tests on Special Reinforcement for the End Support of Hollow-Core Slabs*, PCI Journal, Vol 39, No. 5, pp. 90-105, September-October.

Norton, J.A, King, A.B, Bull, D.K, Chapman, H.E, McVerry, G.H, Larkin, T.J, Spring, KC, (1994), *Northridge Earthquake Reconnaissance Report*, Bulletin of the New Zealand National Society for Earthquake Engineering, December, Vol. 27, No.4.

NZS3101, 1995, *Concrete Structures Standard, NZS 3101, Part 1 & 2*, Standards New Zealand, Wellington, New Zealand

NZS3101, 2003, *Draft Amendment No.3 to 1995 Standard (NZS 3101)*, Standards New Zealand, Wellington, New Zealand

Oliver S. J, 1998, *The Performance of Concrete Topped Precast Hollowcore Flooring Systems Reinforced With and Without Dramix Steel Fibres Under Simulated Seismic Loading*, Master of Engineering Thesis, Department of Civil Engineering, University of Canterbury, Christchurch, New Zealand.

Park R., 1989, *Evaluation of ductility of structures and structural assemblages from laboratory testing*, Bulletin of the New Zealand National Society for Earthquake Engineering, Vol. 22, No. 3, Sept 1989, pp155-166.

Section 3

Implications of Experimental Observation

SECTION SUMMARY

In order to assess the strength and deformation capacity of the hollowcore floor to beam connection details, simplified analytical models are presented and compared with experimental results of component tests. Based on calculated limit states that are verified by a visual assessment of experimental observations, interstorey drift limits in terms of damage states are assigned. Using these results, probabilistic fragility curves for different hollowcore seating details are developed. By using these fragility curves it is possible to provide some insightful implications of the extent of damage that might be expected in a class of hollowcore buildings.

3.1 INTRODUCTION

Concern has been raised regarding the likely performance of New Zealand's precast concrete building during an earthquake, in particular those constructed with hollowcore floor systems. The failure of the Meadow Apartments during the 1994 Northridge (Norton, 1994) has provided some information regarding the potential for poor performance of this class of flooring system if the connection with the supporting beam is not properly detailed. Although much research effort regarding to hollowcore floor system has been conducted previously (Mejia-McMaster and Park, 1994; Oliver, 1998; Herlihy et al, 1995; Matthews, 2004; Bull and Matthews, 2003; and Lindsay, 2004), the research has primarily focused on defining the rotational or elongation capacity of various details. The research presented herein extends the analytical portion of the work of Matthews (2004) and Lindsay (2004) to investigate the likely performance of three different types of hollowcore seating details.

To understand the general behaviour of a beam to hollowcore floor connections joint, the results of the previously tested seating connection details were further analysed. Simple limit methods of analysis are developed to assess the strength of the various connection joint details under both positive and negative moments (drift).

One of the products of this research is to apply visual indicators of damage to hollowcore floor seating connection details for the purpose of assessing the post-earthquake utility of structures. Following an earthquake event, a structure may be tagged according to its perceived safety by a colour code. This tagging system is used to indicate if immediate occupancy is possible, or if life-safety is threatened. Experimental evidence can give guidance to inspectors to understand what to look for in a damaged building following an earthquake. Finally, the visual assessment of all the different types of seating connection details was quantified using fragility theory to explain the implications of the observed damage in terms of New Zealand buildings.

3.2 Strength and Deformation Analysis Models for Hollowcore

3.2.1 Moment Capacity of Reinforced Hollowcore to Beam Connections

Figure 3-1 and 3-2 presents a free body force diagrams of paperclip seating connection detail under positive and negative moments. The estimation of the paperclip seating connection moment capacities are as follows:

Positive Moment Capacity

At full plastification, the paperclip may be assumed to fully yield in tension. Figure 3-1 shows the force diagram of the connection under positive moment with the section analysed as a singly reinforced beam. The connection joint moment strength is made up of two parts. One is from the internal couple forces and the other is from the frictional forces between the beam seating and hollowcore floor unit.

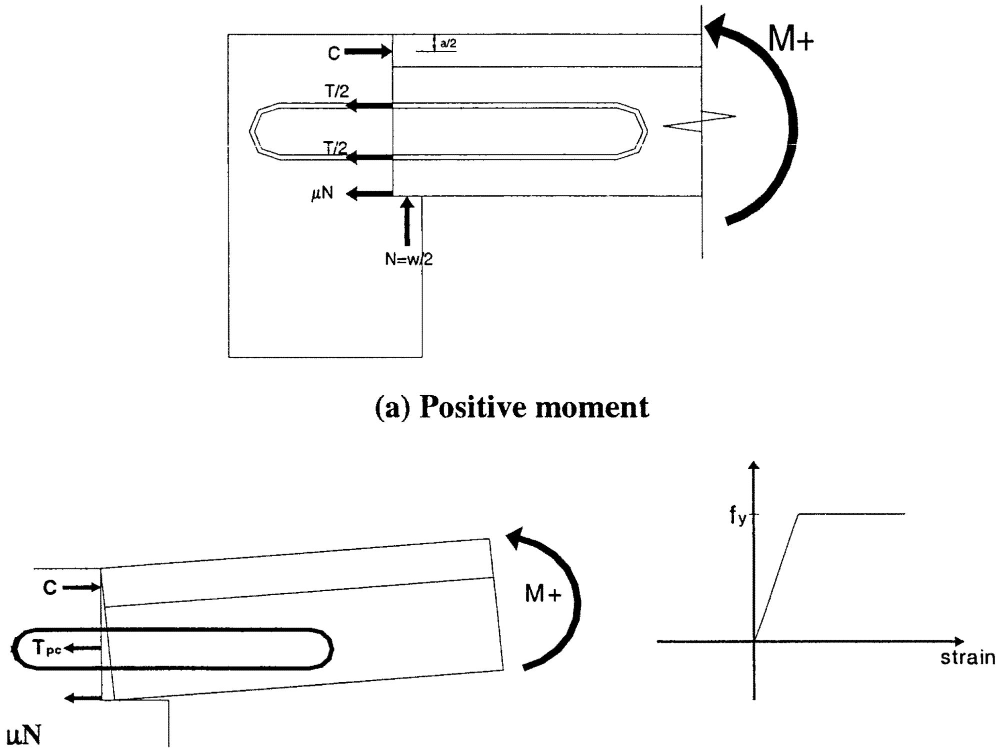

(b) Positive Moment

Figure 3-1 Positive strength capacity of hollowcore seating with cells reinforced with the "Paperclip" detail

$$M_n^+ = M_T + M_\mu \quad \textbf{(3-1)}$$

$$M_T = Tjd \quad \textbf{(3-2)}$$

$$T = A_s f_y \quad \textbf{(3-3)}$$

$$jd = d - \frac{a}{2} \quad \textbf{(3-4)}$$

$$a = \frac{T}{0.85 f'_c\, b} \quad \textbf{(3-5)}$$

where M_T = positive moment capacity contributed by the reinforcement in the connection; T = tension force; A_s = Steel area; f_y = yield strength of paperclip steel; a = depth of compression stress block; f'_c = concrete compressive strength; and b = width of the hollowcore unit.

The frictional moment contribution is given by:

$$M_\mu = \mu Njd \quad \textbf{(3-6)}$$

in which N = supporting force on seating (shear at support); and μ = coefficient of seating friction (taken as 1.2).

Negative Moment Capacity

Figure 3-2 summarises the force diagram of the connection under negative moment. Under a positive moment (drift), the hollowcore unit walked out at the seats and the paperclip reinforcement reach yield in tension as shown in Figure 3-1(b). However in the next cycle of negative moment, cracks open up at the seating connection and the paperclip is in compression as illustrated in Figure 3-2(b). Therefore, the paperclip compression force and the connection's negative moment capacity can be estimate as follows:

$$C_s = T - \mu N \tag{3-7}$$

$$M^- = Te + \mu Ne' \tag{3-8}$$

where C_s = paperclip compression force; e = eccentricity between centre of paperclip to centroid of the starter bars in the topping slab; and e' = eccentricity between centre the of paperclip bars to the bottom support surface.

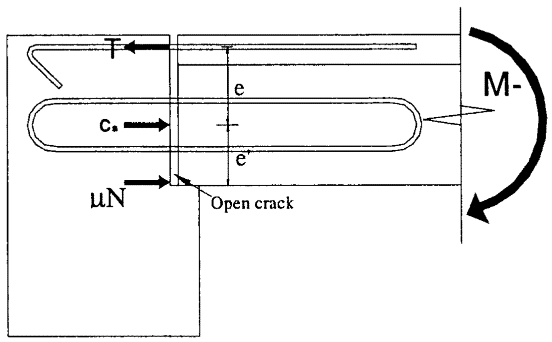

(a) Negative moment

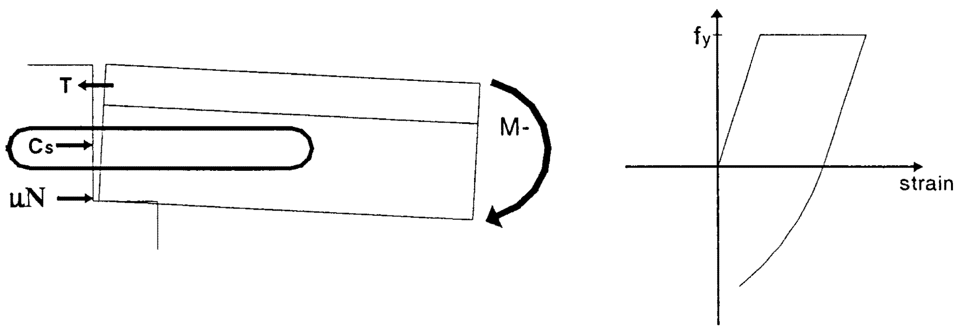

(b) Negative Moment

Figure 3-2 Open crack at the seat connection at negative moment

3.2.2 Moment Capacity of Connection without reinforced cells

Figure 3-3 shows a connection detail without reinforced cells under positive and negative moments. This section presents the strength estimation of the seating connection detail without any tie-bar running into the cells of the hollowcore unit.

Positive moment Capacity:

For a seating connection detail without any tie-bar, under a positive moment the hollowcore unit first develops its cracking moment. Once the cracking moment is reached, diagonal cracks then propagated upward from the bottom of the hollowcore unit toward the concrete topping in a 45° degree inclination with increasing inter-storey drift as shown in Figure 3-3(a). The cracking moment capacity, M_{cr}, of hollowcore unit can be estimated from:

$$M_{cr} = f_{cr}\frac{I_{xx}}{y_{bottom}} = f_{cr}S_x \tag{3-9}$$

in which S_x = section modulus $f_{cr} = 0.36\sqrt{f'_{c\_hollowcore}}$, where f_{cr} = hollowcore unit cracking stress; $f'_{c\_hollowcore}$ = hollowcore unit compressive strength; I_{xx} = Section moment of inertia; and y_{bottom} = distance from the composite section neutral axis to the bottom fibre.

The seating connection joint positive moment strength capacity decreases as the hollowcore cracks propagate upward from the bottom of the hollowcore unit. In order to more accurately estimate the residual strength of the connection, after cracking moment is reach, the tensile stress in the uncracked hollowcore unit should also be taken into account as it also contributes to the positive moment of the connection. Therefore, the residual strength of the connection can be estimate using Equations **(3-1)** to **(3-6)** plus the tensile stress moment contribution from the uncracked section of the hollowcore unit.

Negative Moment Capacity

Figure 3-3(b) summarised the force diagram of a connection detail without reinforced cells under negative moment. The connection joint negative moment capacity can be estimate using Equations **(3-1)** to **(3-6)**. If vertical shear cracks are to form at the end of the starter bars and topping meshes are fractured, the strength capacity of the connection detail would expect to drop significantly. The negative moment residual strength of the unreinforced cells connection following these events can be calculated using the lesser of:

$$M_n^- = Cjd \qquad \textbf{(3-10a)}$$

$$M_n^- = Tjd \qquad \textbf{(3-10b)}$$

$$jd = d - \frac{kd}{3} \qquad \textbf{(3-11)}$$

where

$$C = \frac{1}{2} f_c bkd \qquad \textbf{(3-12a)}$$

$$T \approx A_{strand}\left(0.6 f_{pu}\right) \qquad \textbf{(3-12b)}$$

and

$$k = \sqrt{(\rho n)^2 + 2\rho n} - \rho n \qquad \textbf{(3-13)}$$

$$\rho = \frac{A_{s\_strand}}{A_{concrete}} \qquad \textbf{(3-14)}$$

$$n = \frac{E_{strand}}{E_{hollowcore}} \qquad \textbf{(3-15)}$$

In which ρ = steel concrete ratio; n = transformed ratio; A_{s_strand} = area of hollowcore strand (diameter 12.9mm); $A_{concrete}$ = area of effective concrete; E_{strand} = modulus of elastic of hollowcore strand (200GPa); $E_{hollowcore}$ = modulus of elastic of hollowcore unit ($E_{hollowcore} = 4700\sqrt{f'_{c\_hollowcore}}$); k = neutral axis depth factor; and d = effective depth.

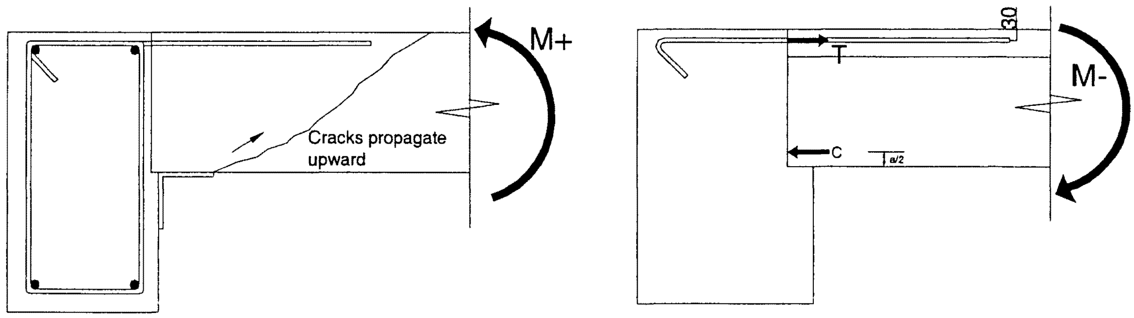

(a) Positive moment **(b) Negative moment**

Figure 3-3 Capacity of hollowcore seats that do not have reinforced cells

3.3 APPLICATION TO HOLLOWCORE COMPONENT TESTS

Simple rational method proposed in the previous section is use to estimate the specimens strength capacity tested in this research and Bull and Matthews (2003) specimens. Full detail calculation of the connection strength capacities is presented in Appendix C.

3.3.1 Specimens with reinforced cells

The connection joint moment strength is made up of two parts. One is from the internal couple forces and the other is from the frictional forces between the beam seating and hollowcore floor unit. Based on Equation **(3-1)** to **(3-6)**, for 4-R16 paperclip specimens $M_T = 171kNm$ and $M_\mu = 15.4kNm$. Therefore, positive moment capacities of $M_n^+ = 171kNm$ and $M_n^+ = 186kNm$ were calculated for Specimens 1 and 2, respectively. Similarly, for 2-R12 paperclip specimen by Bull and Matthews (2003) Equations **(3-1)** to **(3-6)** gives $M_T = 54kNm$ and $M_\mu = 15.4kNm$ and hence, $M_n^+ = 69.4kNm$.

Under negative moments, using Equations **(3-3)** the starter bars forces can be calculated as 226.2*kN*. Based on Equation **(3-8)**, with e = 188mm and e'= 150mm the connection's negative moments capabilities for 4-R16 and 2-R12 paperclips specimens are $M_n^- = 49kNm$. Figure 3-4 and 3-5 compares the theoretical strength capacities calculated for the reinforced cells specimens with the actual observed moment-rotation curve of the specimens.

Figure 3-4 illustrates the effects of a seat at a hollowcore floor to beam connection joint. Both Specimen 1 (no seats) and Specimen 2 (70mm seats) have given a similar peak magnitude in the positive and negative drift amplitudes. Specimen 1 has an incipient failure at 1.6% and failed at 1.75% drift amplitude and Specimen 2 has sustained the entire ±4.0% inter-storey drift. The seat allows more damage to be done at the connection joint and delays the catastrophic collapse of the hollowcore floors. Figure 3-5 compares the moment-rotation curves of 4-R16 paperclip specimen with 2-R12 paperclips specimen by Bull and Matthews (2003). Figure 3-5 shows that the 4-R16 paperclip specimens have reached a higher magnitude, in positive and negative drift amplitude, than the 2-R12 paperclip specimen.

The 2-R12 paperclip specimen has out-performed Specimen 2. However, Figure 3-5, moment-rotation curve of both specimens, has showed otherwise. Figure 3-5 shows that Specimen 2 has dissipated more energy than Bull and Matthews (2003). It is customary to assume that a connection with larger hysteresis loop size has more work done and give a better performance. However, according to experimental observation, Bull and Matthews (2003) was observed to perform better than Specimen 2. Specimen 2 was separated from the supporting beam and suspended by the hollowcore bottom strain at failure (Figure 2-8b(ii)). On the other hand, Bull and Matthews (2003) 2-R12 paperclip specimen did not fail at the end of the experiment. Cracks developed and concentrated at the beam-floor connection interface. Therefore, the size of one hysteresis plot cannot be used to determine the performance of one connection detail as it is the case presented here.

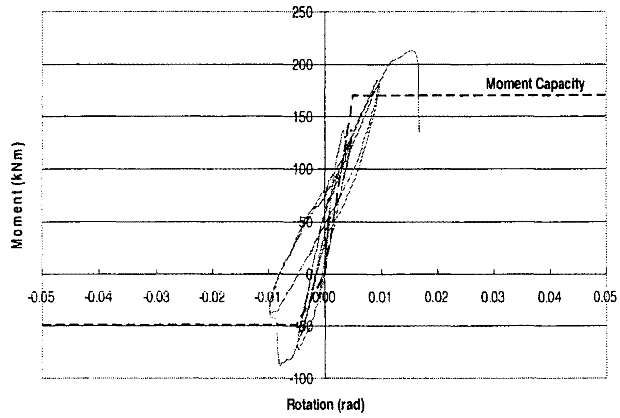

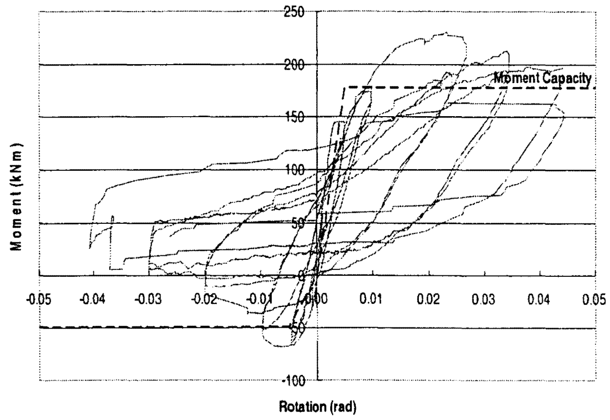

(a) Specimen 1: no seats **(b) Specimen 2: 70mm seat**

Figure 3-4 Comparison of specimen with and without seats

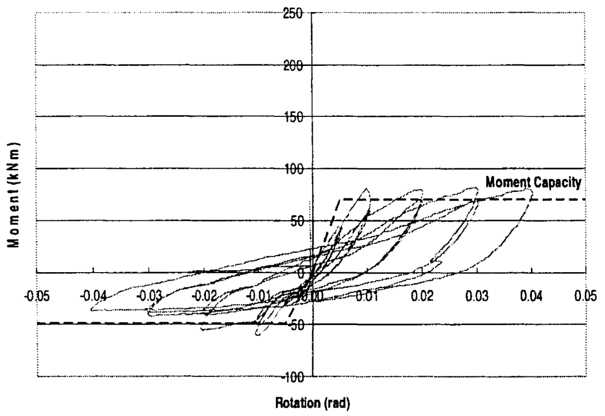

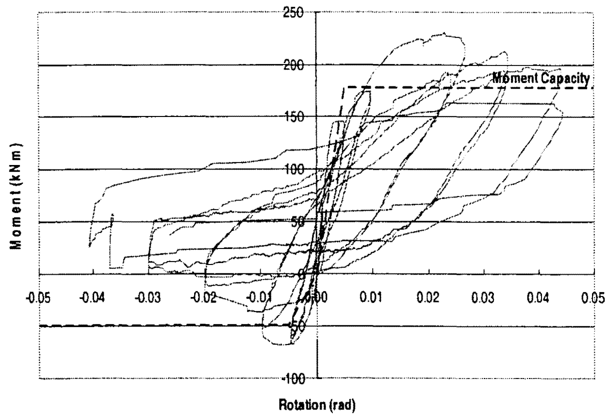

(a) 2-R12 Paperclips (Bull and Matthews) **(b) 4-R16 Paperclips (Specimen 2 of Present Study)**

Figure 3-5 Comparison of specimens with reinforced cells

3.3.2 Specimens without reinforced cells

For connection detail without any tie-bar, the connection joint will reach the hollowcore unit cracking moment first under positive moment. After hollowcore unit cracking moment was reached, bottom hollowcore unit cracks propagated upward. Using Equation **(3-9)**, the cracking moment of the hollowcore unit is $M_{cr} = 59kNm$.

As hollowcore cracks propagated upward from the bottom of the hollowcore unit, the connection joint moment capacity decreases. From experimental observation for Specimen 3, at 3.0% drift amplitude hollowcore cracks propagated and stopped at the hollowcore web. Therefore, using Equation **(3-1)** to **(3-6)**, $M_T = 6kNm$ and $M_\mu = 10.5kNm$. Therefore $M_n^+ = 16.5kNm$, where μ = coefficient of friction between hollowcore and angle seat (taken as 0.8). The tensile stress in the uncracked hollowcore unit should also be taken into account; it also contributes to the positive moment at the connection. Referring to Figure 3-6(a), hollowcore unit can be approximated as an I-section. The shaded area represents the effective area of the uncracked hollowcore unit at 3.0% drift amplitude. Figure 3-6(b) shows the force diagram of the uncracked section. Refer to Appendix C for determination of the hollowcore unit uncracked tensile force and leverarm, *jd*. The tensile strength of the uncracked hollowcore unit can thus be summarised as below:

	b (mm)	Force (kN)	jd (mm)	Moment (kNm)
T1	1017	22.7	49.2	1.19
T2	1200	37.3	90	3.42
T3	343	67.3	170.74	11.54
				Σ = 16.1 kNm

Therefore, the residual connection positive moment capacity is $M_n^+ = 32.6kNm$

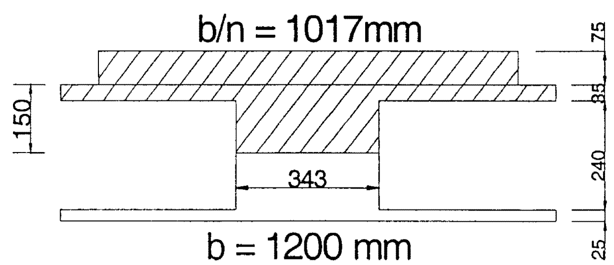

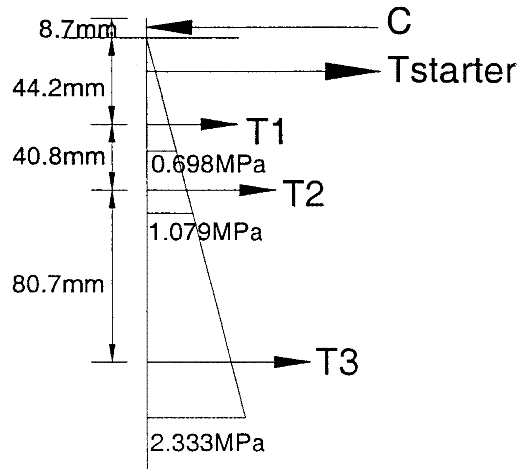

(a) Effective section for 300 series hollowcore **(b) Force diagram**

Figure 3-6 Uncrack effective section and force diagram

Under negative moments, the 4-HD12 starter bars were fully yielded. Based on Equation **(3-2)** to **(3-5)**, the connection's negative moment capacity $M_n^- = -77.4kNm$. Experimental observation of Specimen 3 shows that the connection joint strength capacity dropped suddenly under negative moment when shear cracks formed at the end zone of the starter bars and the mesh fractured. Figure 3-7 shows that a depth of 27mm was taken as the effective hollowcore concrete depth under negative moments after the shear crack formed. Using Equations **(3-10)** to **(3-15)**, with strand diameter of 12.9mm, the residual negative moment strength of Specimen 3 is $M_n^- = 7.04kNm$.

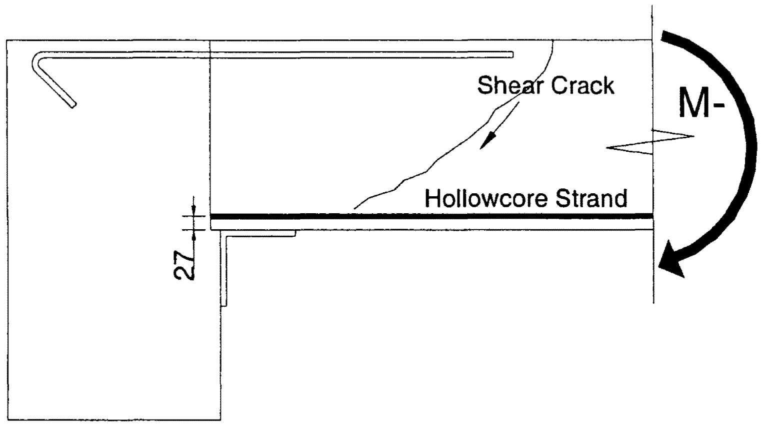

Figure 3-7 Effective hollowcore unit area after shear crack formed

Similar to Specimen 3, for 300 control specimen, the connection joint will reached the hollowcore unit cracking moment of 59kNm under positive moment. After hollowcore unit cracking moment was reached, bottom hollowcore unit cracks propagated upward. The residual strength of the connection joint can thus be estimated with Equations **(3-1)** to **(3-6)** as $M_T = 6kNm$ and $M_\mu = 15.8kNm$. Therefore, the residual positive moment of the 300 control specimen is $M_n^+ = 22kNm$.

Under negative moments, the 4-HD12 starter bars were assumed fully yielded. From Equation **(3-2)** to **(3-5)**, the connection's negative moment capacity is $M_n^- = 77.2kNm$. The calculated and actual strength capacities of the unreinforced cells specimen are shown in Figure 3-8.

Specimen 3 tested in this research where the specimen possessed a retrofit detail, can be directly compared to Bull and Matthews (2003) (pre-retrofit) control specimen. Figure 3-8 presents the moment-rotation curve of both Specimen 3 and Bull and Matthews (2003) specimen. Referring to Figure 3-8, Specimen 3 shows an improved performance (higher positive moment strength–lower sudden drop from cracking moment) in the positive drift amplitude than Bull and Matthews (2003) specimen. However, in the negative drift amplitude, the moment in Specimen 3 dropped suddenly once the shear crack developed and the mesh in the concrete topping fracture, at -2.0% drift. Note both specimens performed poorly under negative moment – they both "broke their backs" off the end of the starter bars (brittle failure). Clearly, some negative moment enhancement is needed. It is suggested that gluing carbon or glass fibre strips to the concrete surface is one potential retrofit measure that could be considered. Finally, the 150 x150 x 12mm angle seat used in Specimen 3 successfully fulfilled its role as a "catcher" but at the same time it has also restrained the rotation of the hollowcore end support at the seating.

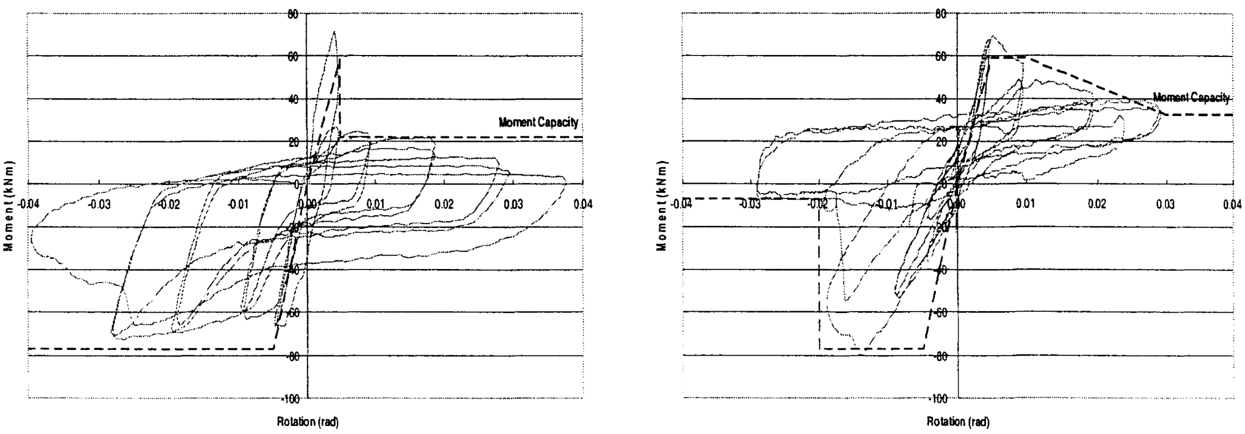

(a) Control Specimen Bull and Matthews (2003) **(b) Specimen 3**

Figure 3-8 Comparison of performance of specimen without reinforced cells

Table 3-1 and Table 3-2 summarise the positive and negative moment capacities of the specimens with and without reinforced cells. Overall, the estimated strength capacities for the specimens give satisfactory agreement with those observed in the experiment.

Table 3-1 Summary of Moment Capacities calculated for Specimens with reinforced cells

	Positive Moment Capacity		Negative Moment Capacity	
	M_n^+	$M_{residual}^+$	M_n^-	$M_{residual}^-$
Specimen 1	171 kNm	-	-49 kNm	-
Specimen 2	186 kNm	-	-49 kNm	-
Paperclip Specimen	69kNm	-	-49 kNm	-

Table 3-2 Summary of Moment Capacities calculated for Specimens without reinforced cells

	Positive Moment Capacity		Negative Moment Capacity	
	M_n^+	$M_{residual}^+$	M_n^-	$M_{residual}^-$
Specimen 3	59 kNm	32.6kNm	-77 kNm	-7kNm
Control Specimen	59kNm	22kNm	-77 kNm	-

3.4 Strength, Rotation and Damage Limit States of Hollowcore Connections

To facilitate the re-occupancy of a building after an earthquake event, it customary practice to tag structures based on an engineers damage inspection using a colour coded format (NZUSAR, 2003). Similarly, for design planning and performance based earthquake engineering a Damage State format is emerging as a popular means of distinguishing levels of damage, reparability and expected outage times (Mander, 2003). For the colour coded format, the level of damage to a building structure is assessed and tagged with one of four colours with increasing severity of damage: green, yellow, orange, and red. Table 3-3 summarizes and gives a description of the colour coding format. The other approach used for tagging is to classify the damage to the building on a numerical scale from one to five. This approached is summarized in Table 3-4. Although by comparing Table 3-3 and 3-4, it is evident that both forms of classification are similar, the application of each system is for different purposes: the colour coded format is applied to Urban Search and Rescue; while the numerical format is for damage and economic analysis.

One of the purposes of this research was to obtain a visual indication of the expected damage to the hollowcore floor unit at different levels of inter-storey drift. It is important that these results can be used as a reference for tagging hollowcore floor buildings in a post-earthquake event during and following the completion of the sub-assembly experiments, it was possible to classify the super-assemblage according to the two classification methods. The damage states of the test specimens assigned in terms of the coloured coding and damage state criteria are presented in Table 3-5 and Table 3-6.

Table 3-3 Description of colour coding used to classify building damage after earthquake

Damage State	Description of Damage State
Green	No Damage, building occupiable
Yellow	Moderate levels of damage. Buildings can be entered to remove belongings
Orange	Heavy damage. Building can be entered for brief periods to remove essential items only
Red	Near collapse. Building can not be entered

Table 3-4 Description of damage states used to classify building damage after earthquake (Mander, 2003)

Damage State	Description of Damage	Post-earthquake utility	Expected Repair or reconstruction time
1	None (pre-yielding)	Normal	-
2	Minor/ Slight	Slight Damage	3 days
3	Moderate	Repairable Damage	3 weeks
4	Major/ Extensive	Irreparable Damage	3 months
5	Complete Damage	Irreparable Damage	3 years

Table 3-5 Colour coding and damage states classification for the reinforced cells connection detail based on observed drift amplitudes

Tag Colour	Damage State	2-R12 Paperclip	Specimen 1	Specimen 2
Green	1	1.0%	0.5%	0.5%
Yellow	2	4.0%	-1% (1), shear crack formed	2%, large cracks extend across connection zone
Orange	3	-	1.75 large horizontal split formed	-2.9%, can see mesh on surface
Red	4	-	2% (1), floor unit dropped	4%, see strand hanging the H/C intact
	5			

Table 3-6 Colour coding and damage states classification for the unreinforced without and with retrofit connection detail based on observed drift amplitudes

Tag Colour	Damage State	Control 300 series	Control 200 series	Specimen 3
Green	1	0.5%	0.5%	0.5%
Yellow	2	2.0% topping separate from unit	-1.8%(1), first mesh fractured	-1.5%, first mesh fracture, visible big cracks
Orange	3	3.0% strand pulling out of fracture end	-2.76%, 24mm vertical separation	-3% (1), unit drops 15mm
Red	4	4%	3.95%, separated from beam, strand holding up	4%
	5			

Note: Number in bracket represent which cycles of that particular drift

3.5 FRAGILITY ANALYSIS

An investigation has been undertaken by Matthews (2004) that determined the expected inter-storey drift on the class of structure tested in this programme. The findings were, in terms of the expected (median) drift as follows

$$\tilde{D}_D = 2.0F_vS_1 \tag{3-16a}$$

or

$$\tilde{D}_D = 2.0PGA \tag{3-16b}$$

where $\tilde{D}_D$ = the median (50th percentile) drift demand as a percentage of the storey height; F_vS_1 = one second spectral acceleration for tall structures (above four stories); and PGA = peak ground acceleration for low rise structures (up to four stories). By inverting Equation **(3-16a)** and **(3-16b)**, the expected (median or 50th percentile) ground motion demand needed to achieve a given median drift capacity can be found such that

$$\tilde{F}_v S_1 = 0.5\tilde{D}_C \tag{3-17a}$$

or

$$P\tilde{G}A = 0.5\tilde{D}_C \tag{3-17b}$$

where $\tilde{D}_C$ = expected drift capacity of the structure.

Analysis by Matthews (2004) showed that the distribution of drift outcomes was lognormal with coefficient of variation of $\beta_D = 0.52$ (note the subscript D stands for demand). When combining these distributions to give an overall composite distribution, Kennedy et al (1980) shows that by using the central limit theorem the coefficient of variation for lognormal distribution can be found from:

$$\beta_{C/D} = \sqrt{\beta_C^2 + \beta_D^2 + \beta_U^2} \tag{3-18}$$

where β_C = coefficient variation for the strength capacity, taken as 0.2 (Dutta, 1999); and β_U = dispersion parameter to account for modelling uncertainty, taken here as 0.2.

Applying Equation **(3-18)**, these values give $\beta_{C/D} = 0.6$.

By using a cumulative distribution that can be described by a unit lognormal variation ξ_β (where the median =1 and the lognormal coefficient of variation, $\beta_{C/D} = 0.6$), the distribution of ground motion demands needed to produce a given state of damage can be found by:

$$F_v S_1 = 0.5 \tilde{D}c(DS)\xi_\beta \qquad \textbf{(3-19a)}$$

or $$PGA = 0.5 \tilde{D}c(DS)\xi_\beta \qquad \textbf{(3-19b)}$$

where $\tilde{D}c(DS)\xi_\beta$ = the expected value (in this case the experimentally observed drift) for a given damage state (*DS*).

Following the above discussed philosophy outlined by Matthews (2004), fragility curves are developed for a typical moment resisting concrete frame where damaged states are classified according to post-earthquake inspection based on colour tagging format as well as the Damage state format. Based on the experimental observations made, expected values of the response parameters for different post-earthquake states of damage in terms of coloured tagging and damage state tagging for connection details with reinforced cells and without reinforced cells is presented in Table 3-7 and Table 3-8.

Figure 3-9 shows the fragility curves for specimens consisted of "paperclip" reinforcement. In each of the graph the 10% in 50 years the Design Basis Earthquake (DBE), F_vS_1 = 0.40g for Wellington, New Zealand and the 2% in 50 years the Maximum Considered Earthquake (MCE), F_vS_1 = 0.72g for Wellington, New Zealand are shown. Figure 3-9(a) shows that for Specimen 1(4-R16 paperclip: zero seat) type connection building, under a DBE, 6% of the building would be expected to tag damage state 5, 4% tagged damage state 4, 25% tagged damage state 3, and 43%

tagged damage state 2. Under a MCE, 29% tagged damage state 5, 8% tagged damage state 4, 36% tagged damage state 3 and 23% tagged damage state 2. For Specimen 2 (4-R16 paperclip: 70mm seat), Figure 3-9(b) shows that after a DBE 2% of the building would tagged damage state 4, 4% tagged damage state 3, and 72% tagged damage state 2. However, under a MCE, 5% of the building would be tagged damage state 5, 8% tagged damage state 4, 15% tagged damage state 3 and 68% tagged damage state 2. Finally, Figure 3-9(c) shows that for a 2-R12 paperclip connection detail 1% of the buildings would sustain moderate damage under DBE, 34% of the buildings sustain minor damage (damage state 2) and the remaining 65% of the buildings would have sustained no damage. However, under a MCE 5% of the buildings would be tagged damage state 3, 68% tagged damage state 2 and remaining 27% of the buildings would be in normal condition.

Figure 3-10 shows fragility curves for the connection details without reinforced cells. Figure 3-10(a) present fragility curve for Specimen 3, retrofit detail. Under a DBE, 3% of the retrofit detail building would be tagged damage state 4, 12% tagged damage state 3 and 63% tagged damage state 2. Under a MCE, 5% tagged damage state 5, 7% tagged damage state 4, 35% tagged damage sate 3 and 49% of the building would be expected to tag damage state 2. Figure 3-10(b) illustrate that, for control specimen buildings, 2.5% of the building would be tagged damage state 4 under a DBE, some 3.5% of the building tagged damage state 3, 70% tagged damage state 2 and the remaining 22% of the structures would have no damage. Under a MCE, 5% of the buildings would be tagged damage state 5, 6% damage state 4, 17% damage state 3 and 68% of the building sustain minor damage. Figure 3-10(c) shows fragility curve for 200 control series specimen. The curve demonstrate that under a DBE, 23% of the buildings would be expected to sustain no significant damage, 69% tagged damage state 2, 6% damage state3 and 2.5% sustain heavy damage. For a MCE, 4% tagged damage state 1, 61% damage state 2, 22% damage state 3, 8% damage state 4 and 5% of the building would be expected to collapse.

Building performance expectation should be surviving the 2500 year event with 90% confidence. Figure 3-9 demonstrate that, for reinforced cells connection, 2-R12 paperclips by Bull and Matthews (2003) gives that best outcome follows by 4-R16 paperclips with 70mm seats (Specimen 2) and 4-R16 paperclip with zero seating (Specimen 1). For unreinforced cells connection, fragility curves present in Figure 3-10 illustrate that the retrofit detail, 300 control specimen and 200 control specimen gives reasonable outcome.

A summary of the fragility analysis under colour coding and damage state format were shown in Table 3-9 and Table 3-10. Table 3-9 clearly shows the superiority of the 2-R12 paperclip detail while table 3-10 highlights that the Specimen 3 retrofit detail gives only marginal enhancement to the expected performance of the typical existing details.

Table 3-7 Relationship between damage level and expected hazard to cause that damage state for reinforced cells

Damage State	Tag Colour	2-R12 Paperclips		Specimen 1		Specimen 2	
		Drift	F_vS_1 or PGA (g)	Drift	F_vS_1 or PGA (g)	Drift	F_vS_1 or PGA (g)
1	Green	1.0%	0.5	0.5%	0.25	0.5%	0.25
2	Yellow	4.0%	2.0	1.0%	0.5	2.0%	1.0
3	Orange	-		1.75%	0.88	2.9%	1.45
4 5	Red	-		2%	1.0	4.0%	2.0

Table 3-8 Relationship between damage level and expected hazard to cause that damage state for specimens without reinforced cells

Damage State	Tag Colour	Control 300		Control 200		Specimen 3	
		Drift	F_vS_1 or PGA (g)	Drift	F_vS_1 or PGA (g)	Drift	F_vS_1 or PGA (g)
1	Green	0.5%	0.25	0.5%	0.25%	0.5%	0.25%
2	Yellow	2.0%	1.0	1.5%	0.75%	1.5%	0.75%
3	Orange	3.0%	1.5	3.0%	1.5%	3.0%	1.5%
4 5	Red	4.0%	2.0	4.0%	2.0%	4.0%	2.0%

Table 3-9 Summary of the fragility analysis for specimens with reinforced cells

Damage State	Tag Colour	Specimen 1		Specimen 2		2 R-12 Paperclip	
		DBE	MCE	DBE	MCE	DBE	MCE
1	Green	22%	4%	22%	4%	65%	27%
2	Yellow	43%	23%	72%	68%	34%	68%
3	Orange	25%	36%	4%	15%	1%	5%
4	Red	4%	8%	2%	8%	-	-
5		6%	29%	0%	5%	-	-

Table 3-10 Summary of the fragility analysis for specimens without reinforced cells

Damage State	Tag Colour	Specimen 3		300 control		200 control	
		DBE	MCE	DBE	MCE	DBE	MCE
1	Green	22%	4%	23%	4%	23%	4%
2	Yellow	63%	49%	70%	68	69%	61%
3	Orange	12%	35%	3.5%	17%	6%	22%
4	Red	3%	7%	2.5%	6%	2.5%	8%
5		0%	5%	-	5%		5%

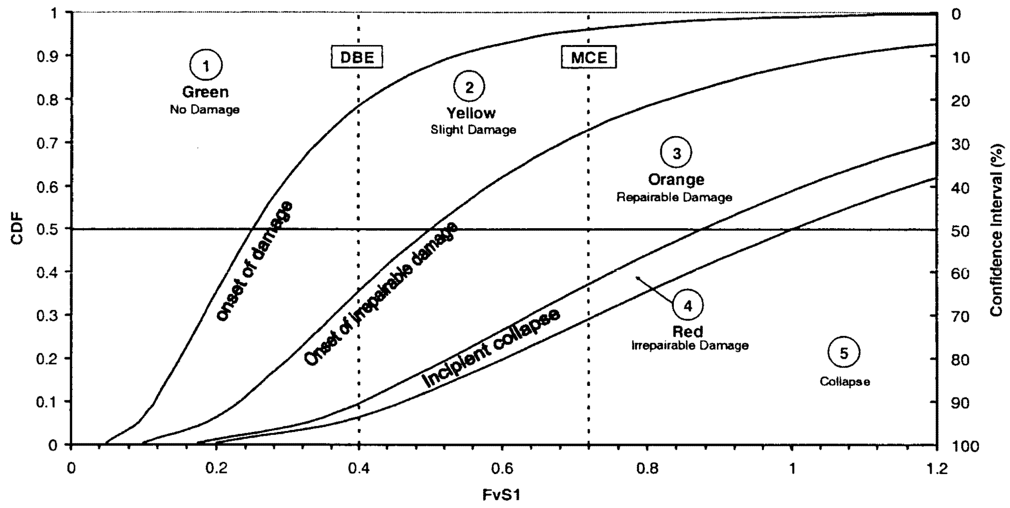

(a) Specimen 1: 4-R16 Paperclip (no seating)

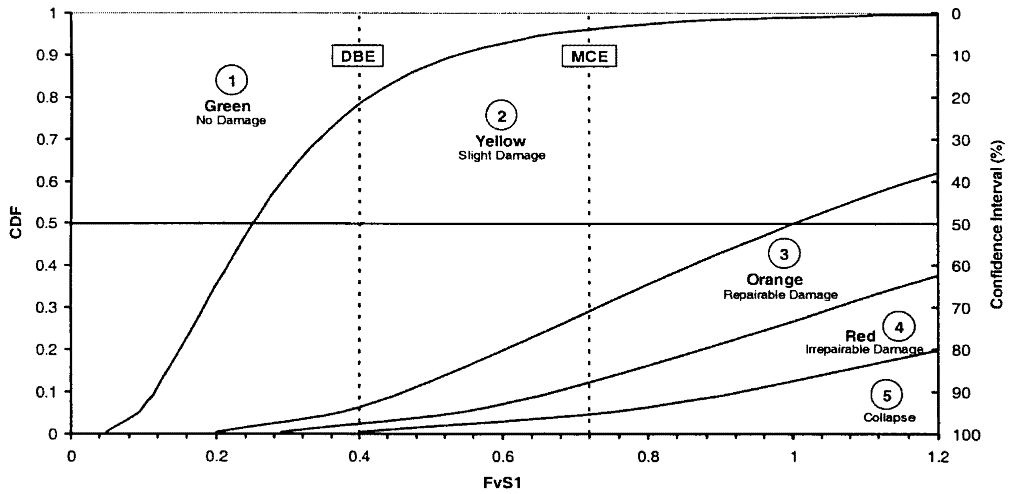

(b) Specimen 2: 4-R16 Paperclip (70mm seating)

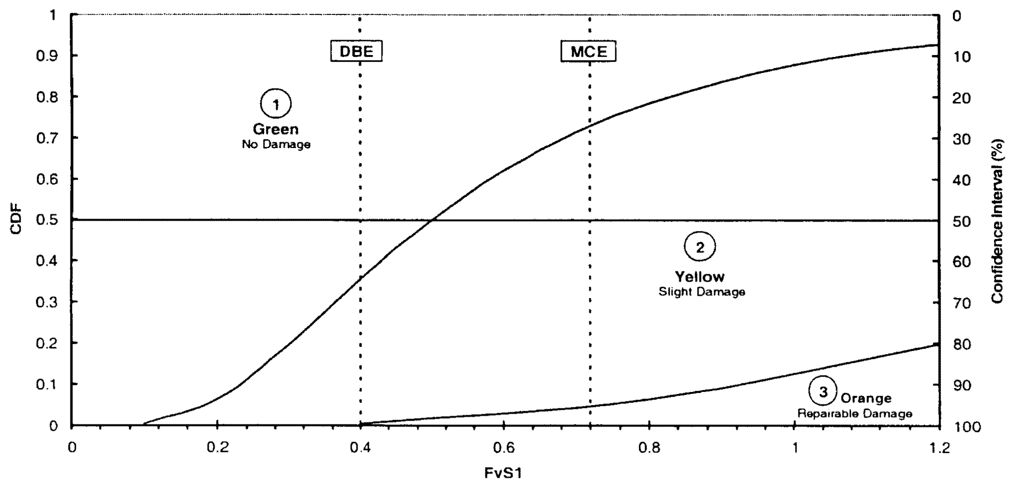

(c) 2-R12 Paperclip specimen

Figure 3-9 Fragility curves for reinforced cells connections

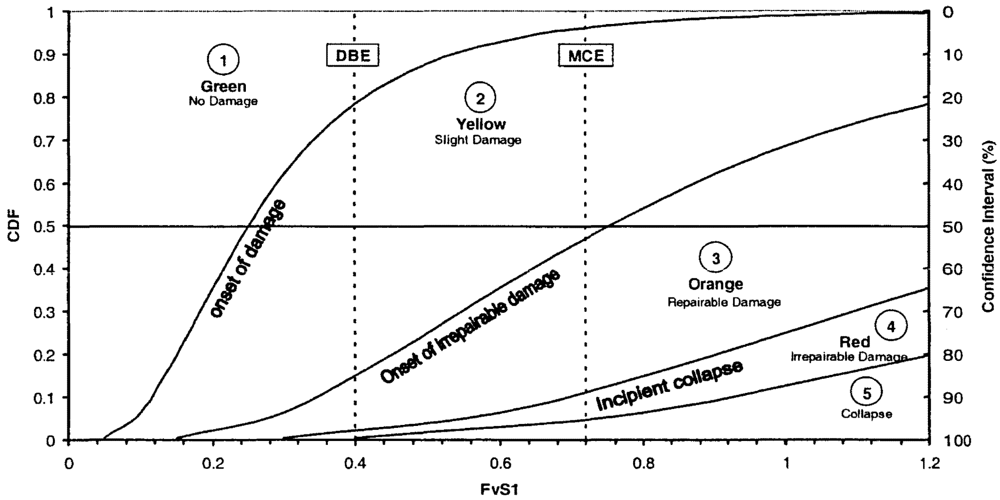

(a) Specimen 3: Retrofit detail

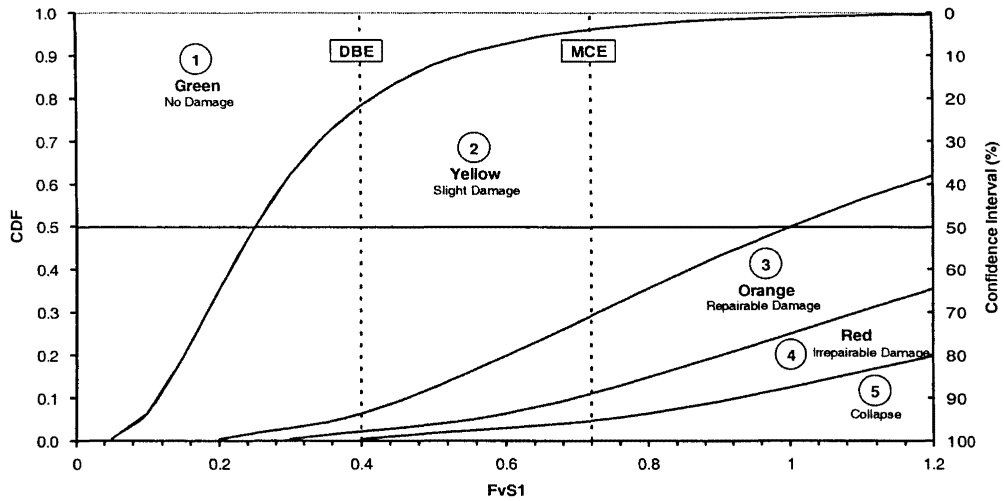

(b) 300 control specimen

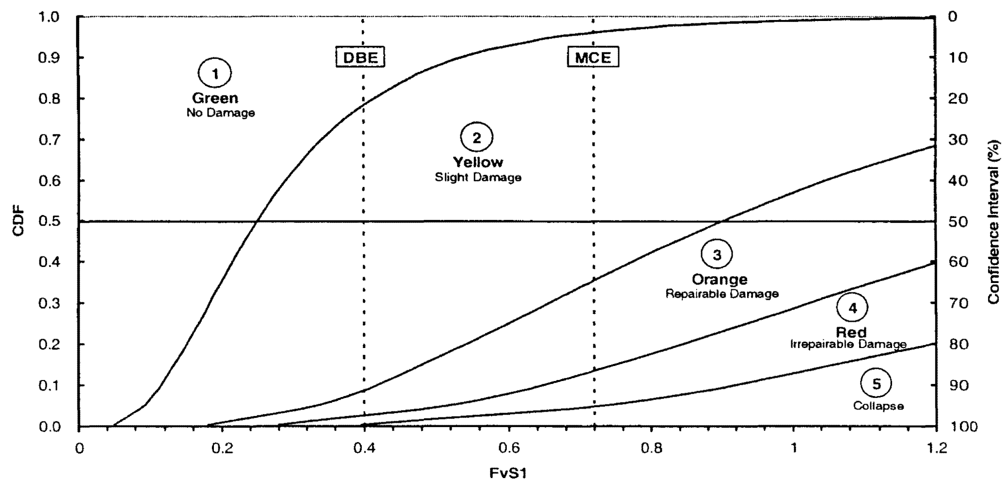

(b) 200 control specimen

Figure 3-10 Fragility curves for unreinforced cells connections

3.6 CONCLUSIONS

The following conclusions are drawn from the experimental study and analysis presented herein:

1. Simple methods, based on rational mechanics, were proposed to assign nominal strength capacities for hollowcore to beam connections. Methods are given for connections that are either unreinforced or reinforced and filled cells with paperclips. Results appear to agree well with experimental observations.
2. The specimen reinforced with 2-R12 paperclips by Bull and Matthews (2003) out-performed the two specimens with 4-R16 paperclip investigated herein. The lightly reinforced paperclip specimen did not fail during their experiment although significant cracking were developed and concentrated at the beam-floor connection interface. From the present experiments, Specimen 1, due to absence of seating, collapsed at 1.75% drift. Specimen 2, which had a 70mm seat, was observed to cease functioning properly at 2.9% drift.
3. Bull and Matthews control specimen and Specimen 3 showed poor performance under negative moments and as a result, both specimens "broke their back". Both specimens recorded a sudden drop of the connection joint strength capacity. However, the retrofit measures included in Specimen 3 were effective under positive moments when compared with Bull and Matthews (2003) un-retrofitted control specimen. Clearly some negative moment enhancement is also required to complete the retrofit measures.
4. Probabilistic fragility curves were developed both for colour coded and Damage state formats based on experimental observations. By using fragility curves to assess individual elements of a system it is possible to determine the implications of the drift damage on New Zealand constructed buildings of this type.

5. Building performance expectation should be surviving the 2500 year event with 90% confidence. Fragility analysis shows that for reinforced cells hollowcore connection details, 2-R12 paperclip specimen by Bull and Matthews (2003) gives the best outcome. 4-R16 paperclips with zero seat specimens is not recommend and 4-R16 paperclips with 70mm seats gives satisfactory outcome.

3.7 REFERENCES

Bull D.K, Matthews J.G, 2003, *Proof of Concept Tests for Hollowcore Floor Unit Connections*, Precast NZ report, Feb 2003.

Dutta A, 1999, On *Energy-Based Seismic Analysis and Design of Highway Bridges*. Ph.D Thesis, Science and Engineering Library, State University of New York at Buffalo, Buffalo, NY.

Herlihy M.D, Park R. and Bull D.K, 1995, *Precast Concrete Floor Unit Support and Continuity*, Research Report 93/103, Department of Civil Engineering, University of Canterbury, Christchurch, New Zealand

Kennedy R.P, Cornell C.A, Campbell R.D, Kaplan S, Perla H.F. 1980, *Probabilistic Seismic Safety Study of an Existing Nuclear Power Plan,* Nuclear Engineering and Design, No.59, pp315-338.

Lindsay R, Mander J.G and Bull D.K, 2004, *Experiments On the Seismic Performance of Hollow-core Floor Systems in Precast Concrete Buildings*, Master of Engineering Thesis, Department of Civil Engineering, University of Canterbury, Christchurch.

Mander J. B., 2003, *Beyond the Ductility: The Quest Goes On*, Proceedings to celebrate the lifetime contribution of professors emeriti Tom Paulay and Bob Park, pp76-89, Christchurch, New Zealand.

Matthews J.G, 2004, *Hollow-core floor slab performance following a severe earthquake,* PhD Thesis, Department of Civil Engineering, University of Canterbury, Christchurch, New Zealand.

Mejia-McMaster J.C and Park R., 1994, *Tests on Special Reinforcement for the End Support of Hollow-Core Slabs*, PCI Journal, Vol 39, No. 5, pp. 90-105, September-October.

Norton, J.A, King, A.B, Bull, D.K, Chapman, H.E, McVerry, G.H, Larkin, T.J, Spring, KC, (1994), *Northridge Earthquake Reconnaissance Report*, Bulletin of the New Zealand National Society for Earthquake Engineering, December, Vol. 27, No.4.

NZS3101, 1995, *Concrete Structures Standard, NZS 3101, Part 1 & 2*, Standards New Zealand, Wellington, New Zealand

Oliver S. J, 1998, *The Performance of Concrete Topped Precast Hollowcore Flooring Systems Reinforced With and Without Dramix Steel Fibres Under Simulated Seismic Loading*, Master of Engineering Thesis, Department of Civil Engineering, University of Canterbury, Christchurch, New Zealand.

Paulay T and Priestley M.J.N, 1992, *Seismic Design of Reinforced Concrete and Masonry Buildings,* J. Wiley and Sons Inc, New York.

Section 4

Summary, Conclusions and Recommendations

4.1 SUMMARY

This research has followed on recently completed experimental work conducted by Bull and Matthews (2003). Under the sponsorship of Precast NZ Inc, Bull and Matthews (2003) has conducted two-dimensional sub-assemblage tests on past precast concrete connection detail and a further two new seating connection details recommended by an industry based Technical Advisory Group on precast floors (TAG). These two new seating details were included into the Amendment No.3 to NZS 3101:1995 (2003). This research has looked into the "paperclip" connection detail used in present practice and a potential retrofit connection detail.

The setup of these two dimensional component experiments were different from the past studies conducted by Mejia-McMaster and Park (1994), Herlihy et al (1995) and Oliver and Restrepo (1998) where the hollowcore unit was pulled off the supporting beam by a cyclic horizontal loading. In this research, the rotation effect between the hollowcore unit and the supporting beam was fully developed. The construction of the specimen was carried out in a way that matches the on-site construction as close as possible. These connection details were tested under cyclic loading up to interstorey drifts of ±4.0%.

Experimental and instrumental observations from the experiment were outlined.

The behaviour of the connection details was examined carefully to illuminate understanding of the observed failure modes of each specimen.

4.2 REVIEW OF RESULT

4.2.1 Specimen 1

There are some concerns with the performance of this connection experiment. The primary function of the paperclip in each cell is to transfer the vertical loading from the floor unit to the supporting beam. From the experimental study, it is found that the paperclip hardly did any work throughout the experiment. This is because once the shear crack has formed at the tip of the starter bar new bearing path has also formed, bypassing the paperclip. As a result, cracks have propagated along the web of the unit and the hollowcore unit was seen separated from the beam at the end of the experiment. The heavily reinforced connection joint has significantly increased the flexural strength of the connection. At the same time, it has also resulted in a greater stresses being developed within the hollowcore unit and the concrete topping. Specimen 1 shows that the bond between concrete topping and the precast was not sufficient to carry the vertical shear. Besides, the ductile mesh also demonstrated a positive result and did not fracture by the end of testing.

4.2.2 Specimen 2

Specimen 2 gave a similar crack pattern with Specimen 1. Similarly, the paperclip also did little work. Again, the overly reinforced connection joint had significantly raised the flexural strength of the connection and cause the end support to act like a rigid end block. Therefore, shear crack has occurred. After the shear crack has formed, new bearing path was formed and horizontal cracks were seen propagating along the bottom of the unit. Since Specimen 2 provided a 70mm seating, the hollowcore unit did not fail in the same manner as Specimen 1(no seating). The bottom section of the hollowcore unit at the end support was totally damaged and the web of hollowcore unit at the shear crack was also crushed. Ductile mesh used in this connection detail snapped at first cycles of -3.0% drift.

4.2.3 Specimen 3

The performance of this connection detail produced a positive result. The angle seat used in this connection served its purpose as a "catcher". The addition of the angle seat also has improved the positive drift moment capacity of the seating connection detail. However, this specimen shows poor performance under negative moments. The angle seat underneath the floor unit had somehow restrained the rotation movement of the hollowcore unit when subject to a rotation effect. This has changed the crack pattern formation within the hollowcore unit as compared with Matthews and Bull (2003) control detail (traditional detail). A shear crack was seen forming at the end zone of the starter bar and propagated toward the end support. High strength mesh was fractured at -2.0% drift cycles. As inter-storey drift increases, bottom section of the hollowcore floor near the end support was totally damaged and it cannot prevented the hollowcore unit from collapsing even with the angle seat in-place (Figure 2-8c(iii)).

4.3 CONCLUSIONS

Based on the research presented in this thesis, the following conclusions may be drawn:

1. Early researchers did not fully understand the importance of the relative rotation between the hollowcore unit and the supporting beam. It is this relative rotation that causes a snapping action at the ends of the hollowcore units. However, Matthews (2004) and Bull and Matthews (2003) has addressed this issue. Matthews (2004) has shown that the hollowcore unit failure mechanism observed under cyclic loading was very similar to that seen in Northridge earthquake.
2. Specimen 1 and 2 have suggested that over reinforced connection detail is not highly recommended. However the intention of these connection details testing is not to send the message that paperclip is bad for connection joint. Indeed, Bull and Matthews (2003) paperclip detail (2 R12 paperclips) has shown very positive result. These experiments were to educate engineers that only a certain amount of reinforcement can be tolerated at the connection joint, overly reinforcement at the connection joint is not recommended and should be avoided.
3. An angle seat has proved to be a possible retrofit solution that can be used for existing structure. The angle seat functions well to catch the floor when it may have a tendency to drop, but at the same time a totally different failure mechanism may also form. However, this experiment has shown that the retrofit solution is still incomplete. Improvements still can be made to the retrofit solution to further enhance performance, especially in the negative moment direction.

4. Floor delamination between the precast hollowcore floor unit and the concrete topping was observed at the end of experiment of Specimen 1 and 2. It has agreed with Mejia-Master and Park (1994), Herlihy et al (1995) and Oliver (1998) that the bond between the topping and precast is not enough and cannot be reliable to carry the vertical shear.
5. Ductile mesh has shown to perform better compared with high strength mesh as the ductile mesh has fractured at later drift amplitude. Ductile mesh had slightly increased the ductility performance of the connection joint.
6. All the connections tested are only a one off tests. Therefore it is unclear as to whether the observed results are conservative, unconservative or at mean value. These tests should be considered as an indication of the connection performance up to a point by recognising the limitations of the programme discussed.
7. The setup of these sub-assembly component experiments has ignored the three dimensional effect such as net horizontal tension in the floor slab, no plastic hinge forming in the beam in which hollowcore unit is seated, vertical acceleration, second order effects or a 45° earthquake attack, and no services loading have been included.
8. Specimen 2 out-performed Specimen 1. Specimen 2 demonstrated the importance of a seat. Adequate seating must be provided at all times. The presence of seating can significantly increase the life-span of hollowcore unit before collapse. The 70mm seating provided in Specimen 2 has allowed more damage to be inflicted to the connection joint, but without collapses.

9. Simple rational mechanics method was proposed to assess strength capacities of hollowcore to beam connection joint. Methods given are categorised for connections that are either reinforced or unreinforced cells with paperclips. The results appear to agree well with experimental observations.

4.4 RECOMMENDATIONS FOR PROFESSIONAL PRACTICE

1. The paperclip details tested in Specimen 1 and 2 has identified that over reinforcement at the connection joint is not suitable. These tests showed that the very rigid end had pushed the hinge further away from the beam face. Reviewing the 2-R12 paperclip test done by Bull and Matthews (2003), it has performed better than both Specimen 1 and 2 which had 4-R16. Therefore, it is recommended that only 2 paperclip should be used for each unit. The used of the bearing strip is also highly recommended.
2. Major strength discontinuity has been caused by the inclusion of paperclip. This has resulted in the formation of shear crack. In order to remedy this, it is recommended a longer starter bar length, which span approximately 3 to 4 meter from the beam face, be used so that the paperclip and the starter bars do not end at the same point.
3. Specimen 3 "broke its back" forming a shear crack at the end of starter bars. Obviously, the retrofit detail is not yet perfected. Therefore, it is recommended that a carbon fibre strip be used to enhance the connection detail negative

moment capacity. The carbon fibre strip should span 3m length from the beam face.

4. All connections should provide a seat of at least 75mm. This has take into account of construction tolerances and expected beam elongation effect at the supporting beam.

5. Specimen 2 has showed that the presence of a seat can significantly delay the collapse of a hollowcore unit. In a situation where a hollowcore unit has a negative seating, angle seat should be inserted to give adequate vertical support.

4.5 RECOMMENDATIONS FOR FURTHER RESEARCH

1. The next step up to conduct a connection testing is to include three dimensional effect particularly net tensions in slab-beam connection. To what extend the net tension played in connection is still unknown. It is the feeling that the hollowcore units would have dropped earlier, but how much earlier is unknown. The challenge of this will be to determine the amount of horizontal tension force should be inserted into the floor unit.

2. Longer development starter bar length should be used typically at the connection joint to avoid extreme strength discontinuity. From Specimen 1 and 2, it was identified that shear crack has formed at the point where both starter bar and paperclips tie reinforcement end. However, the true performance of the seating connection detail with longer starter bars is still unknown. Figure 4-1 shows a

seating connection detail with a starter bar span about 3m long from the starter bar.

3. Test specimens in this research demonstrated poor performance under negative moments. The brittle type failure with diagonal shear crack plane forming at the end of the starter bars caused a sudden drop in the connection moment capacity. Clearly, some negative moment enhancement is needed. Carbon fiber strips can be used to increase the negative moment capacity of the seating connection. Figure 4-2 shows a carbon fiber strips glued to the top of the floor from the end of the specimen to about 3 meters length. The question now lies in how much the carbon fiber strips can improved the overall performance of the seating connection detail.

4. Over reinforcement at a connection joint must be avoided. However, there is no clear defining boundary on how much steel is defined as over-reinforcement. Therefore, future research is required to work out a mathematical model that can be apply to common connection design for determining the appropriate amount of steel that can be use at a connection joint.

5. Hollowcore floors are certainly not the only common precast floor typed used in New Zealand. All the major precast floor types such as T-slab used in New Zealand should be tested to determine their vulnerability to catastrophic damage.

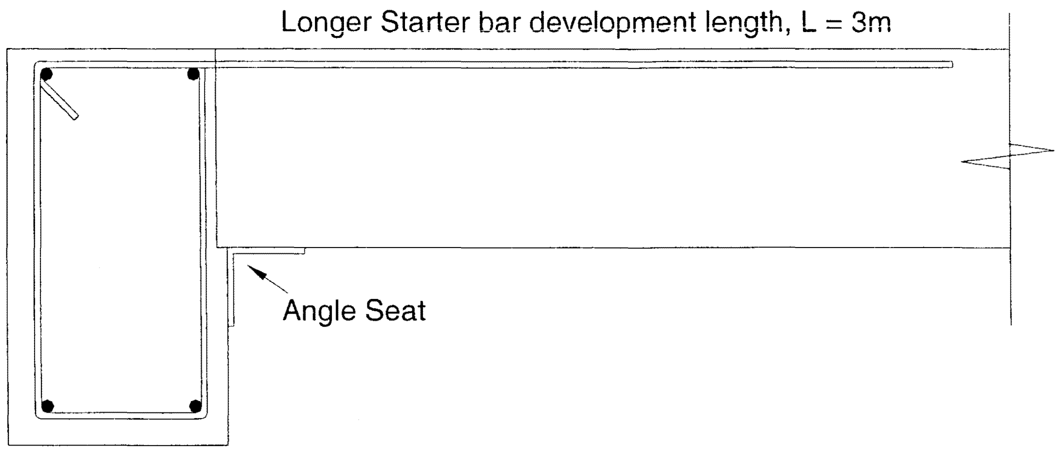

Figure 4-1 Seating connection detail with 3m long starter bar

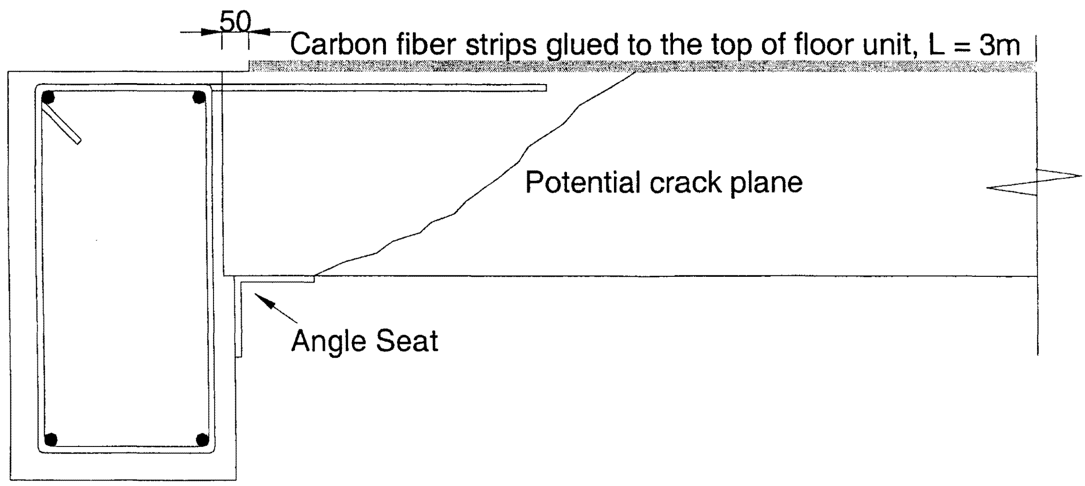

Figure 4-2 Carbon fiber strips glued to the top of the floor

4.6 REFERENCE

Bull D. k, Matthews J.G, 2003, *Proof of Concept Tests for Hollowcore Floor Unit Connections*, Precast NZ report, Feb 2003, pp25.

Herlihy M.D, Park R. and Bull D.K, 1995, *Precast Concrete Floor Unit Support and Continuity*, Research Report 93/103, Department of Civil Engineering, University of Canterbury, Christchurch, New Zealand

NZS3101, 1995, *Concrete Structures Standard, NZS 3101, Part 1 & 2*, Standards New Zealand, Wellington, New Zealand

NZS3101, 2003, *Draft Amendment No.3 to 1995 Standard (NZS 3101)*, Standards New Zealand, Wellington, New Zealand

Mejia-McMaster J.C and Park R., 1994, *Tests on Special Reinforcement for the End Support of Hollow-Core Slabs*, PCI Journal, Vol 39, No. 5, pp. 90-105, September-October.

Oliver S. J and Restrepo J, 1998, *The Performance of Concrete Topped Precast Hollowcore Flooring Systems Reinforced With and Without Dramix Steel Fibres Under Simulated Seismic Loading*, Master of Engineering Thesis, Department of Civil Engineering, University of Canterbury, Christchurch, New Zealand.

Appendix A:

A.1 DETAIL OF TEST SPECIMEN

Figure A-1 summarises three different types of hollowcore unit end connection details that is being investigated in this research. Two of the seating connection details, Specimen 1 and 2, in this research possessed paperclip detail as shown in Figure A-1 (a) and (b). These seating connection details consisted of 4-R16 (Grade 500) paperclips; HD-12 (Grade 500) starter bars and a ductile mesh centrally positioned in a 75mm deep cast in-place 30 MPa concrete topping. The difference between these specimens is Specimen 2 has 70mm seating and Specimen 1 has zero seating. Finally, Specimen 3 (Figure A-1(c)) is a potential retrofit detail utilizing a 150 x 150 x 12mm equal angle seat. This angle seat was tightly bolted to the side of the supporting beam underneath the hollowcore unit. The function of this angle seat is to act as a "catcher" when the hollowcore unit loss it's seating under severe seismic action. This specimen used a traditional connection detail which consisted of 50mm mortar bed seating, HD-12 (Grade 500) starter bars; high strength mesh and a bearing strip beneath the hollowcore unit attached to the angle seat. Figure A-1 (d) shows a cross section of the 300 series hollowcore unit used in this experiment and Figure A-2 shows the plain view of the paperclip and retrofit detail.

In order to obtain a direct comparable result between the present experiments and the work of Bull and Matthews (2003), the supporting beam's dimensions and hollowcore unit used in these testing was chosen to be the same. Figure A-3 shows the layout of the supporting beam and details of the transverse reinforcement in the beam. The supporting beam was 750 mm deep, 2600 mm long and nominally 670 mm wide. The beam width varies slightly depending on the seat length used in each of the test. It consisted of a 6-D24 (Grade 300) longitudinal bars top and bottom and 25-R12 stirrups at 100 mm centers to centers. Details of the HD-12 (Grade 500) starter bars, 4-R16 paperclip and 150 x 150 x 12mm (Grade 320) angle seat are shown in Figure A-4 and Figure A-5, respectively.

A.1.1 Load to be resisted

Test specimens in this research are modelled on a 12m span long hollowcore floor unit as shown in Figure A-6. Therefore, dead load and live load of the 12m long hollowcore floor unit can be calculated as:

Dead Load:

Hollowcore unit self-weight	= 3.2 kPa
Topping weight	= Density of concrete x topping thickness
	= 23.5 kN/m^2 x 0.075mm
	= 1.76 kPa
Superimposed dead load	= 0.5 kPa

Therefore Total dead load, G = 3.2 + 1.76 + 0.5 = 5.46 kPa

Live Load:

New Zealand loading code (NZS4203:1992) specifies that the factored live load for ultimate limit state, Q_u, shall be obtained by multiplying the reduced live load, $Q_{reduced}$, by the live load combination factor, ψ_u, shown in Equation A-1.

$$Q_u = \Psi_u Q_{reduced} \tag{A-1}$$

where $$Q_{reduced} = \Psi_a Q_b \tag{A-2}$$

and $$\Psi_a = 0.5 + \frac{4.6}{\sqrt{A}} \leq 1.0 = 0.5 + \frac{4.6}{\sqrt{12 \times 1.2}} = 1.71 \leq 1.0 \tag{A-3}$$

where ψ_u = 0.4 for office use only (NZS4203:1992) and Q_b = basic live load (2.5 kPa for office use only). Hence for a 12m length hollowcore unit and width of 1.2m, $Q_{reduced}$ = 2.5 kPa and Q_u = 1 kPa. The loading code (NZS4203:1992) has identified six ultimate limit state load combination that should be considered when designing concrete structures. Of these, the combinations:

$$1.2G \,\&\, 1.6Q = 1.2(5.46) + 1.6(1.0) = 8.15kPa \tag{A-4}$$

are the most critical when designing for the connection detail. The vertical reaction or design shear force, V^*, demanded at the connection joint can thus be calculated as:

$$V^* = \frac{wl}{2} = \frac{8.152 \times 12 \times 1.2}{2} = 58.7kN \tag{A-5}$$

A.1.2 Starter bars Design

According to New Zealand Concrete Standard (NZS3101:1995) the basic development length of a deformed bar in tension, L_{db}, can be calculated from:

$$L_{db} = \frac{0.5\alpha_a f_y}{\sqrt{f'_c}} d_b = \frac{0.5 \times 1.0 \times 500}{\sqrt{30}} \times 12 = 548mm \approx 600mm \tag{A-6}$$

where f'_c = specified compressive strength of concrete (30 MPa for topping); d_b = nominal bar diameter (12mm diameter starter bar); f_y = lower characteristic yield strength of the reinforcement (Grade 500 for starter bars) and α_a = development length parameter taken (1.0 for less than 300 mm of fresh concrete cast below the bar). The Concrete Code (NZS 3101:1995) also specified that the minimum bend diameter of a hook bar, d_i, measured to the inside of the bar should be given as:

$$d_i \geq 0.92\left(0.5 + \frac{d_b}{s_b}\right)\left(1 - \frac{L_b}{L_{db}}\right)\frac{f_y}{f'_c} d_b \tag{A-7}$$

$$d_i = 0.92\left(0.5 + \frac{12}{35}\right)\left(1 - \frac{341}{548}\right)\frac{500}{30} \times 12 = 58mm$$

where s_b = starter bar diameter plus concrete cover (35mm); L_b = distance from critical section to start of bend (341mm) and L_{db} (=548mm), f_y (=500 MPa), f'_c (=30MPa) and d_b (=12mm) are previously defined. Concrete code (Table 7-1, NZS 3101:1995) states that the minimum bend diameter for bar diameter in the range of 6 to 20 mm should not be smaller than 5 d_b. Therefore bend diameter of the starter bar is 60 mm.

A.1.3 Paperclips Design

According to Concrete Code (NZS3101:1995) shear force, V_n, transferred across a rough, irregular crack by shear friction is given by:

$$V_n = \phi \mu_f (A_{vf} f_y + N^*) \tag{A-8}$$

Rearranging Equation A-8, the minimum required amount of shear reinforcement, A_{vf}, at the connection joint can be calculated as:

$$A_{vf} \geq \frac{V_n}{\phi \mu_f f_y} = \frac{58700}{0.75 \times 1.4 \times 500} = 111.8mm^2 \tag{A-9}$$

where V_n = 58.7kN; φ = strength reduction factor (0.75 for shear); μ_f = coefficient of friction in the concrete (assumed 1.4 for situation where monolithic concrete exists in the predicted crack location); f_y = lower characteristic yield strength (Grade 500 for R16 reinforcing steel) and N* = design axial load (taken as zero since the setup of this experiment ignored net tension within the beam-floor connection).

However, when the principles of shear friction no longer apply when beam elongation occurs and significant axial tension exists across a crack the kinking mechanism take over. Once the hollowcore floor unit loss the seating, all shears will be taken by the paperclips and the NZ guideline for precast concrete buildings (CAE, 1999) recommends that the kinking angle α < 30. The paperclip shears strength in kinking mechanism is described in Equation 1-2. Rearranging Equation 1-2 and it becomes:

$$A_s \geq \frac{V_n}{f_y \sin \alpha} = \frac{58700}{500 \times \sin 30} = 235mm^2 \tag{A-10}$$

Therefore, a minimum of 235 mm^2 of reinforcing area is required across the crack. Only 1 paperclip, $A_s = 402.1 mm^2$ (2 leg), is required for each hollowcore unit. Hence the 4-R16 paperclip used in Specimen 1 and 2 has more than enough strength capacity to carry the hollowcore unit.

A.1.4 Angle Seat Design

Angle seat was used in Specimen 3. Its function is to support the hollowcore unit when it lost its seating under seismic action. Therefore it is prefer to have a longer angle seat. Low friction bearing strip was placed on the angle seat to exert a compression force at the bottom strand and consequently improved shear capacity of the unit. The largest possible seat length that is available, from manufacture guide, is 150x 150mm equal angle. The bolt hole in the angle seat was located as high up as possible. This is to minimise the rotation or the movement of the angle seat as much as possible when bolted onto the supporting beam. Figure A-7 shows the bending moment diagram of the angle seat when the floor weight acted onto the seat. The design bending moment, M^*, of the angle seat is therefore given by:

$$M^* = (V^*)\, x \text{ (seat length)} = 8.85 \text{ kNm} \qquad \text{(A-11)}$$

According to Steel structure code (NZS3404:1997), the nominal member moment capacity, M_n, of the angle seat can be calculated as follows:

$$M^* \leq M_n = \phi \alpha_m \alpha_s M_s \qquad \text{(A-12)}$$

where $M_s = f_y Z_e$ (A-13)

and $Z_e = \frac{1}{4} b t^2$ (A-14)

where, M_s = Section capacity moment; f_y = lower characteristic strength of the angle seat (320 MPa); ϕ = strength reduction factor (= 0.9 for moment); α_m = moment modification factor; α_s = slenderness reduction factor; Z_e = effective section modulus;

b = width of the angle seat (= 1.2m) and t = thickness of angle seat. Substituting Equation A-13 to A-14 into Equation A-12, the minimum angle seat thickness, t, required for a 150 x150mm angle seat (with $\alpha_m\alpha_s$ = 1.0) is given by:

$$t \geq \sqrt{\frac{4M*}{\phi\alpha_m\alpha_s f_y b}} = \sqrt{\frac{4\times 8850}{0.9\times 1.0\times 320\times 1.2}} = 10.13mm \qquad \text{(A-15)}$$

The next size up for angle seat thickness is 12 mm.

Bolts (Ramset's Spatec safety anchor) were used to anchor the angle seat onto the supporting beam. Four bolts were used to carry a total shear force of 59 kN. Table A-2 shows the properties and dimension for each of the bolts.

A.1.5 Vertical Loading

In order to calculate the vertical loading at midspan for the indeterminate structure, the sum of right hand side end deflection of Case 1, 2 and 3 shown in Figure A-8 should be equal to zero.

$$\delta_{Total} = \delta_1 + \delta_2 + \delta_3 = 0 \qquad \text{(A-16)}$$

$$R = \frac{3}{2}\frac{Pa^2}{L^3}\left(L - \frac{a}{3}\right) + \frac{3wL}{8} \qquad \text{(A-17)}$$

The vertical loading, P, can hence be expressed in term of the vertical shear force, V*, required at the seating.

$$V* = wL + P - R \qquad \text{(A-18)}$$

$$P = \frac{V* - \frac{11}{8}wL}{\left(1 - \frac{3}{2}\frac{a^2}{L^2} + \frac{1}{2}\frac{a^3}{L^3}\right)} \qquad \text{(A-19)}$$

Using a = 3m, L = 6m, V*=58.7kN and w = 9.78kNm, the vertical loading required to match the in-situ shear force at the seating connection is P = 32kN. A force of 35 kN was applied at all time during testing.

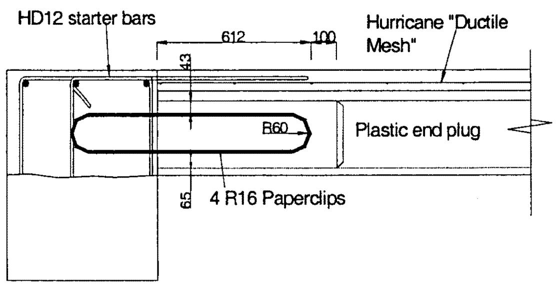

(a) Hollowcore unit 1 dimensions

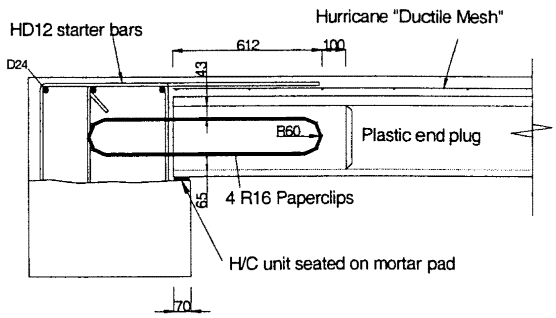

(b) Hollowcore unit 2 dimensions

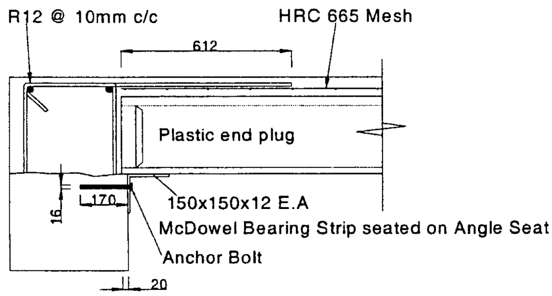

(c) Hollowcore unit 3 dimensions

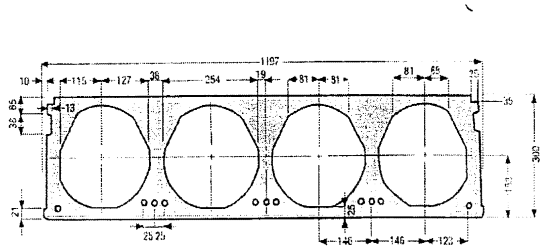

(d) Cross section of hollowcore unit

Figure A-1 Dimensions of test specimen

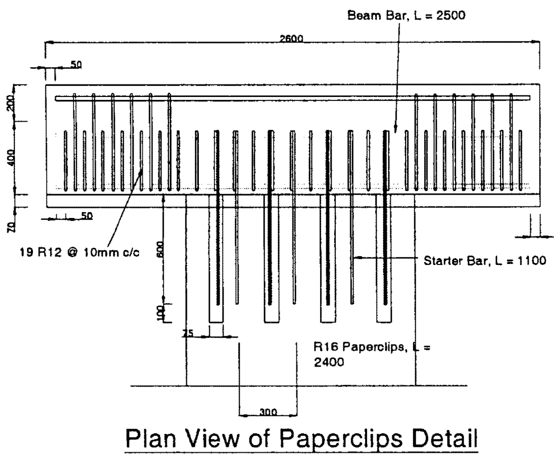

(a) Plain view of paperclip detail

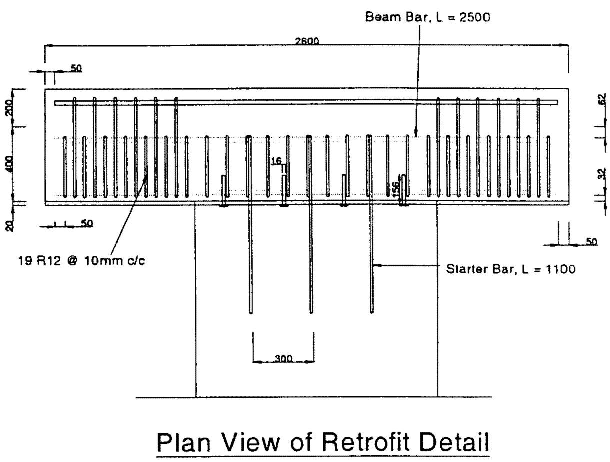

(b) Plain view of retrofit detail

Figure A-2 Plain view of the test specimen

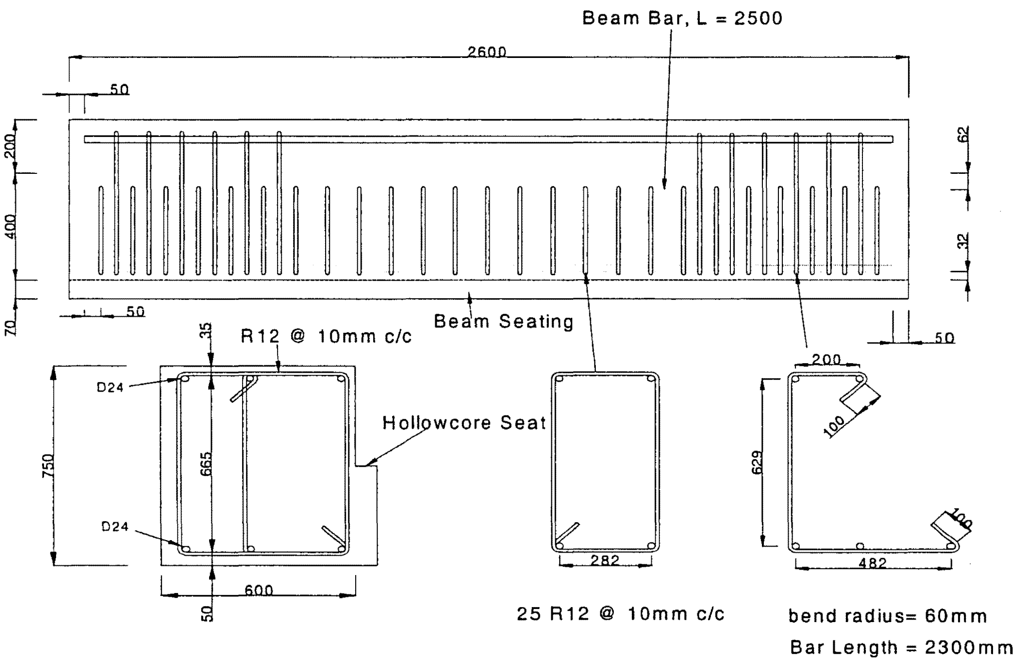

Figure A-3. Dimensions of supporting beam

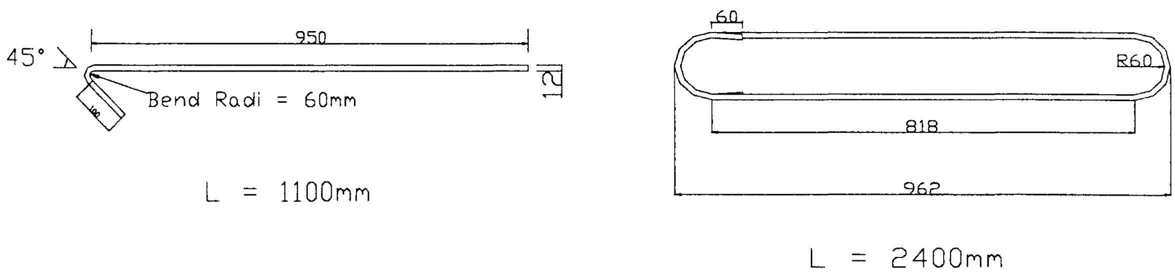

(a) HD-12 starter bar

(b) R-16 paperclip

Figure A-4 Detail of starter bars and paperclip used in the Test Specimen

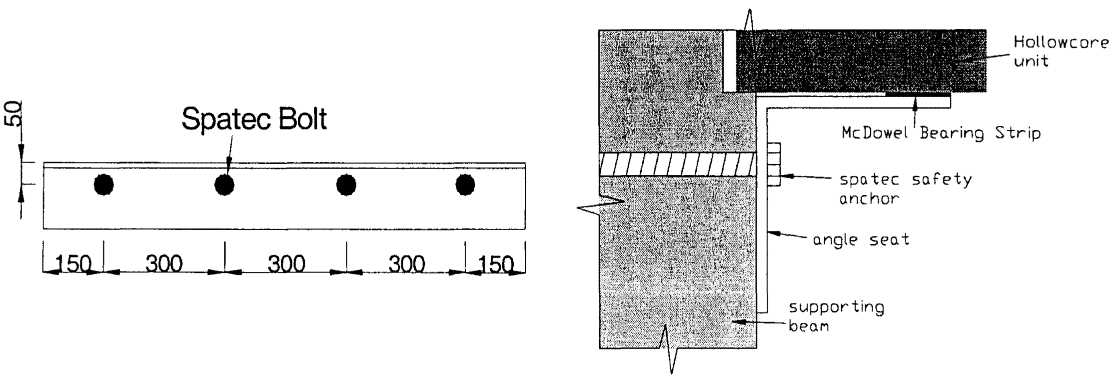

(a) Plain view of Angle Seat

(b) Bearing strip positioned on angle seat

Figure A-5 Details of angle seat

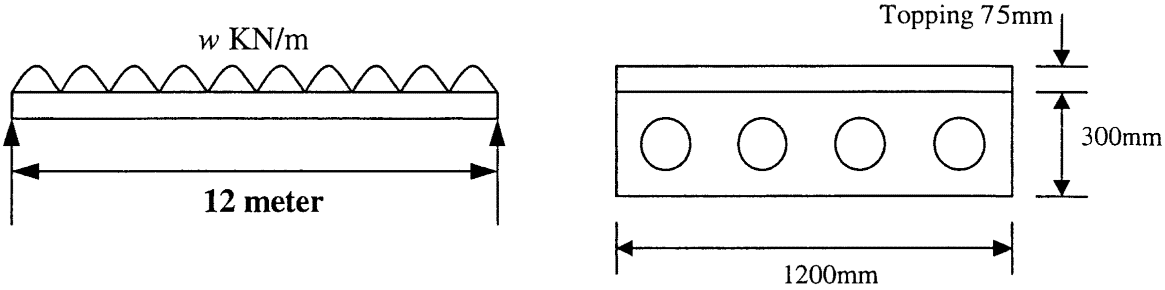

Figure A-6 Model dimension of test specimen

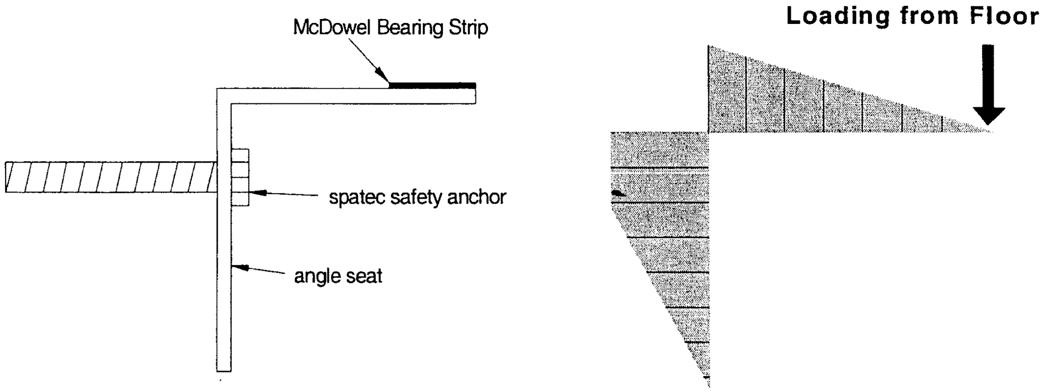

Figure A-7 Bending moment diagram on the angle seat

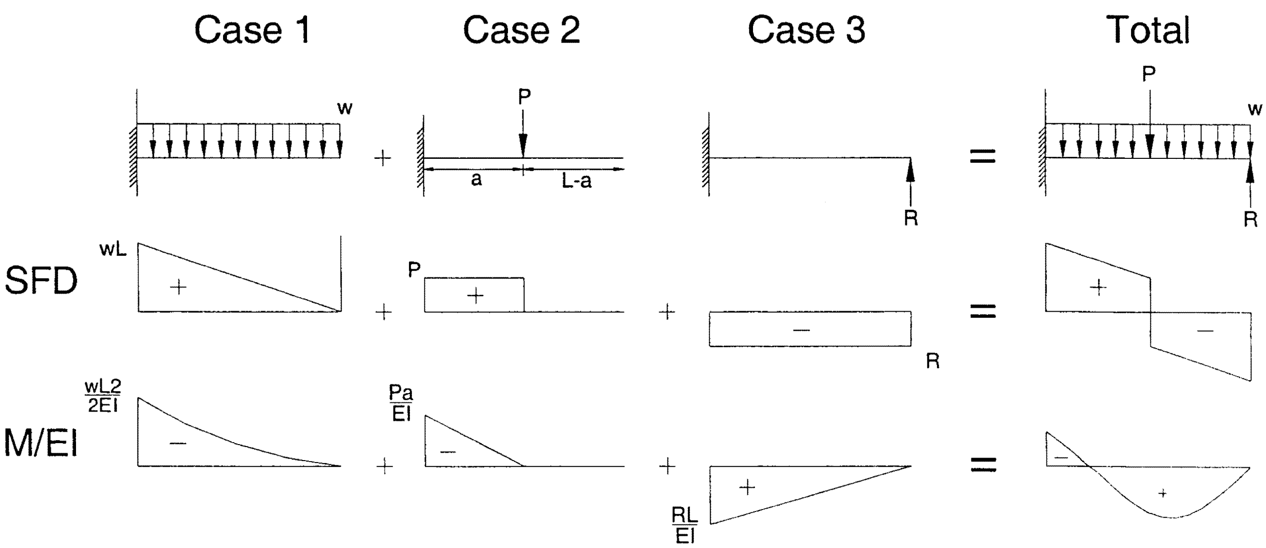

Figure A-8 Determination of SDF and BMD using superposition

A.2 MATERIAL PROPERTIES

A.2.1 Hollowcore Properties

The propriety 300 series "Dycore" precast hollowcore units were used in these investigations. Hollowcore units are constructed by means of an extrusion process on a long line prestressing bed. In this research project, the hollowcore floor used was supplied by Stresscrete Division of Firth Industries in Christchurch. Table A-1 summarised the section properties of the 300 series hollowcore unit.

Table A-1 Section properties of 300 series Dycore

Unit	Area (m^2)	Y_b (mm)	I (m^4)	Self Weight (KPa)	f'_c (@28days)
300 Dycore/partek	0.6106	153	2.04×10^{-3}	3.20	42 MPa

A.2.2 Safety Bolt Properties

Table A-2 summarised the properties and dimension of the anchor bolt used in the Test Specimen.

Table A-2 Properties and dimension of the Spatec Safety Bolt

No. of Bolt	Shear/bolt	Tensile capacity	Anchor size	Length
4	14.75 KN	29.5 KN	16 mm	170 mm

A.2.3 Concrete Compressive strength tests

In this experiment, all the concrete pours used a 30 MPa mix with a maximum aggregate size of 19mm (3019AW). The mix also has a specify slump of 100mm. Table A-3 shows the concrete compressive strength of the beam and concrete topping.

Table A-3 Concrete compressive strength

	7 day	28 day	At testing
Beam	24.5	39.3	32.6 MPa
Topping	35.9	43.7	39.8 MPa

A.2.4 Steel Testing

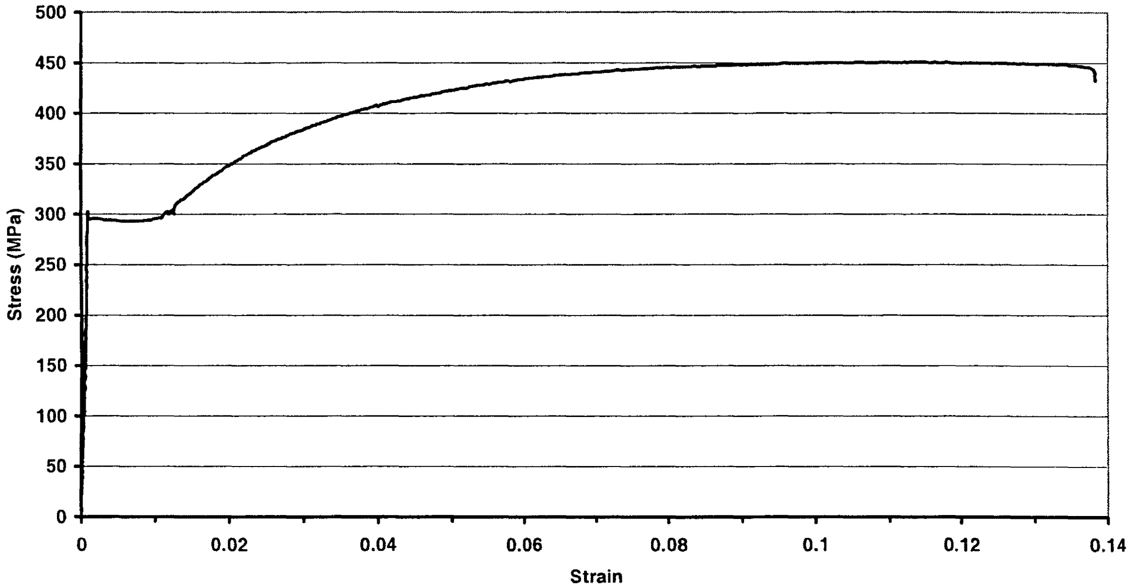

(a) Beam longitudinal reinforcement (D24)

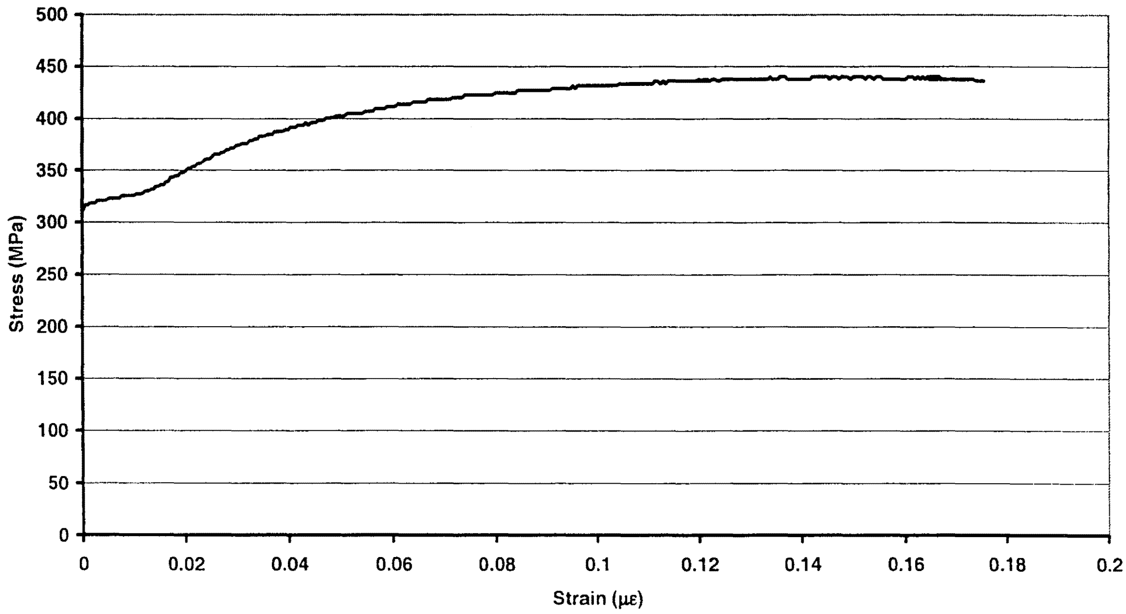

(b) Longitudinal beam transverse reinforcement (R12)

Figure A-9(a) Stress-strain curve for steel reinforcement

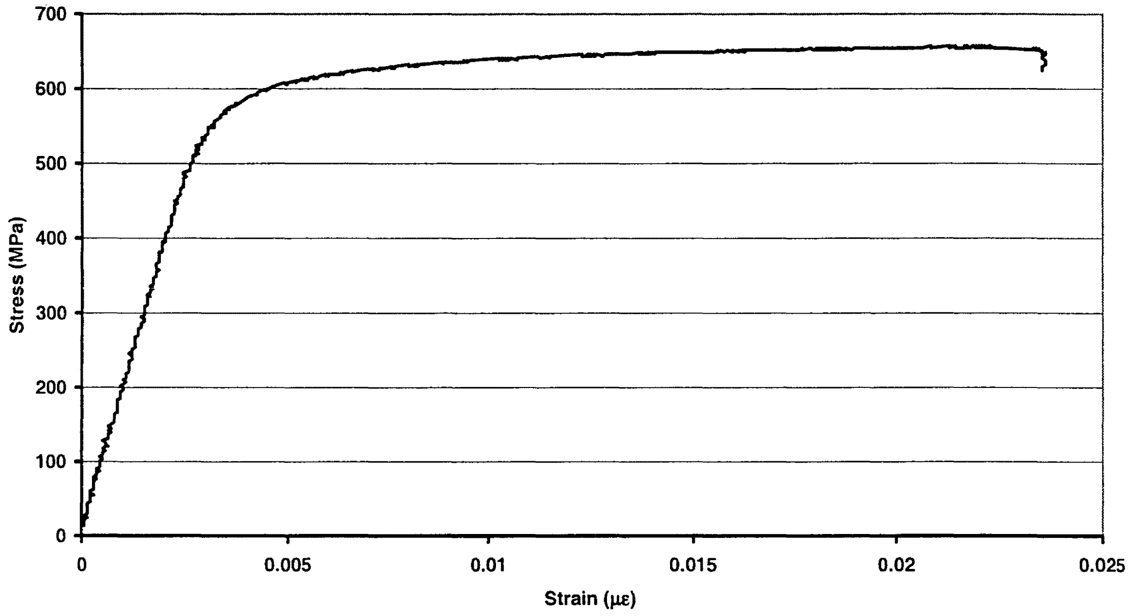

(c) Cold drawn wire mesh (665)

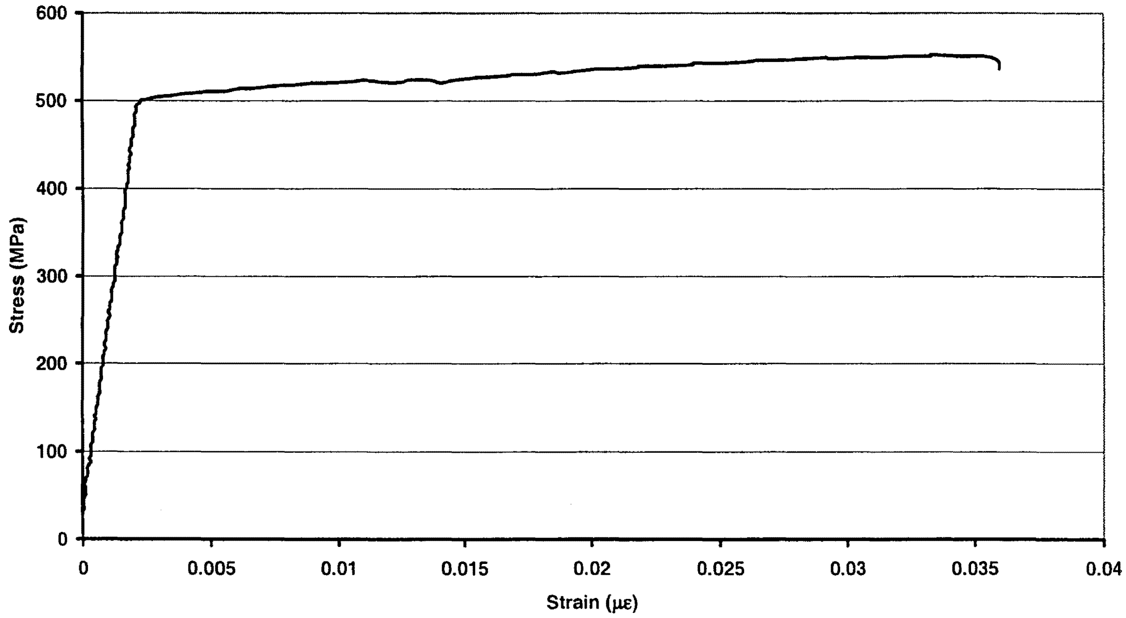

(d) Hurricane ductile mesh

Figure A-9(b) Stress-strain curve for steel reinforcement

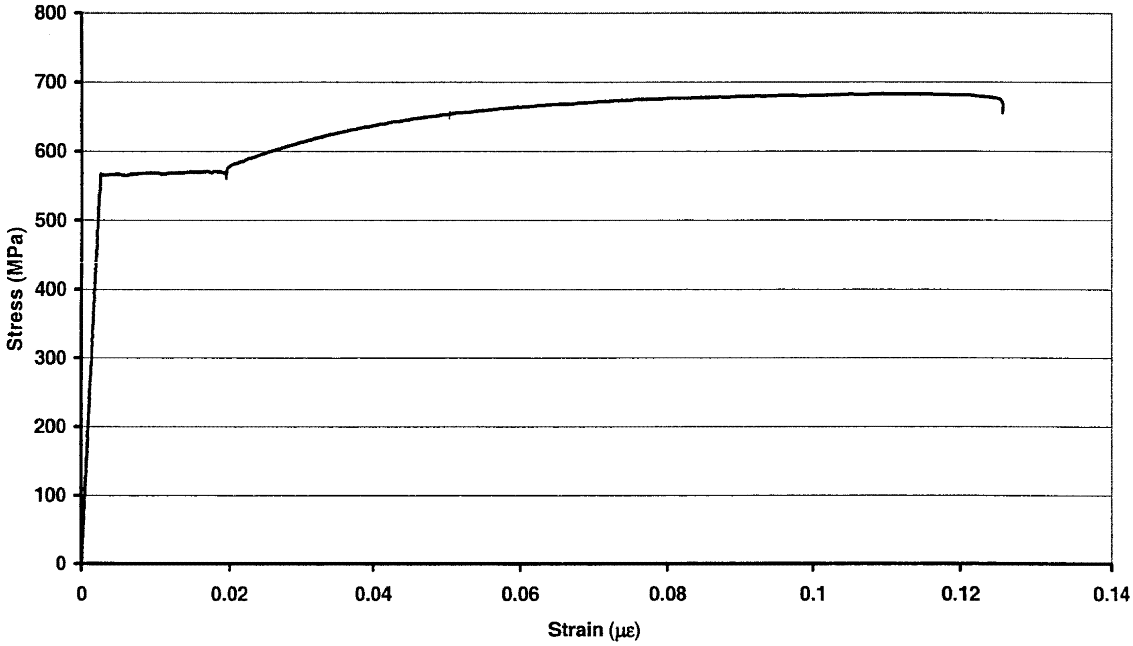

(f) Grade 500E starter bar (HD12)

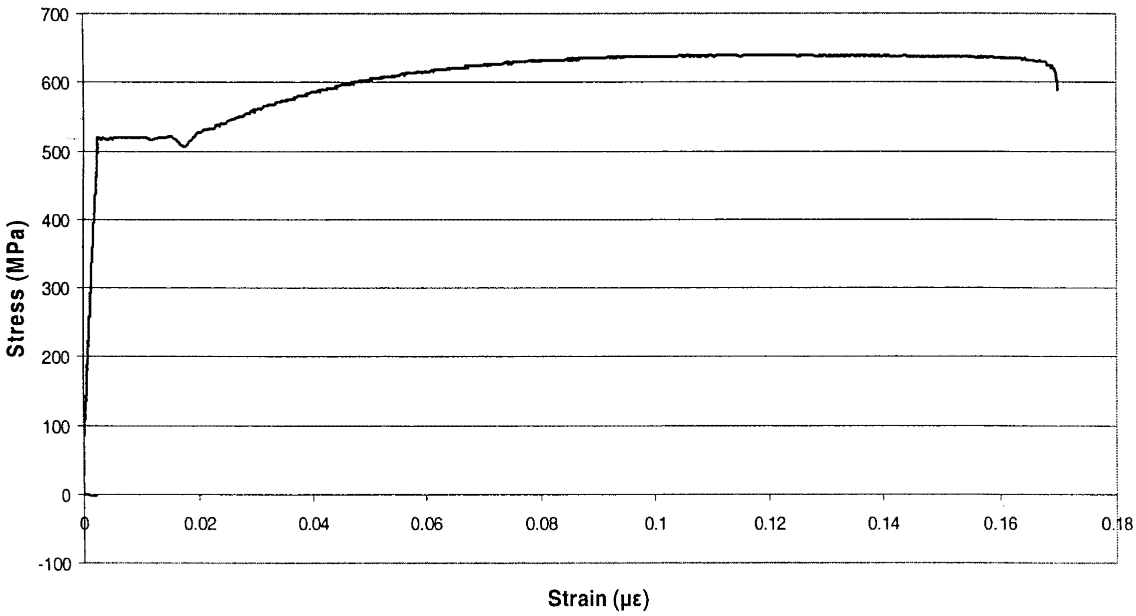

(g) Grade 500E paperclip (R16)

Figure A-9(c) Stress-strain curve for steel reinforcement

A.3 FURTHER RESULT OF TEST SPECIMEN

Further details of the instrumental observations made during each experiment are presented for the southern starter bars and paperclip strain distribution in what follows. It should be noted that upon the completion of the data analysis the target drifts from ±0.5% to ±4.0% were not always achieved during the testing due to beam flexibility. Table A-4 has presented the corrected target drift of the experiment.

Table A-4 Target inter-storey drift versus actual inter-storey drift

Target Drift (%)	H/C Test 1	H/C Test 2	H/C Test 3
0.5	0.49	0.499	0.462
-0.5	-0.48	-0.472	-0.436
0.5(2)	0.49	0.491	0.4585
-0.5(2)	-0.48	-0.471	-0.44
1.0	0.97	0.982	0.959
-1.0	-0.99	-0.979	-0.898
1.0(2)	0.96	0.972	0.958
-1.0(2)	-0.99	-0.979	-0.912
2.0	1.99	2.678	1.939
-2.0	N/A	-1.999	-1.876
2.0(2)	N/A	2.412	1.937
-2.0(2)	N/A	-1.990	-1.924
3.0	N/A	3.439	2.92
-3.0	N/A	-3.0	-2.915
3.0(2)	N/A	3.416	2.906
-3.0(2)	N/A	-2.997	-2.917
4.0	N/A	4.406	N/A
-4.0	N/A	-4.084	N/A

A.3.1 Specimen 1

Figure A-10(a) and (b) presented the southern starter bars and paperclip instrumental observation of Specimen 1. Figure A-10(a) shows the southern starter bar strain profile in the positive and negative drift directions. Majority of the strains were recorded to concentrate at the end of the starter bars concrete topping. The starter bars remained in the elastic range in the positive drift direction but have slightly yielded in the negative drift at the beam-floor interface. After shear crack has formed, the starter bars carried little loads.

Figure A-10(b) shows southern paperclip strain distribution of Specimen 1 in positive and negative drift direction. The paperclip did not yield during the experiment and it has carried little load after the diagonal shear crack plane has formed at the end zone of the starter bars. It should be noted that both top and bottom paperclip strain registered tensile strains throughout the experiment under both positive and negative drift. The overall performance of the northern and southern paperclip was shown in Figure A-11. Both paperclips have registered similar result in both drift direction.

Figure A-12 shows the vertical and horizontal movements of the hollowcore end unit with relative with the supporting beam. Note that the hollowcore unit has recorded a huge drop of approximately 48mm at 2.0% drift amplitudes.

A.3.2 Specimen 2

Figure A-13(a) and (b) shows the southern starter bars and paperclip strain distribution profile of Specimen 2. Figure A-13(a) show that majority of the strains were concentrated at the end of the starter bars concrete topping. Figure A-13(b) shows that the bottom chord of the southern paperclip has recorded yield in the positive drift. However, the top chord of the paperclip has done little work under both drift amplitude direction. The overall performance of the northern and southern paperclip was shown in Figure A-14. Both paperclips have registered similar result.

Figure A-15 explained the horizontal and vertical movement of the Hollowcore floor unit relative to the supporting beam. However these displacements cannot represent the true displacement of the unit since the potentiometer only measure the displacement at the end support while most of the movement occurred at or near the shear cracks. Then again, the potentiometer recorded its largest horizontal and vertical movement of 2.6mm and 1.1mm at 2.0% drift.

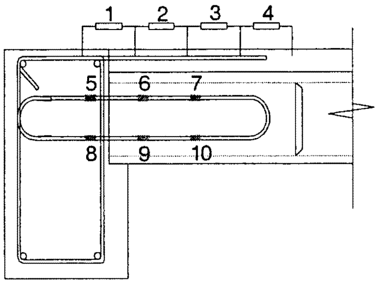

Instrument Layout

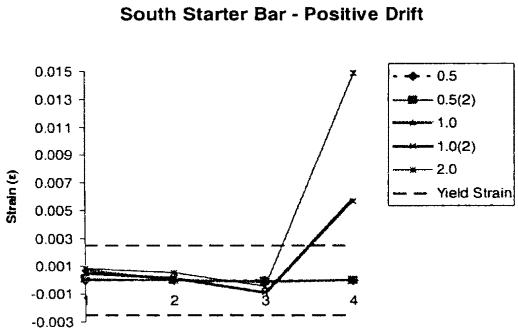

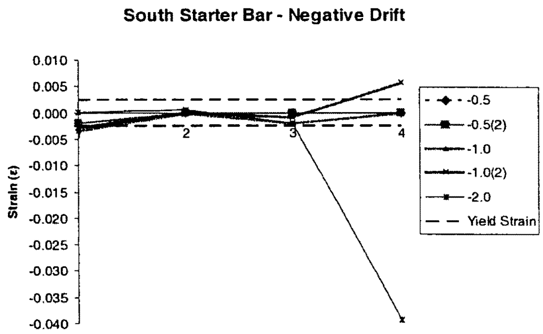

(i) Positive drift **(ii) Negative drift**

(a) Southern starter bar strain distribution

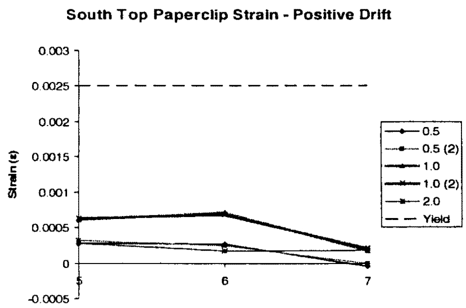

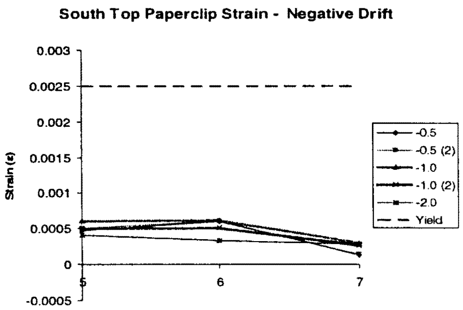

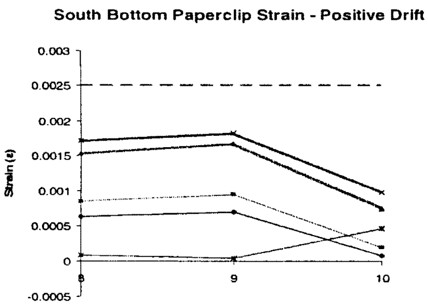

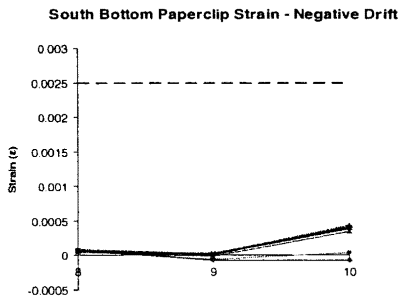

(i) Positive drift direction **(ii) Negative drift direction**

(b) Southern paperclip strain distribution

Figure A-10 Southern starter bars and paperclip strain distribution of Specimen

1

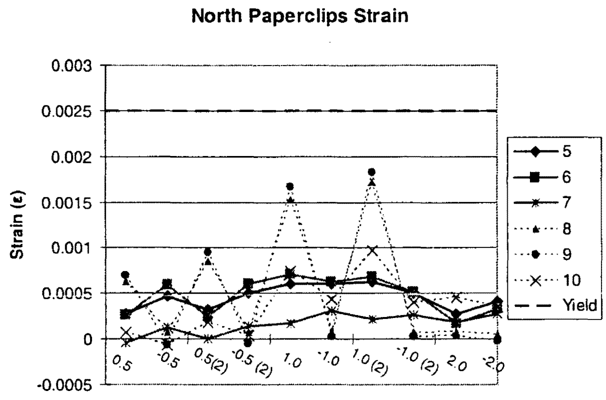

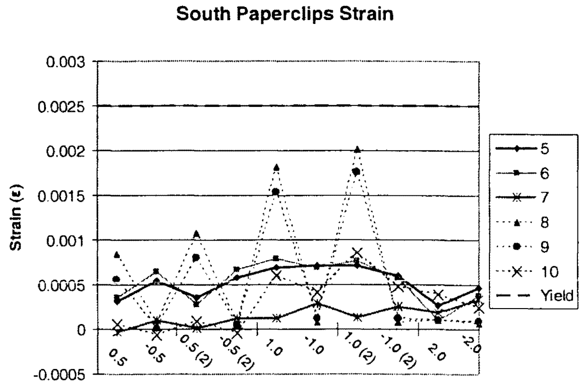

(a) Northern Paperclip strain **(b) Southern Paperclip strain**

Figure A-11 Specimen 1 Northern and Southern paperclip strain distribution

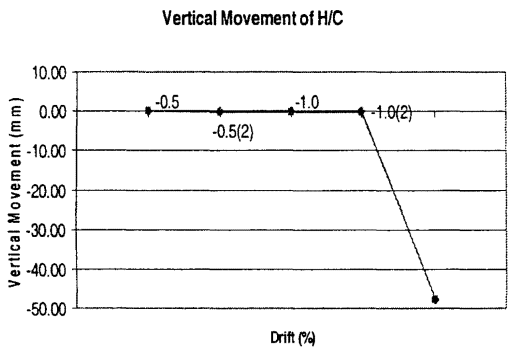

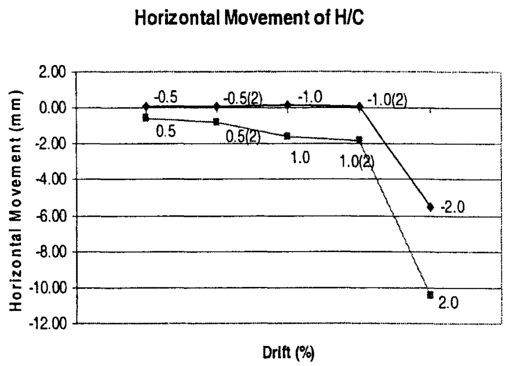

(a) Vertical movement of hollowcore unit **(b) Horizontal movement of hollowcore unit**

Figure A-12 Relative movement between the supporting beam and hollowcore unit of Specimen 1

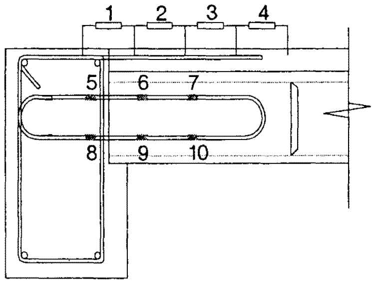

Instrument Layout

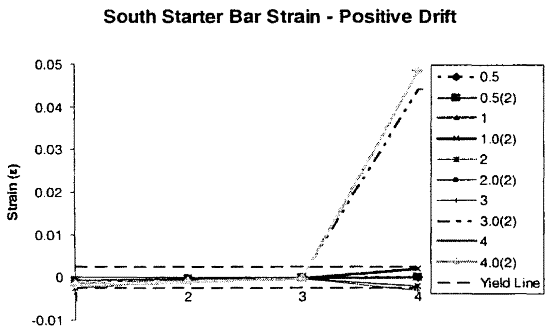

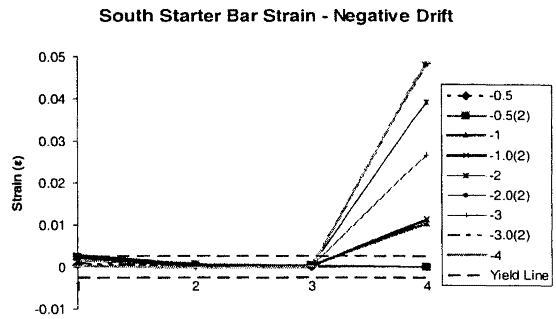

(i) Positive drift **(ii) Negative drift**

(a) Southern starter bar strain distribution

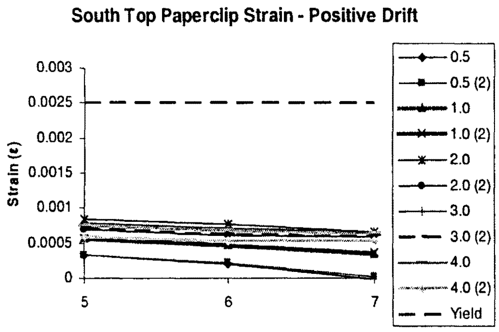

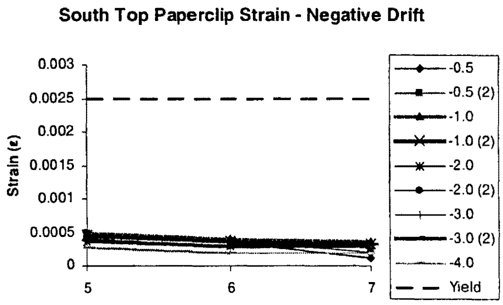

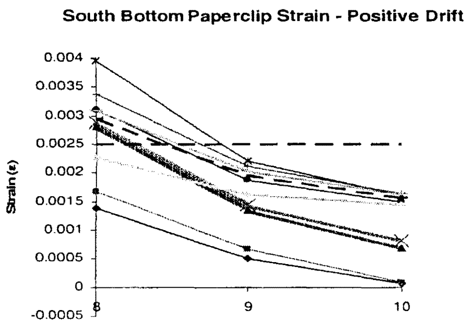

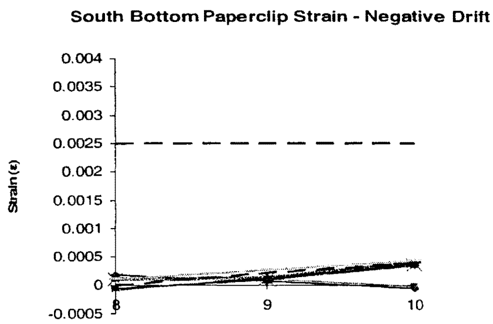

(i) Positive drift direction **(ii) Negative drift direction**

(b) Southern paperclip strain distribution

Figure A-13 Southern starter bars and paperclip strain distribution of Specimen 2

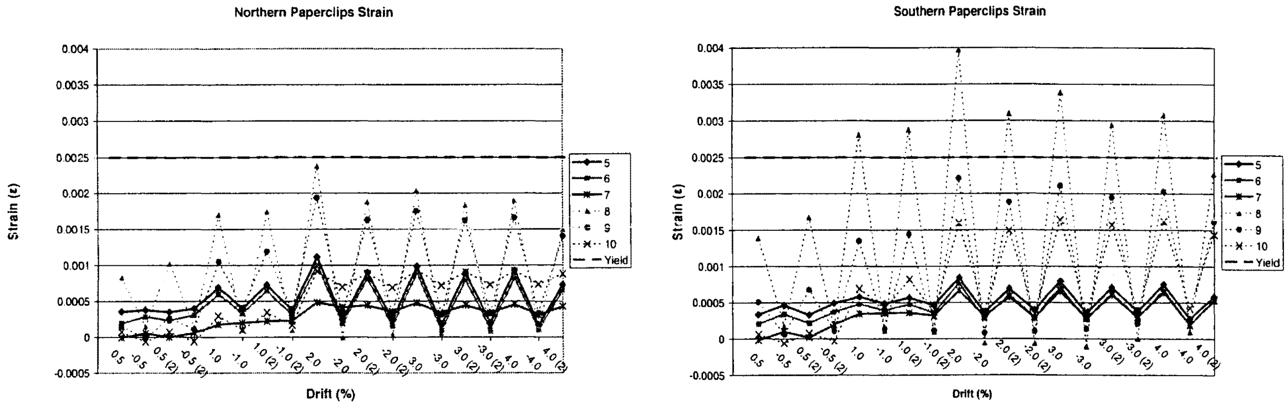

(a) Northern Paperclip strain (b) Southern Paperclip strain

Figure A-14 Specimen 2 Northern and Southern paperclip strain distribution

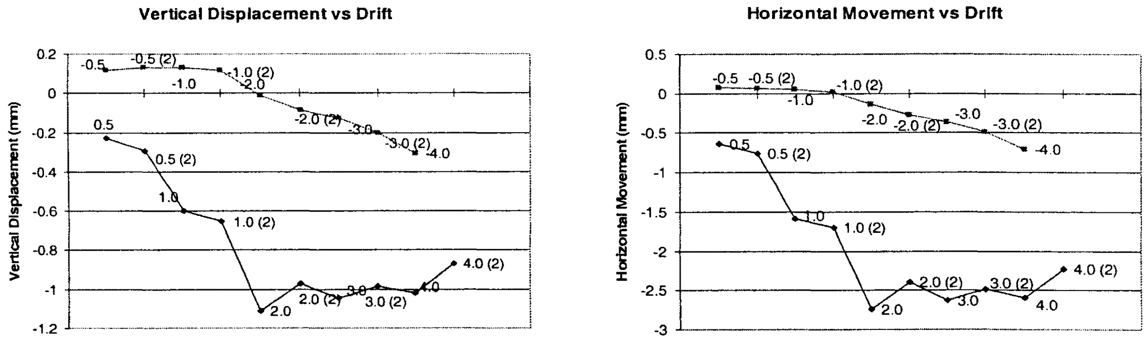

(a) Vertical movement of hollowcore unit (b) Horizontal movement of hollowcore unit

Figure A-15 Relative movement between the supporting beam and hollowcore unit of Specimen 2

Appendix C: Full Detail Calculations

C.1 MOMENT CAPACITY OF SPECIMENS

C.1.1 Specimen 1: 4-R16 with zero seats

Positive Moments:

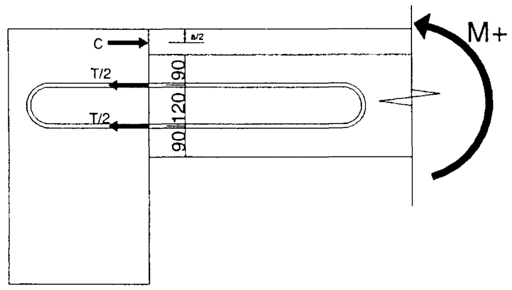

The moment capacity of the connection is estimate by multiplying the tension reinforcement within the flange with the lever arm, *jd*, between the centroids of the compression force and the tension reinforcement.

$$T = A_{spaperclip} f_y = \left(4 \times 2 \times \frac{\pi}{4} \times 16^2\right)(500) = 804.2kN$$

$$a = \frac{T}{0.85 f'_c b} = \frac{804000}{0.85 \times 30 \times 1200} = 26.3mm$$

$$jd = 150 + 75 - \frac{26.3}{2} = 212mm$$

$$M_T^+ = Tjd = 804 \times 0.212 = 171kNm$$

Negative Moments:

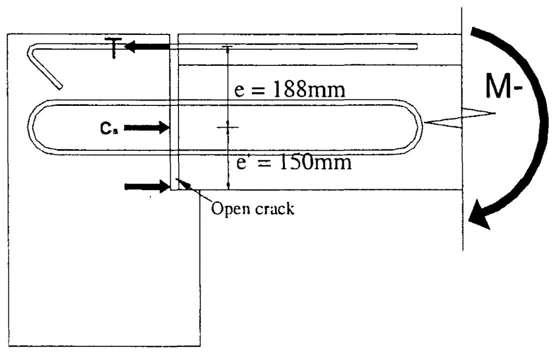

$$T = A_{starter} f_y = \left(4 \times 2 \times \frac{\pi}{4} \times 12^2\right)(500) = 226.2kN$$

$$M_n^- = Te + \mu Ne' = 226.2 \times 0.188 + 1.2 \times 5.4 \times 0.15 = 49kNm$$

C.1.2 Specimen 2: 4-R16 with 70mm seats

Positive Moments:

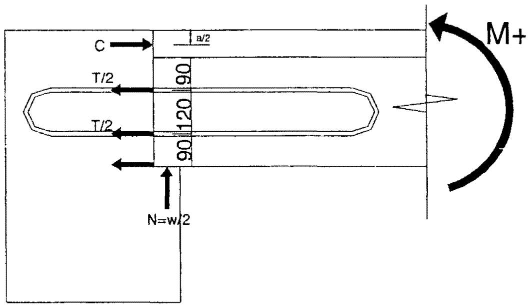

$$T = A_{spaperclip} f_y = \left(4 \times 2 \times \frac{\pi}{4} \times 16^2\right)(500) = 804.2kN$$

$$a = \frac{T}{0.85 f'_c b} = \frac{804000}{0.85 \times 30 \times 1200} = 26.3mm$$

$$jd = 150 + 75 - \frac{26.3}{2} = 212mm$$

$$M_T^+ = Tjd = 804 \times 0.212 = 171kNm$$

The frictional moment, M_μ, contribution is:

$$N = \frac{w}{2} = \frac{1}{2}(4.96 \times 1.2 \times 6 + 35) = 35.4kN$$

$$M_\mu^+ = \mu Njd = 1.2 \times 35.4 \times (0.375 - 0.013) = 15.4kNm$$

$$M_n^+ = M_T^+ + M_\mu^+ = 171 + 15.4 = 186kNm$$

Negative Moments:

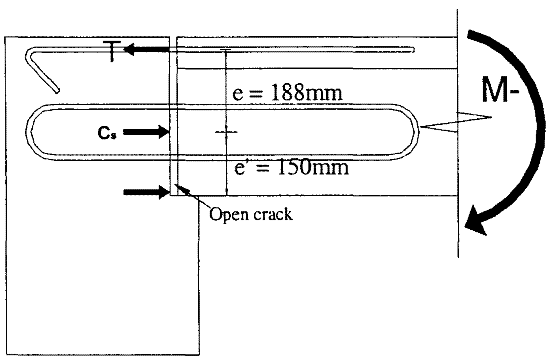

$$T = A_{starter} f_y = \left(4 \times 2 \times \frac{\pi}{4} \times 12^2\right)(500) = 226.2kN$$

$$M_n^- = Te + \mu Ne' = 226.2 \times 0.188 + 1.2 \times 5.4 \times 0.15 = 49kNm$$

C.1.3 Specimen 3

Positive Moment Capacity

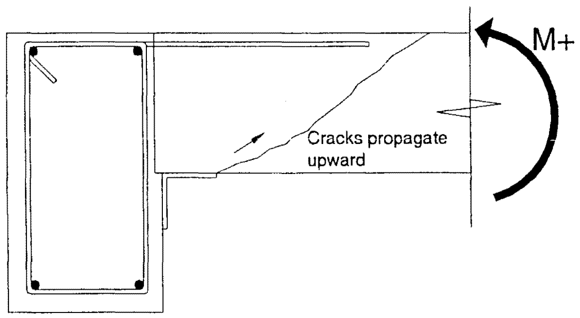

Under a positive moment, the hollowcore unit first develops its cracking moment. Once the cracking moment is reached, diagonal cracks then propagated upward from the bottom of the hollowcore unit toward the concrete topping. First calculate the transformed section moment of inertia.

Calculate the N.A depth, $\overline{Y}$ (with reference to the bottom fibre of the floor), of the transformed section.

$$n = \frac{E_{hollowcore}}{E_{topping}} = \frac{4700\sqrt{f'_{c\_hollowcore}}}{4700\sqrt{f'_{c\_topping}}} = \sqrt{\frac{42}{30}} = 1.18$$

where n = transformed ratio; $f'_{c\_topping}$ = concrete topping compressive strength and $f'_{c\_hollowcore}$ = hollowcore unit compressive strength. The transformed section of the floor unit is shown below.

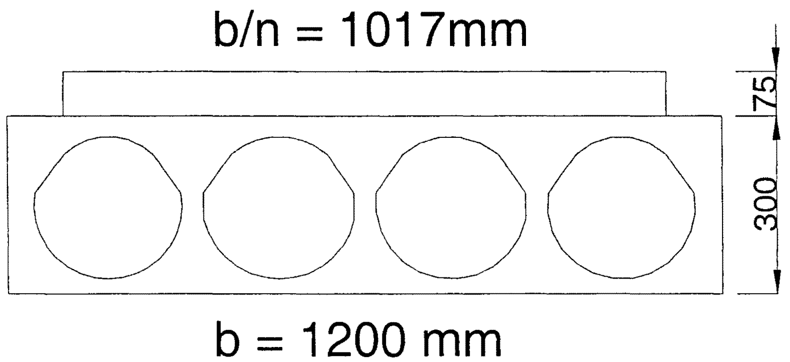

	A (mm^2)	$\bar{y}$ (mm)	A $\bar{y}$ (mm^3)
Concrete Topping	76063.9	337.5	2.567 x 10^7
Hollowcore unit	610600	153	9.342 x 10^7
	$\sum A = 686664$		$\sum A\bar{y} = 1.191 \text{ x } 10^8$

$$\bar{Y} = \frac{\sum A\bar{y}}{\sum A} = \frac{1.191 \times 10^8}{686664} = 173.4mm$$

Next, the moment of inertia of the floor unit can be calculated as:

$$I_{topping} = \frac{bd^3}{12} + Ad^2 = \frac{1014.2 \times 75^3}{12} + (1014.2 \times 75)\left(375 - 173.4 - \frac{75}{2}\right) = 2.083 \times 10^9 mm^4$$

$$I_{hollowcore} = I + Ad^2 = 2.04 \times 10^9 + (610600)(173.4 - 153)^2 = 2.259 \times 10^9 mm^4$$

$$I_{total} = I_{topping} + I_{hollowcore} = 2.083 \times 10^9 + 2.259 \times 10^9 = 4.378 \times 10^9 mm^4$$

Therefore, the connection cracking moment is:

$$M_{cr} = f_{cr} \frac{I_{xx}}{y}$$

$$f_{cr} = 0.36\sqrt{f'_{c\_hollowcore}} = 2.333MPa$$

$$M_{cr} = f_{cr} S_x = 2.333 \times \frac{4.378 \times 10^9}{173.4} = 59kNm$$

Residual Positive Moment Capacity

After cracking moment develops, the connection joint moment capacity decreases as the hollowcore unit cracks propagated upward from the bottom of the hollowcore unit. The residual strength of the connection joint at 3.0% drift amplitude is

$$T = A_{starter} f_y = \left(4 \times 2 \times \frac{\pi}{4} \times 12^2\right)(500) = 226.2kN$$

$$a = \frac{T}{0.85 f'_c b} = \frac{226.2}{0.85 \times 30 \times 1200} = 7.4mm$$

$$jd = 30 - \frac{7.4}{2} = 26.3mm$$

$$M_T^+ = Tjd = 226.2 \times 0.0263 = 6kNm$$

$$M_\mu^+ = \mu Njd = 0.8 \times 35.4 \times (0.375 - 0.013) = 10.5kNm$$

$M_n^+ = 6 + 10.5 = 16.5kNm$

The diagram below shows the tensile stress profile of an uncracked hollowcore unit.

The hollowcore can be approximate as an I-section.

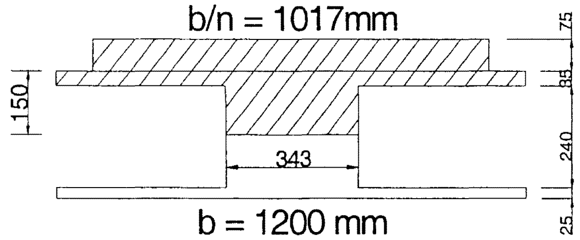

(a) Effective section

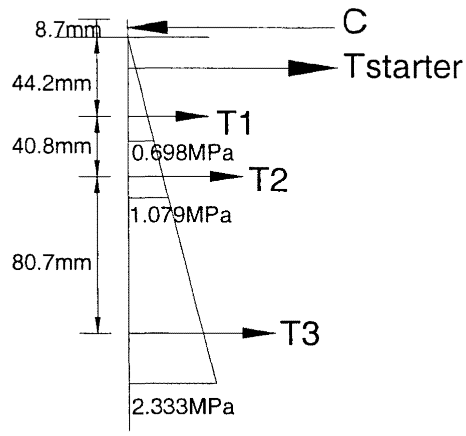

(b) Force diagram

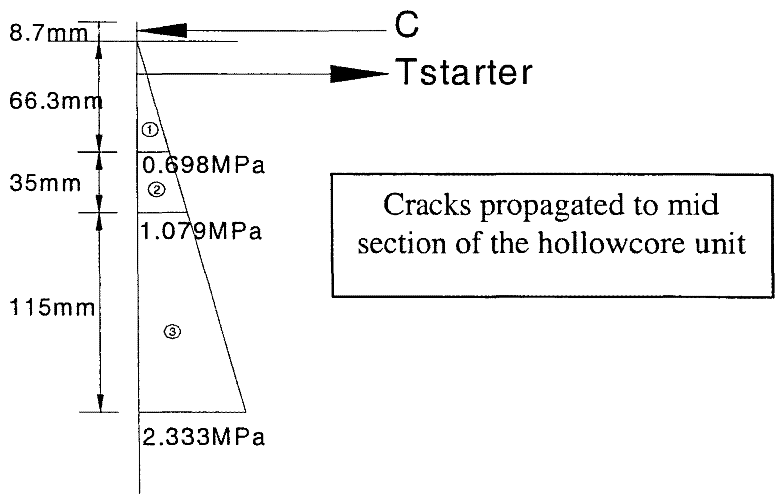

(c) Area under the stress triangle

The tensile force is determined by calculating the area inside the stress profile. In order to calculate connection moment capacity, the tension force within the section is multiplied by the leverarm, *jd*, between the centroids of the compression force and the tension reinforcement. Therefore the centroids (with references to the top) and the leverarm for each area is summarised as below.

	b (mm)	Force (kN)	Centroid (mm)	jd (mm)	Moment (kNm)
T1	1017	24.11	44.2	49.20	1.19
T2	1200	37.96	18.7	90.02	3.42
T3	343	67.56	64.44	170.74	11.54
					Σ = 16.1 kNm

Therefore the total residual positive moment capacity at 3.0% drifts:

$$M_n^+ = 16.5 + 15.9 = 32.4kNm$$

Negative Moment Capacity

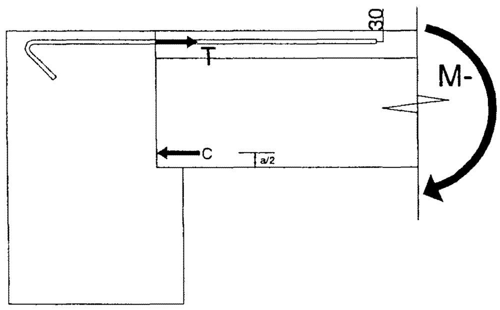

$$T = A_{starter} f_y = \left(4 \times 2 \times \frac{\pi}{4} \times 12^2\right)(500) = 226.2kN$$

$$a = \frac{T}{0.85 f'_c b} = \frac{226.2}{0.85 \times 42 \times 1200} = 5.3mm$$

$$jd = 375 - 30 - \frac{a}{2} = 342.4mm$$

$$M_n^- = Tjd = 226.2 \times 0.342 = 77.4kNm$$

Residual Negative Moment Capacity

Experimental observations of Specimen 3 show that the connection joint strength dropped suddenly under negative moment when shear cracks formed.

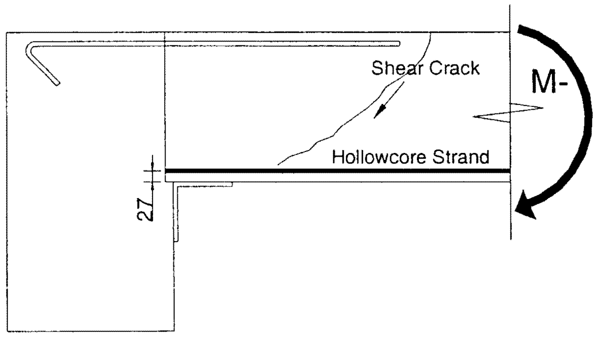

$$\rho = \frac{A_{s\_strand}}{A_{concrete}} = \frac{7\times\pi\times(12.9/2)^2}{27\times1200} = 0.0282$$

$$n = \frac{E_{strand}}{E_{hollowcore}} = \frac{200000}{4700\sqrt{42}} = 6.57$$

$$k = \sqrt{(\rho n)^2 + 2\rho n} - \rho n = 0.4511$$

$$kd = 0.4511\times 27 = 12.18mm$$

$$C = \frac{1}{2} f_c bkd = \frac{1}{2}\times 42\times1.2\times12.18 = 307kN$$

$$T \approx A_{strand}(0.6 f_{pu}) = 7\times\pi\times(12.9/2)^2(0.6\times1840) = 1010kN$$

$$jd = d - \frac{kd}{3} = 27 - \frac{12.18}{3} = 23mm$$

$$M_n^- = Cjd = 307\times0.023 = 7.04kNm$$

C.2 Moment Capacity of Bull and Matthews (2003) Specimens

C.2.1 2-R12 Paperclip Specimen

Positive Moment Capacity

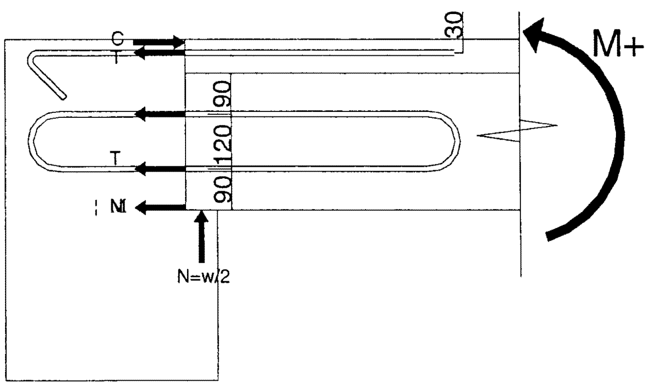

$$T = A_s f_y = (4\times\frac{\pi}{4}\times12^2 + 2\times2\times\frac{\pi}{4}\times12^2)(500) = 452.4kN$$

$$a = \frac{T}{0.85 f'_c b} = \frac{452400}{0.85 \times 30 \times 1200} = 14.7mm$$

The centroid of the tensile force with references to the top can be estimated by:

$$x = \frac{T_{starter} x_1 + T_{paperclip} x_2 + T_{paperclip} x_3}{T_{starter} + 2T_{paperclip}} = 127.5mm$$

$$jd = 127.5 - \frac{14.7}{2} = 120.2mm$$

$$M_T^+ = Tjd = (226.2 + 226.2) \times 0.1202 = 54kNm$$

$$N = \frac{w}{2} = \frac{1}{2}(4.96 \times 1.2 \times 6 + 35) = 35.4kN$$

$$M_\mu^+ = \mu Njd = 1.2 \times 35.4 \times (0.375 - 0.013) = 15.4kNm$$

$$M_n^+ = M_T^+ + M_\mu^+ = 54 + 15.4 = 69.4kNm$$

Negative Moment Capacity

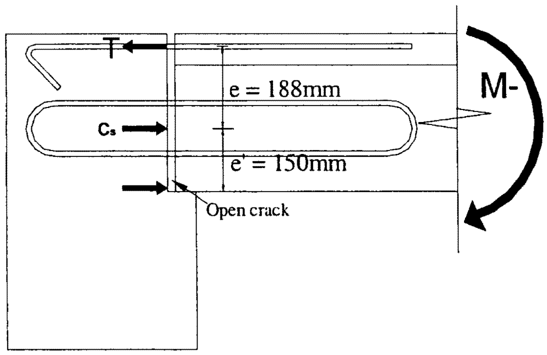

$$T = A_{starter} f_y = \left(4 \times 2 \times \frac{\pi}{4} \times 12^2\right)(500) = 226.2kN$$

$$M_n^- = Te + \mu Ne' = 226.2 \times 0.188 + 1.2 \times 5.4 \times 0.15 = 49kNm$$

C.2.2 Control Specimen

Positive Moment Capacity

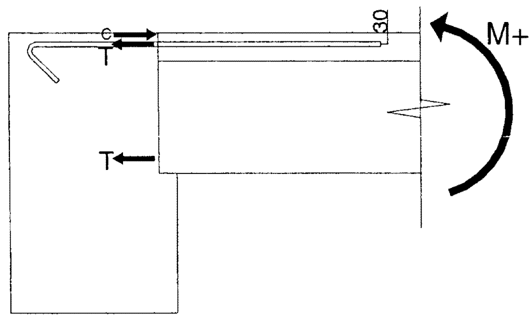

$$M_{cr} = f_{cr}\frac{I_{xx}}{y}$$

$$f_{cr} = 0.36\sqrt{f'_{c\_hollowcore}}$$

$$M_{cr} = f_{cr}S_x = 2.333\times\frac{4.378\times10^9}{173.4} = 59kNm$$

The residual strength of the connection after cracking moments develops:

$$T = A_{starter}f_y = \left(4\times2\times\frac{\pi}{4}\times12^2\right)(500) = 226.2kN$$

$$a = \frac{T}{0.85f'_c\,b} = \frac{226.2}{0.85\times30\times1200} = 7.4mm$$

$$jd = 30 - \frac{7.4}{2} = 26.3mm$$

$$M_T^+ = Tjd = 226.2\times0.0263 = 6kNm$$

$$M_\mu^+ = \mu Njd = 1.2\times35.4\times\left(0.375 - \frac{0.0074}{2}\right) = 15.8kNm$$

$$M_n^+ = M_T^+ + M_\mu^+ = 6 + 15.8 = 22kNm$$

Negative Moment Capacity

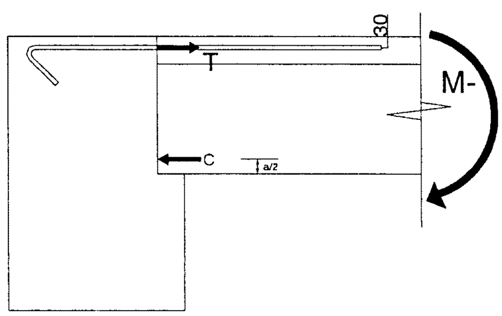

$$T = A_{starter} f_y = \left(4 \times \frac{\pi}{4} \times 12^2\right)(500) = 226.2kN$$

$$a = \frac{T}{0.85 f'_c b} = \frac{226.2}{0.85 \times 30 \times 1200} = 7.4mm$$

$$jd = 375 - 30 - \frac{a}{2} = 341.3mm$$

$$M_n^- = Tjd = 226.2 \times 0.3413 = 77.2kNm$$

Appendix B: Experimental Photos

B.1 Photographs of Experiment Setup

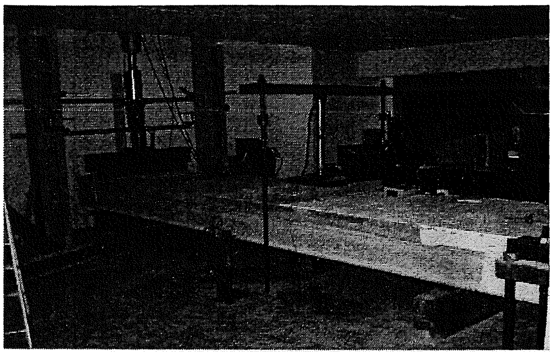

(a) Overview of the test specimen setup

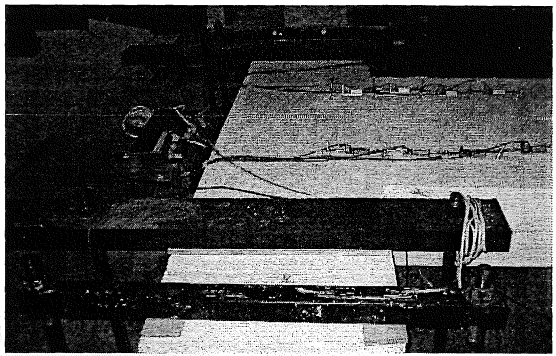

(b) Clamp down of the supporting beam

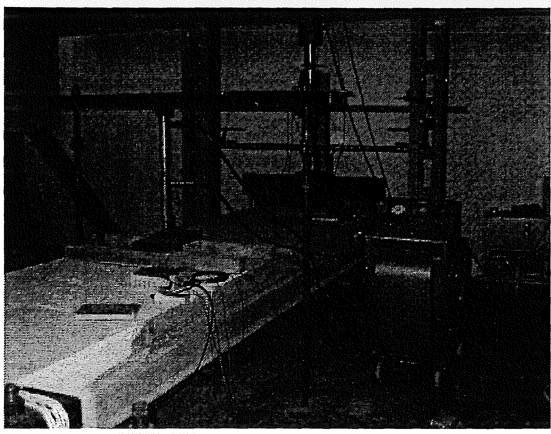

(c) Vertical loading applied on the Hollowcore floor system

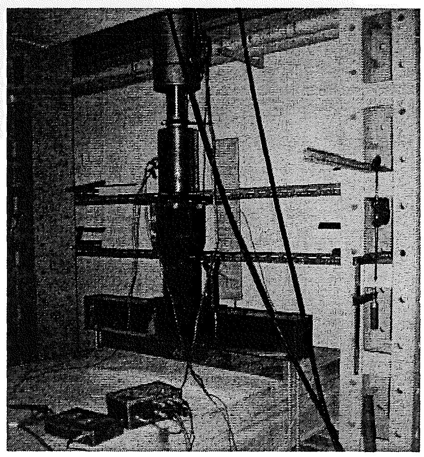

(d) Hydraulic ram used to stimulate rotation effect at connection

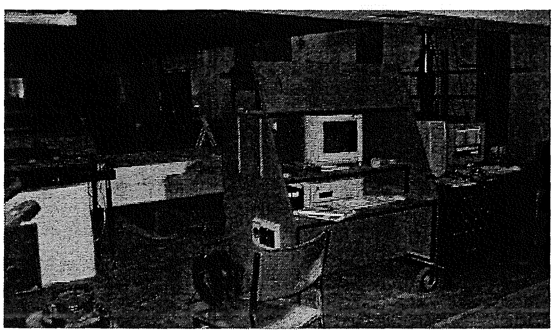

(e) Computers used to monitor and control the experiment

Figure B-1 Photographs of experiment setup

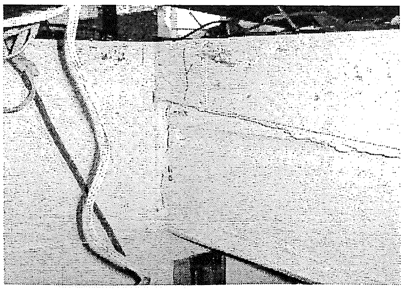

(i) Northern View of connection

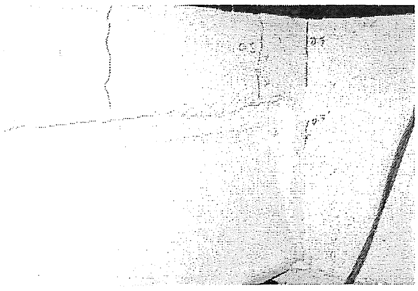

(ii) Southern View of connection

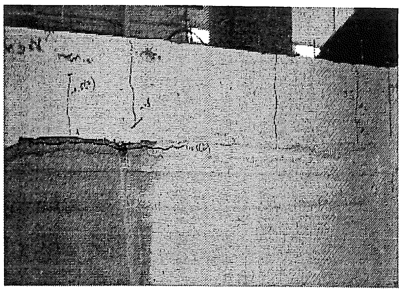

(iii) cracks between topping and floor unit

(a) Damage of hollowcore unit at ±0.5%

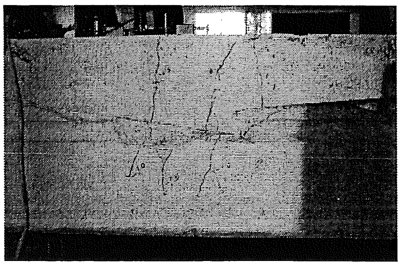

(a) Northern View

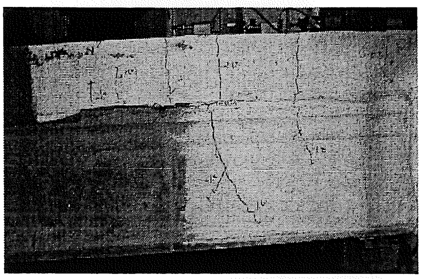

(b) Southern View

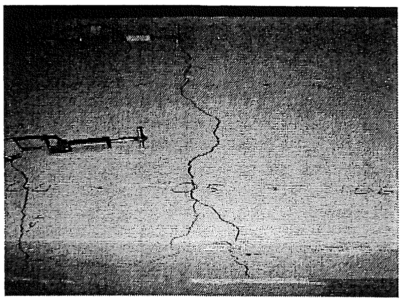

(iii) Shear crack formed

(b) Damage to hollowcore unit at -1.0%

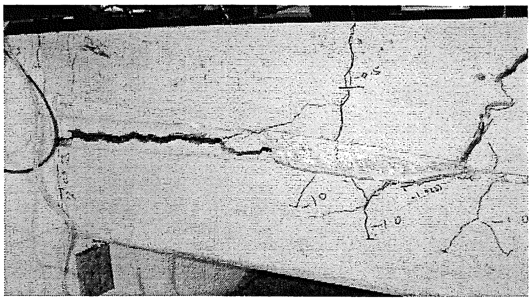

(i) North Side

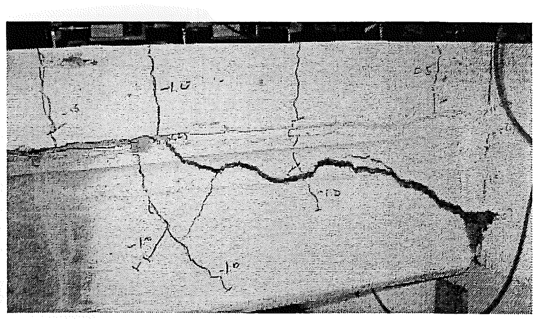

(ii) South Side

(c) Photos of floor unit at 2%

Figure B-2 Photographs of Specimen 1 at 0.5%, -1.0% and 2.0%

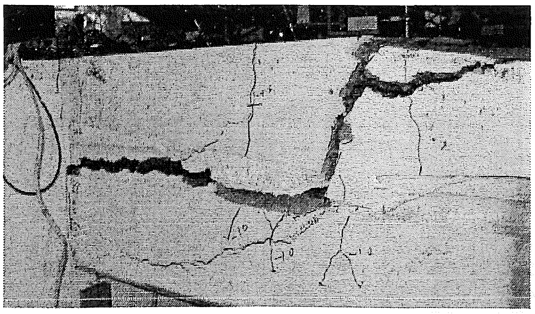

(i) North Side

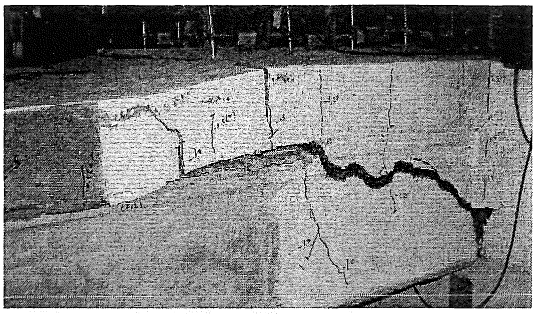

(ii) South Side

(a) Crack shifted toward bottom of the hollowcore unit at -2.0%

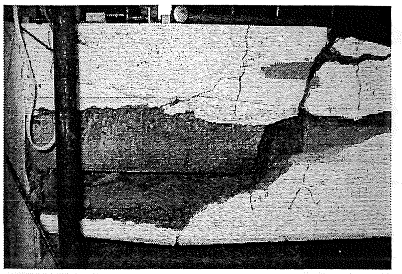

(i) Floor unit broken off from supporting beam.

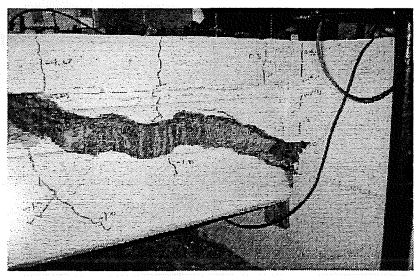

(ii) Southern view of hollowcore unit at failure

(iii) hollowcore unit had dropped at the end of testing

(b) Floor unit at failure

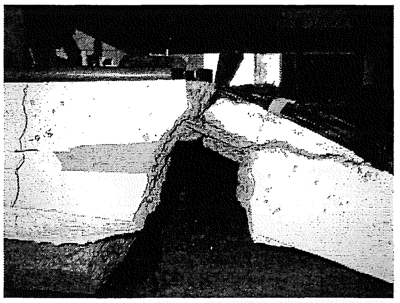

(i). Kinking of ductile mesh at end of testing

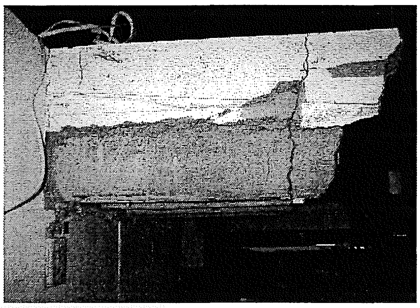

(ii) supporting beam at removal

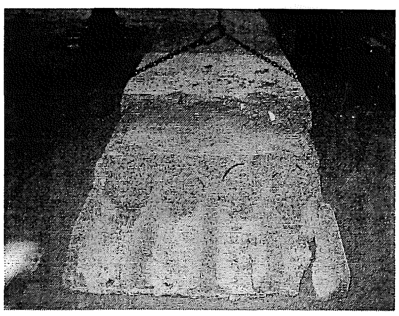

(iii) hollowcore floor unit at removal

(c) Photograph of Specimen 1 at removal

Figure B-3 Photographs of Specimen 1 at -2.0%, at failure and at removal

Test Specimen 2: Paperclip Detail with 70 mm Seating

(i) North side cracks pattern

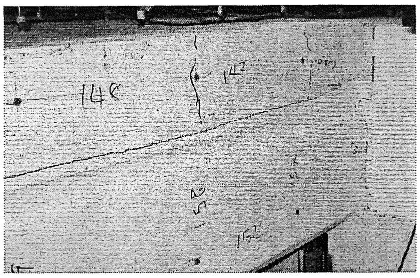

(ii) South side cracks pattern

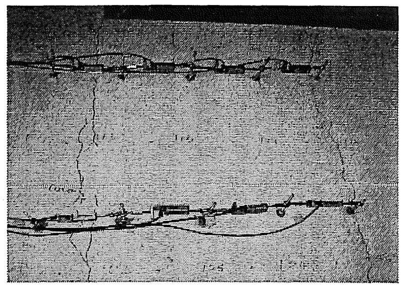

(iii) concrete topping

(a) Damage of hollowcore unit at ±0.5%

(i) Cracks at the underside of the unit at 1.0%

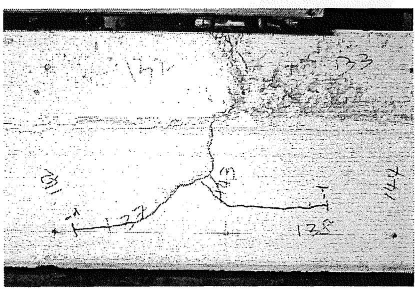

(ii) Northern view at -1.0%

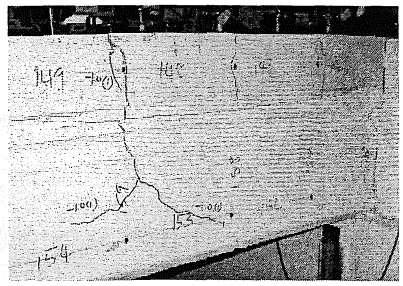

(iii) Southern view at -1.0%

(b) Damage of hollowcore unit at ±1.0%

(i) Shear crack at -2.0% drift at northern side

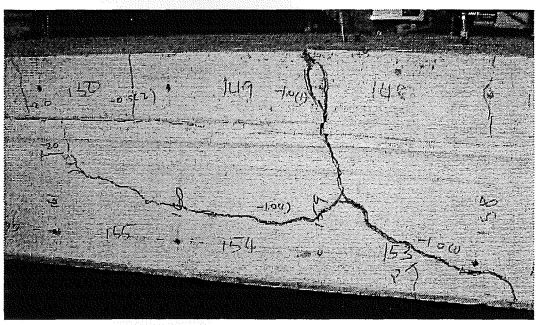

Photos of crack pattern at -2.0% at southern side

(c) Damage of hollowcore unit at -2.0%

Figure B-4 Photographs of Specimen 2 at 0.5%, 1.0% and -2.0%

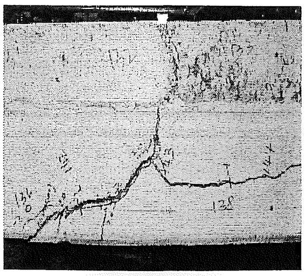

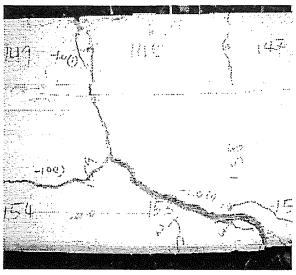

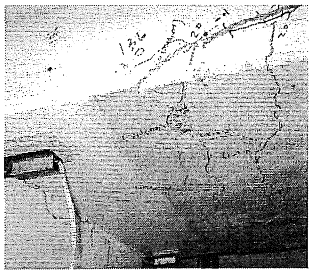

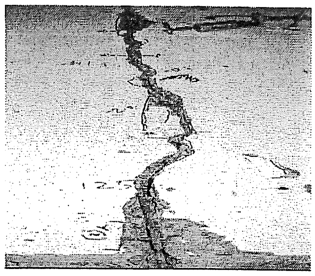

(i) Northern view at 3.0%

(ii) Southern view at 3.0%

(iii) Crack at bottom at 3.0%

(iv) Fracture topping mesh evident at -3.0%

(a) Damage of hollowcore unit at ±3.0%

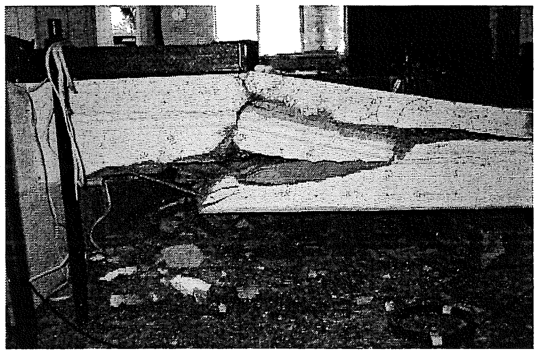

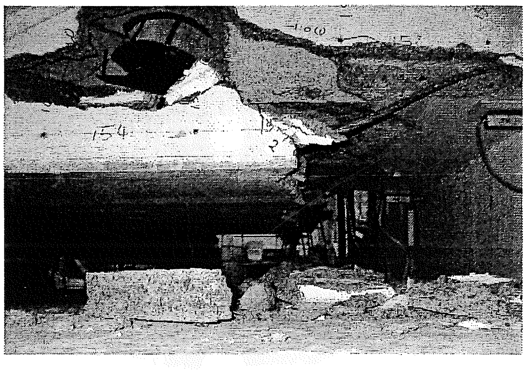

(i) Northern view of unit at failure

(ii)Unit hang up by strand at failure

(b) Connection at failure

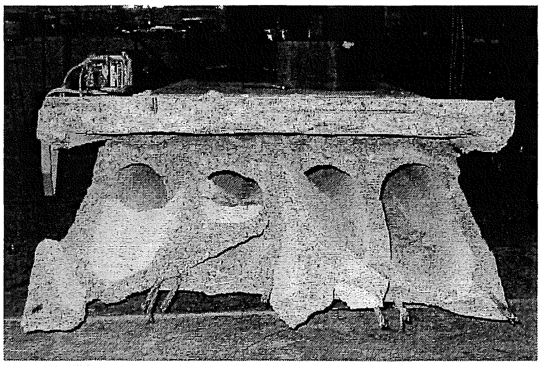

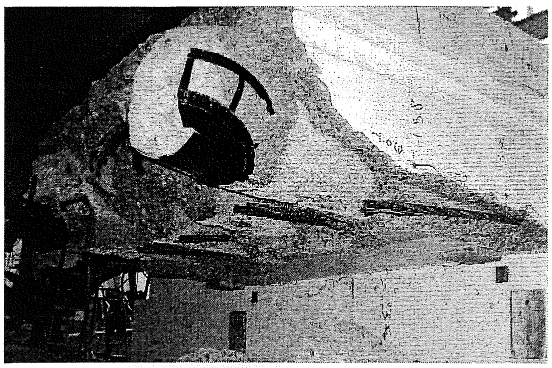

(i) The end of the hollowcore unit after removal

(ii) Section of hollowcore unit attached to the beam

(c) Removal photographs of Specimen 2

Figure B-5 Photographs of Specimen 2 at 3.0%, at failure and at removal

Test Specimen 3: Retrofit Detail with Angle Seat

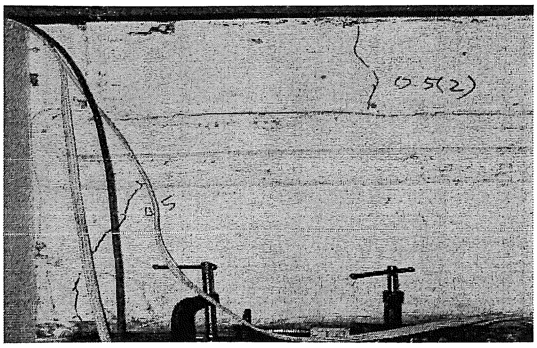

(i) Cracks on the side of the unit

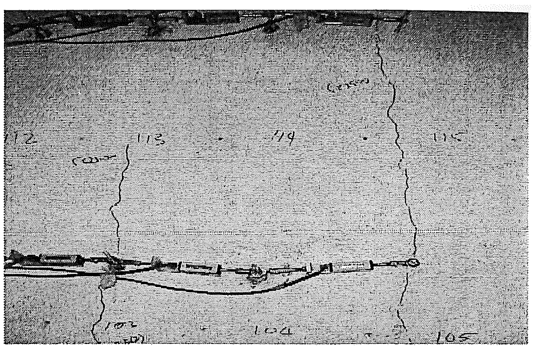

(ii) Cracks at concrete topping

(a) Damage to hollowcore unit at ±0.5%

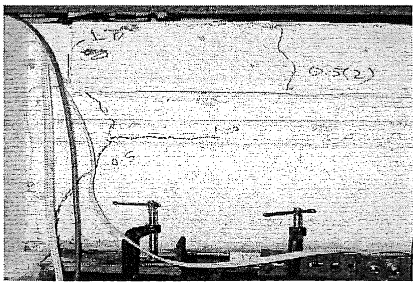

(i) Northern view

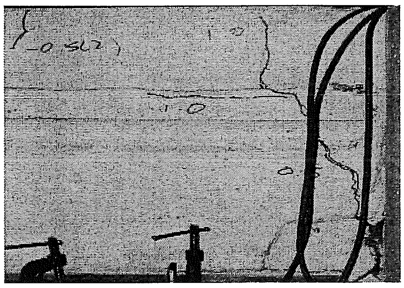

(ii) Southern view

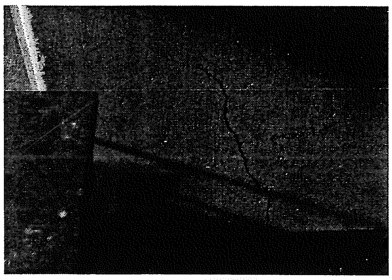

(iii) Cracks at underside of hollowcore unit

(b) Damage to hollowcore unit at 1.0%

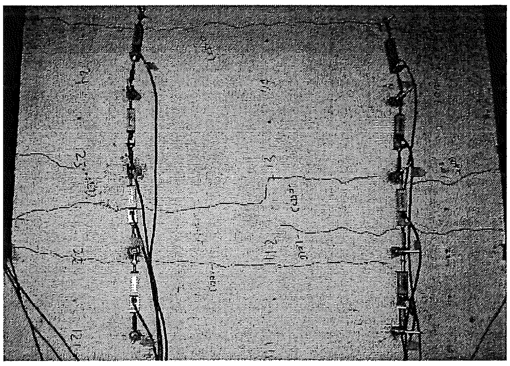

(i) Topping cracks at -1.0%

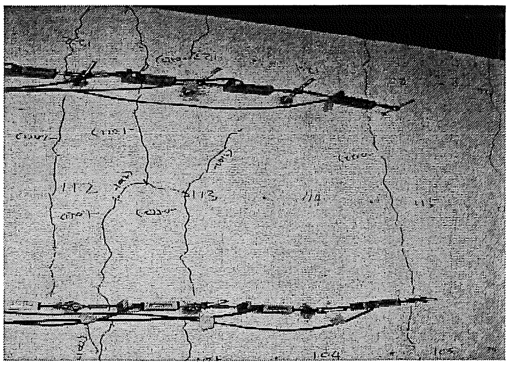

(ii) Topping cracks at 2nd cycle of -1.0%

(c) Damage to hollowcore unit at -1.0%

Figure B-6 Photographs of Specimen 3 at 0.5%, 1.0% and -1.0%

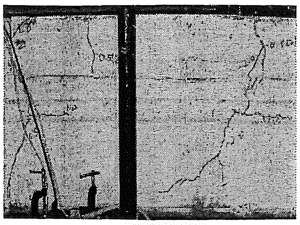

(i) Northern view at --2.0%

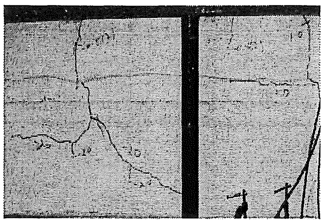

(ii) Southern view at -2.0%

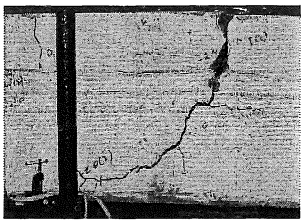

(iii) Northern view at 2nd cycle of -2.0%

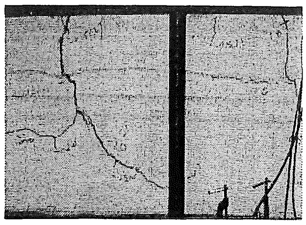

(iv) Southern view at 2nd cycle of -2.0%

(a) Damage of hollowcore unit at ±2.0%

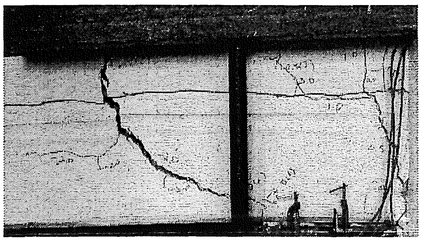

(i) Cracks at -3.0% drift

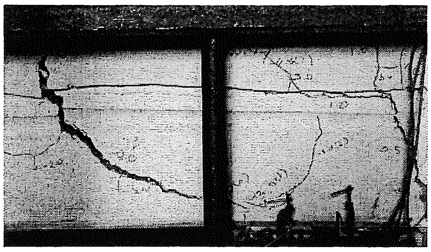

(ii) Cracks at 2nd cycles -3.0% drift

(b) Southern view of damage of hollowcore unit at -3.0%

(e) Bearing strip slipped

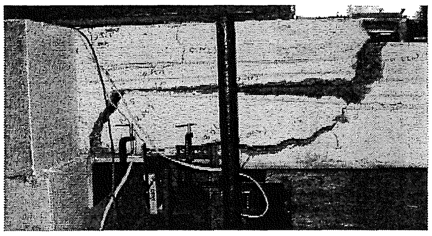

(f) Floor unit broken off

(c) Damage of hollowcore unit at failure

(i) Floor unit at failure

(ii) Unit being hang on by strand at failure

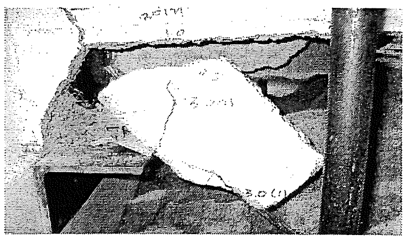

(iii) Hollowcore strand been pull off

(c) Floor unit at failure

Figure B-7 Photographs of Specimen 3 at 2.0%, -3.0% and at failure